

คุณลักษณะและสมบัติการเป็นตัวเร่งปฏิกิริยาของตัวเร่งปฏิกิริยาไทเทโนซีนบนตัวรองรับ
สำหรับการโคพอลิเมอไรเซชันของเอทิลีนกับหนึ่งออกทีน



นางสาวชนินทร เกตุลอย

สถาบันวิทยบริการ
จุฬาลงกรณ์มหาวิทยาลัย

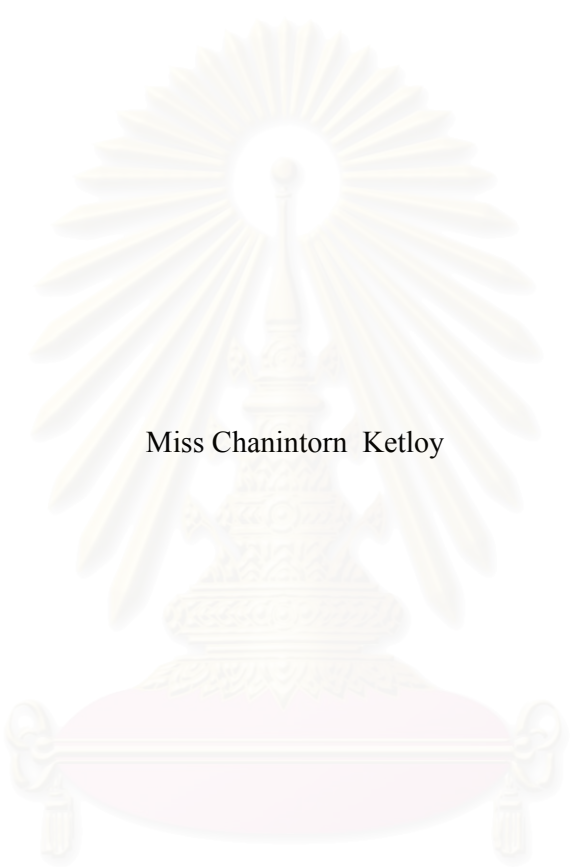
วิทยานิพนธ์นี้เป็นส่วนหนึ่งของการศึกษาตามหลักสูตรปริญญาวิศวกรรมศาสตรมหาบัณฑิต

สาขาวิชาวิศวกรรมเคมี ภาควิชาวิศวกรรมเคมี
คณะวิศวกรรมศาสตร์ จุฬาลงกรณ์มหาวิทยาลัย

ปีการศึกษา 2549

ลิขสิทธิ์ของจุฬาลงกรณ์มหาวิทยาลัย

CHARACTERISTICS AND CATALYTIC PROPERTIES OF SUPPORTED TITANOCENE
CATALYST FOR ETHYLENE/1-OCTENE COPOLYMERIZATION



Miss Chanintorn Ketloy

สถาบันวิทยบริการ
จุฬาลงกรณ์มหาวิทยาลัย

A Thesis Submitted in Partial Fulfillment of the Requirements
for the Degree of Master of Engineering Program in Chemical Engineering

Department of Chemical Engineering

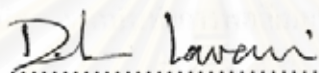
Faculty of Engineering

Chulalongkorn University

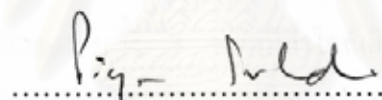
Academic Year 2006

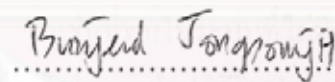
Thesis Title CHARACTERISTICS AND CATALYTIC PROPERTIES OF
SUPPORTED TITANOCENE CATALYST FOR
ETHYLENE/1-OCTENE COPOLYMERIZATION
By Miss Chanintorn Ketloy
Filed of study Chemical Engineering
Thesis Advisor Assistant Professor Bunjerd Jongsomjit, Ph.D.

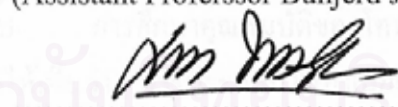
Accepted by the Faculty of Engineering, Chulalongkorn University in Partial
Fulfillment of the Requirements for the Master's Degree



..... Dean of the Faculty of engineering
(Professor Direk Lavansiri, Ph.D.)

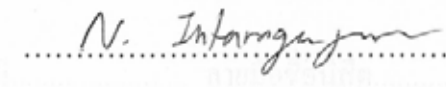
THESIS COMMITTEE


..... Chairman
(Professor Piyasan Praserttham, Dr.Eng)


..... Thesis Advisor
(Assistant Professor Bunjerd Jongsomjit, Ph.D.)


..... Member
(Associate Professor ML. Supakanok Thongyai, Ph.D.)


..... Member
(Assistant Professor Muenduen Phisalaphong, Ph.D.)


..... Member
(Nawaporn Intaragamjon, D.Eng)

ชวินธร เกตุลอย : คุณลักษณะและสมบัติการเป็นตัวเร่งปฏิกิริยาของตัวเร่งปฏิกิริยาไทเทเนียม
บนตัวรองรับสำหรับการ โคพอลิเมอไรเซชันของเอทิลีนกับหนึ่งออกทีน.

(CHARACTERISTICS AND CATALYTIC PROPERTIES OF SUPPORTED
TITANOCENE CATALYST FOR ETHYLENE/1-OCTENE
COPOLYMERIZATION) อ. ที่ปรึกษา : ผศ.ดร. บรรเจิด จงสมจิตร, 137 หน้า.

ในงานวิจัยนี้ได้ทำการศึกษาคุณลักษณะ และสมบัติการเป็นตัวเร่งปฏิกิริยาของระบบที่ใช้ตัวเร่งปฏิกิริยาเททราโบรโมไทลอะมิโดไซลิลไดเมทิลฟลูออรีนไททาเนียมไดเมทิล ($(t\text{-BuNSiMe}_2\text{Flu})\text{TiMe}_2$) บนตัวรองรับสำหรับการ โคพอลิเมอไรเซชันของเอทิลีนกับหนึ่งออกทีน โดยมีตัวเร่งปฏิกิริยาร่วมคือ โมดิฟายเมทิลอะลูมิเนียมออกไซด์ (d-MMAO) ซึ่งได้นำไปผสมกับตัวรองรับ 3 ชนิด คือ ซิลิกา ซิลิกาผสมไทเทเนีย และไทเทเนีย จากนั้นทำการพอลิเมอไรเซชันทั้งในระบบที่มีและไม่มีตัวรองรับในตัวทำละลายที่ต่างกัน ได้แก่ โทลูอีน และคลอโรเบนซีน พบว่าระบบจะมีความว่องไวสูงสุดเมื่อใช้ซิลิกาผสมไทเทเนียเป็นตัวรองรับ เนื่องจากแรงกระทำระหว่างตัวรองรับกับตัวเร่งปฏิกิริยาร่วมในระบบนี้ลดลง นอกจากนี้เมื่อทำการศึกษาผลของโคโมโนเมอร์ตัวที่สอง พบว่าค่าความว่องไวจะเพิ่มขึ้นมากเมื่อทำการเติมแอลฟา-โอเลฟินลงในระบบการพอลิเมอไรเซชันของเอทิลีน แต่ในระบบเอทิลีนนี้พบว่าค่าความว่องไวของระบบที่มีตัวรองรับทั้ง 3 ชนิดมีค่าใกล้เคียงกัน จากการศึกษาผลของตัวทำละลายสามารถสรุปได้ว่าตัวทำละลายส่งผลทำให้เกิดการเปลี่ยนแปลงธรรมชาติของตัวเร่งปฏิกิริยาได้ 2 ทางคือ (1) เปลี่ยนแรงกระทำที่มีระหว่างตัวรองรับกับตัวเร่งปฏิกิริยาร่วม (2) เปลี่ยนรูปแบบของตัวเร่งปฏิกิริยาที่ใช้ในการเข้าทำปฏิกิริยา ดังเช่นที่พบในระบบที่ไม่มีตัวรองรับ อย่างไรก็ตามพบว่าการเปลี่ยนตัวทำละลายไม่มีผลต่อค่าความว่องไวในการทำปฏิกิริยาในระบบการ โคพอลิเมอไรเซชันของเอทิลีนกับหนึ่งออกทีนแบบไม่มีตัวรองรับ การศึกษาคุณสมบัติของ โคพอลิเมอไรท์ที่ได้จากการสังเคราะห์ด้วยตัวเร่งปฏิกิริยาไทเทเนียมแสดงให้เห็นว่า สารประกอบไททาเนียมมีความสามารถในการเข้าร่วมของแอลฟาโอเลฟินซึ่งก็คือหนึ่งออกทีนได้ดีโดยดูจากปริมาณของออกทีนเข้าร่วมที่วิเคราะห์ได้ พอลิเมอร์และโคพอลิเมอร์ที่ได้ทั้งหมดจะนำมาวิเคราะห์ เพื่อวัดคุณสมบัติและโครงสร้างย่อยของพอลิเมอร์ด้วยเครื่องเจลเพอมีเอชันโครมาโตกราฟี (GPC) เครื่องดิฟเฟอเรนเชียลสแกนนิ่งแคลอริมิเตอร์ (DSC) และเครื่องนิวเคลียร์แมกเนติกเรโซแนนซ์ (^{13}C NMR)

ภาควิชา.....วิศวกรรมเคมี..... ลายมือชื่อนิสิต..... ชวินธร เกตุลอย
สาขาวิชา.....วิศวกรรมเคมี..... ลายมือชื่ออาจารย์ที่ปรึกษา.....
ปีการศึกษา.....2549.....

4870267621 : MAJOR CHEMICAL ENGINEERING

KEY WORD: SUPPORTED METALLOCENE CATALYST / COPOLYMERIZATION OF ETHYLENE / 1-OCTENE / SUPPORTING EFFECT / SOLVENT EFFECT

CHANINTORN KETLOY : CHARACTERISTICS AND CATALYTIC PROPERTIES OF SUPPORTED TITANOCENE CATALYST FOR ETHYLENE/1-OCTENE COPOLYMERIZATION. THESIS ADVISOR : ASST. PROF. BUNJERD JONGSOMJIT, Ph.D., 137 pp.

In the present study, the characteristics and catalytic properties of [*t*-BuNSiMe₂Flu]TiMe₂/dMMAO catalyst dispersed on various supports towards ethylene/1-octene copolymerization were investigated. First, the dMMAO was impregnated onto various supports such as SiO₂, SiO₂-TiO₂, and TiO₂. Then, copolymerization of ethylene/1-octene was conducted with and without the presence of supports in different solvent mediums such as toluene and chlorobenzene. It revealed that the SiO₂-TiO₂ support exhibited the highest activity among the other supports. The high activity observed for the SiO₂-TiO₂ support can be attributed to fewer interactions between the support and dMMAO as confirmed by XPS and TGA results. Moreover, ethylene polymerization was also conducted in this study. The activities of polymerization dramatically increased with the insertion of α -olefin due to the second comonomer effect. The slightly difference in the polymerization activities were apparently found in the supported system. It can be proposed that the different solvents can possibly alter the nature of catalyst in two ways; (i) changing the interaction between the support and cocatalyst and/or (ii) changing the form of active species i.e., active ion-pair and solvent-separated ion-pair as seen in the homogeneous system. However, there was no effect with regards to activity of the solvent mediums employed for the homogeneous system in ethylene/1-octene copolymerization. It is worth noting that the Ti-complex rendered pronouncedly high incorporation of 1-octene having the triblock (OOO) and diblock (EOO) copolymers. All the obtained polymers were characterized by GPC, DSC, and ¹³C NMR to determine the polymer properties and polymer microstructure.

Department....Chemical Engineering.....Student's signature.....Chanintorn Ketloy

Field of study...Chemical Engineering.....Advisor's signature.....Bunjerd Jongsomjit

Academic year.....2006.....

ACKNOWLEDGEMENTS

I would like to give special recognition to Assistant Professor Dr. Bunjerd Jongsomjit, my advisor, for his generosity in providing guidance and sharing his ideas on the interesting work. His advices are always worthwhile and without him this work could not be possible.

I wish to thank Professor Dr. Piyasan Prasertdam as a chairman and the entire member of thesis committee including Associate Professor Dr. ML. Supakanok Thongyai, Assistant Professor Dr. Muenduen Phisalaphong and Dr. Nawaporn Intaragamjon for their valuable guidance and revision throughout my thesis. Especially, Dr. Nawaporn Intaragamjon who always advice and discuss the problems with me. His kind advices are valuable for this project.

Sincere thanks are given to the graduate school and department of chemical engineering at Chulalongkorn University for the financial support of this work. And many thanks are given to PTT Chemical Public Company Limited for ethylene gas supply and MEKTEC Manufacturing Corporation (Thailand) Limited for DSC and NMR measurements.

I wish to extend my thanks to my friends for giving my strength and encouragement, and all of senior researchers for their kind advice in my experiment.

Finally, I would like to express my highest gratitude to my parents and sister for their tremendous support and overwhelming encouragement.

สถาบันวิทยบริการ
จุฬาลงกรณ์มหาวิทยาลัย

CONTENTS

	Page
ABSTRACT (IN THAI)	iv
ABSTRACT (IN ENGLISH)	v
ACKNOWLEDGEMENTS	vi
CONTENTS	vii
LIST OF TABLES	xi
LIST OF FIGURES	xii
CHAPTER I INTRODUCTION	1
CHAPTER II LITERATURE REVIEWS	5
2.1 Polyolefin Catalysts.....	5
2.1.1 Metallocene Catalysts.....	5
2.1.2 Structure of Metallocene Catalysts.....	6
2.1.3 Cocatalysts.....	8
2.1.4 Polymerization Mechanism.....	11
2.1.5 Chain Transfer Mechanism	12
2.1.6 Catalyst Deactivation.....	14
2.2 Heterogeneous System.....	16
2.2.1 Supported Metallocene Catalyst Methods.....	17
2.2.2 Effect of Supported Methods.....	19
2.3 The Parameters Affecting Catalyst Activity and Polymer Characteristic.....	23
2.3.1 Comonomer Effect.....	24
2.3.2 Supporting Effect.....	26
2.3.3 Solvent Medium Effect.....	28
CHAPTER III EXPERIMENTAL	30
3.1 Objectives of the Thesis.....	30
3.2 Scopes of the Thesis.....	30
3.3 Research Methodology.....	30
3.4 Experimental.....	32
3.4.1 Chemicals.....	32
3.4.2 Equipments.....	33
3.4.2.1 Cooling system.....	33

	Page
3.4.2.2 Inert gas supply.....	33
3.4.2.3 Magnetic stirrer and heater.....	34
3.4.2.4 Reactor.....	34
3.4.2.5 Schlenk line.....	34
3.4.2.6 Schlenk tube.....	35
3.4.2.7 Vacuum pump.....	35
3.4.2.8 Polymerization line.....	36
3.4.3 Catalyst Synthesis.....	36
3.4.3.1 Synthesis of <i>t</i> -BuNHSiMe ₂ Flu.....	36
3.4.3.2 Synthesis of [<i>t</i> -BuNMe ₂ SiFlu]TiMe ₂	36
3.4.4 Supporting Procedure.....	37
3.4.4.1 Preparation of Mixed oxides.....	37
3.4.4.2 Preparation of dMMAO.....	37
3.4.4.3 Preparation of Supported dMMAO.....	38
3.4.5 Ethylene and Ethylene/1-Octene Polymerization Procedures.....	38
3.4.6 Characterization Method of Supports and supported dMMAO.....	39
3.4.6.1 X-ray diffraction (XRD).....	39
3.4.6.2 Raman spectroscopy.....	39
3.4.6.3 Scanning electron microscopy (SEM) and energy dispersive X-ray spectroscopy (EDX).....	39
3.4.6.4 X-ray photoelectron spectroscopy (XPS).....	39
3.4.6.5 Thermogravimetric analysis (TGA).....	39
3.4.7 Characterization Method of Polymer.....	40
3.4.7.1 Gel permeation chromatography (GPC).....	40
3.4.7.2 Differential scanning calorimetry (DSC).....	40
3.4.7.3 ¹³ C NMR spectroscopy (¹³ C NMR).....	40
CHAPTER IV RESULTS AND DISCUSSION.....	41
4.1 Characterization of supports and supported dMMAOs.....	41
4.1.1 Characterization of supports with X-ray diffraction (XRD).....	41
4.1.2 Characterization of supports with Raman spectroscopy.....	42

	Page
4.1.3 Characterization of supports and supported dMMAO with scanning electron microscopy (SEM) and energy dispersive X-ray spectroscopy (EDX).....	43
4.1.4 Characterization of supports and supported dMMAO with X-ray photoelectron spectroscopy (XPS).....	45
4.1.5 Characterization of supports and supported dMMAO with Thermogravimetric analysis (TGA).....	47
4.2 Characteristics and catalytic properties of ethylene/1-octene copolymerization.....	48
4.2.1 The effect of various supports and solvent mediums on the catalytic activity.....	48
4.2.2 The effect of various supports and solvent mediums on the molecular weight of copolymers.....	51
4.2.3 The effect of various supports and solvent mediums on the microstructure of copolymers.....	52
4.2.4 The effect of various supports and solvent mediums on the thermal properties of copolymers.....	54
4.3 Comparative study of ethylene and ethylene/1-octene polymerization.....	54
4.3.1 The effect of various supports and solvent mediums on the catalytic activity.....	54
4.3.2 The effect of various supports and solvent mediums on the molecular weight of polymers.....	56
4.3.3 The effect of various supports and solvent mediums on the thermal properties of polymers.....	58
CHAPTER V CONCLUSIONS AND RECOMMENDATION.....	60
5.1 Conclusions.....	60
5.2 Recommendations.....	61
REFERENCES.....	62
APPENDICES.....	72
APPENDIX A.....	73
APPENDIX B.....	82
APPENDIX C.....	91

	Page
APPENDIX D	100
APPENDIX E	103
APPENDIX F	106
VITA	137



สถาบันวิทยบริการ
จุฬาลงกรณ์มหาวิทยาลัย

LIST OF TABLES

Table	Page
4.1 The content of $[Al]_{dMMAO}$ on various supports.....	43
4.2 XPS data of Al 2p core-level of cocatalysts.....	46
4.3 Copolymerization activity.....	50
4.4 Copolymer characterization.....	51
4.5 Triad distribution and %octene incorporation of copolymer obtained from ^{13}C NMR.....	53
4.6 Polymerization activity.....	56
4.7 Polymer characterization.....	57
4.8 Melting temperature and %crystallinity of polymer produced.....	58



สถาบันวิทยบริการ
จุฬาลงกรณ์มหาวิทยาลัย

LIST OF FIGURES

Figure	Page
2.1	Typical chemical structure of a metallocene catalyst..... 6
2.2	Schematic representations of metallocene symmetry..... 7
2.3	Several kinds of MAO..... 8
2.4	The general proposed structure of MAO..... 9
2.5	Cossee mechanisms for Ziegler-Natta olefin polymerization..... 12
2.6	Chain transfer via β -H elimination..... 13
2.7	Chain transfer via β -CH ₃ elimination..... 13
2.8	Chain transfer to aluminum..... 13
2.9	Chain transfer to monomer..... 14
2.10	Chain transfer to hydrogen..... 14
2.11	Mechanism showing the deactivation of active center for Cp ₂ ZrCl ₂ -MAO catalyst system..... 15
2.12	Mechanism of reversible second-order deactivation..... 16
2.13	Supporting methods of metallocene catalyst..... 18
2.14	Structure of Et(Ind) ₂ ZrCl ₂ supported on silica..... 19
2.15	Effect of surface hydroxyl groups on ionic metallocene catalysts..... 20
2.16	Structure of some silica supported metallocene catalysts..... 21
2.17	Modification of silica with Cp(CH ₂) ₃ Si(OCH ₂ CH ₃) ₃ and preparation of supported metallocene catalysts..... 22
2.18	Mechanism for supporting metallocene catalysts on silica using spacer molecules..... 23
3.1	Flow diagram of research methodology..... 31
3.2	Inert gas supply system..... 34
3.3	Schlenk line..... 35
3.4	Schlenk tube..... 35
3.5	Diagram of system in slurry phase polymerization..... 36
3.6	Synthetic pathway of [<i>t</i> -BuNSiMe ₂ Flu]TiMe ₂ 37
4.1	XRD patterns of various supports prior to impregnation with dMMAO..... 42
4.2	Raman spectra of various supports prior to impregnation with dMMAO..... 43

Figure	Page
4.3 A typical spectrum of the supported dMMAO from EDX analysis used to measure the average [Al]dMMAO concentration on various supports.....	44
4.4 SEM/EDX mapping for Al distributions.....	45
4.5 A typical XPS spectrum of Al 2p core-level of dMMAO and dMMAO on various supports.....	46
4.6 TGA profiles of supported dMMAO on various supports.....	47
A-1 GPC curve of ethylene/1-octene copolymer produce with homogeneous in toluene.....	74
A-2 GPC curve of ethylene/1-octene copolymer produce with SiO ₂ in toluene.....	74
A-3 GPC curve of ethylene/1-octene copolymer produce with SiO ₂ -TiO ₂ in toluene.....	75
A-4 GPC curve of ethylene/1-octene copolymer produce with TiO ₂ in toluene.....	75
A-5 GPC curve of ethylene/1-octene copolymer produce with homogeneous in chlorobenzene.....	76
A-6 GPC curve of ethylene/1-octene copolymer produce with SiO ₂ in chlorobenzene.....	76
A-7 GPC curve of ethylene/1-octene copolymer produce with SiO ₂ -TiO ₂ in chlorobenzene.....	77
A-8 GPC curve of ethylene/1-octene copolymer produce with TiO ₂ in chlorobenzene.....	77
A-9 GPC curve of polyethylene produce with homogeneous in toluene.....	78
A-10 GPC curve of polyethylene produce with SiO ₂ in toluene.....	78
A-11 GPC curve of polyethylene produce with SiO ₂ -TiO ₂ in toluene.....	79
A-12 GPC curve of polyethylene produce with TiO ₂ in toluene.....	79
A-13 GPC curve of polyethylene produce with homogeneous in chlorobenzene.....	80
A-14 GPC curve of polyethylene produce with SiO ₂ in chlorobenzene.....	80
A-15 GPC curve of polyethylene produce with SiO ₂ -TiO ₂ in chlorobenzene.....	81
A-16 GPC curve of polyethylene produce with TiO ₂ in chlorobenzene.....	81

Figure	Page
B-1 ^{13}C NMR spectrum of ethylene/1-octene copolymer produces with homogeneous in toluene.....	83
B-2 ^{13}C NMR spectrum of ethylene/1-octene copolymer produces with SiO_2 support in toluene.....	84
B-3 ^{13}C NMR spectrum of ethylene/1-octene copolymer produces with $\text{SiO}_2\text{-TiO}_2$ support in toluene.....	85
B-4 ^{13}C NMR spectrum of ethylene/1-octene copolymer produces with TiO_2 support in toluene.....	86
B-5 ^{13}C NMR spectrum of ethylene/1-octene copolymer produces with homogeneous in chlorobenzene.....	87
B-6 ^{13}C NMR spectrum of ethylene/1-octene copolymer produces with SiO_2 support in chlorobenzene.....	88
B-7 ^{13}C NMR spectrum of ethylene/1-octene copolymer produces with $\text{SiO}_2\text{-TiO}_2$ support in chlorobenzene.....	89
B-8 ^{13}C NMR spectrum of ethylene/1-octene copolymer produces with TiO_2 support in chlorobenzene.....	90
C-1 DSC curve of ethylene/1-octene copolymer produce with homogeneous in toluene.....	92
C-2 DSC curve of ethylene/1-octene copolymer produce with SiO_2 support in toluene.....	92
C-3 DSC curve of ethylene/1-octene copolymer produce with $\text{SiO}_2\text{-TiO}_2$ support in toluene.....	93
C-4 DSC curve of ethylene/1-octene copolymer produce with TiO_2 support in toluene.....	93
C-5 DSC curve of ethylene/1-octene copolymer produce with homogeneous in chlorobenzene.....	94
C-6 DSC curve of ethylene/1-octene copolymer produce with SiO_2 support in chlorobenzene.....	94
C-7 DSC curve of ethylene/1-octene copolymer produce with $\text{SiO}_2\text{-TiO}_2$ support in chlorobenzene.....	95
C-8 DSC curve of ethylene/1-octene copolymer produce with TiO_2 support in chlorobenzene.....	95

Figure	Page
C-9 DSC curve of polyethylene produce with homogeneous in toluene.....	96
C-10 DSC curve of polyethylene produce with SiO ₂ support in toluene.....	96
C-11 DSC curve of polyethylene produce with SiO ₂ -TiO ₂ support in toluene.....	97
C-12 DSC curve of polyethylene produce with TiO ₂ support in toluene.....	97
C-13 DSC curve of polyethylene produce with homogeneous in chlorobenzene.....	98
C-14 DSC curve of polyethylene produce with SiO ₂ support in chlorobenzene.....	98
C-15 DSC curve of polyethylene produce with SiO ₂ -TiO ₂ support in chlorobenzene.....	99
C-16 DSC curve of polyethylene produce with TiO ₂ support in chlorobenzene.....	99



สถาบันวิทยบริการ
จุฬาลงกรณ์มหาวิทยาลัย

CHAPTER I

INTRODUCTION

In the recent years, polyolefins are one of the largest productions in plastic industry and widely used in our life. They are a fast growing segment of the polymer industry with the highest amount of nearly 4 million tons a year [1]. For the commercial scale, polyethylene is the major usage polymer in many kinds of industry. In 1996, worldwide production of ethylene/ α -olefin copolymers exceeded 24 million metric tons [2] or approximately 30% of the market share of polymer products from ethylene [3]. Linear low-density polyethylene (LLDPE) which produces by ethylene copolymer of higher α -olefins such as 1-butene, 1-hexene, and 1-octene is industrially important materials [4]. As far, industrial efforts have been directed towards finding novel and efficient polymerization catalysts for the synthesis of the desired copolymer. Some recent reviews and books give detailed information on olefin catalysis especially by metallocene and other metal complexes [2].

The first homogeneous Ziegler-Natta catalyst was discovered independently by Breslow and Natta in 1957 [5]. The catalyst, Cp_2TiCl_2 activated with alkylaluminum chloride exhibited a low polymerization activity for ethylene and none for propylene. It was found later that small amounts of impurities such as oxygen, ether and even moisture had a beneficial effect on the polymerization [6]. The reaction between water and aluminum alkyls was shown to produce alkyl alumoxanes. The hydrolysis of the trimethylaluminum, $\text{Al}(\text{CH}_3)_3$ is cause of formation the cocatalyst methylaluminoxane (MAO) which precede to the high activity [5]. In 1980, Kaminsky and coworkers [7] used oligomeric methylaluminoxane (MAO) with group 4B metallocene compounds to obtain ethylene polymerization catalysts having extremely high activities. The active species in the catalyst system were homogeneous and produced polyethylene with narrow molecular weight distribution (MWD). The discovery brought the way to expand possibilities of new olefin polymerization and good property of the resulting polyolefins [8].

The rapid market penetration of metallocene-based PE is due to its high-value attributes, such as greater stiffness and impact strength, greater stretch and puncture

resistance, and improved stability [9]. The single-site characteristic of metallocene makes it possible to improve polymer properties; control the degree of α -olefin insertion upon the stereochemistry and provide higher activity, than those obtained by conventional Ziegler-Natta catalyst. They can also result in a narrow MWD and the uniform distribution of short-chain branches in the polymer chain as well [10]. It should be noted that different distributions and compositions in the polymer backbone would result in various properties for polymer [11-13]. Therefore, by knowing the nature of catalysts, properties of polymer can be altered.

Several studies comparing different group 4 metallocene structures in ethylene/ α -olefin copolymerization have been reported [14-17]. Nevertheless, the homogeneous catalyst systems based on metallocene require high aluminum-to-transition metal molar ratios and extensive polymer washing, so as to remove residual aluminum. In addition, they are not suitable for industrial applications such as slurry and gas phase polymerization processes. Because most of the existing polymerization plants use these processes with heterogeneous catalyst systems, these soluble catalysts are unsuitable for the production of polyolefins on an industrial scale. To overcome this problem, metallocenes can be immobilized on inert or inorganic carriers such as SiO_2 , Al_2O_3 , TiO_2 and zeolites [18-20]. These carriers have been extensively studied for supported cocatalyst for years. This approach should permit the replacement of conventional Ziegler-Natta catalysts in existing processes. Remarkably, using immobilized metallocenes should result in the formation of uniform polymer particles with narrow size distribution and high bulk density compared to those provided by Ziegler-Natta-supported catalysts [21]. The heterogeneous metallocene system is necessary to produce polymer particle of desired morphology to avoid reactor fouling with finely dispersed swelling of polymers [13].

In many inorganic supports, SiO_2 is perhaps the most attractive support so far [22]. However, the properties of SiO_2 itself may not be completely satisfied for all purposes based on the polymer produced. In addition, due to the support effect, it is found that the catalytic activity of catalysts in heterogeneous system is usually lower than the homogeneous one. Therefore, a modification of the support properties is required. TiO_2 - SiO_2 mixed oxide has been considered to be very attractive as catalysts and supports, which have brought much attention in recent years. It was

reported that $\text{TiO}_2\text{-SiO}_2$ mixed materials have been used as catalysts and supports for various reactions [23]. Such titania-silica materials not only take advantage of both TiO_2 (an n-type semiconductor and an active catalytic support) and SiO_2 (high thermal stability and excellent mechanical strength), but also extend their applications through the generation of new catalytic active sites due to the interaction of TiO_2 with SiO_2 [24].

It is known that the catalytic behaviors depend on polymerization conditions, catalytic compositions, metal dispersion, and types of supports used. In the case of solution and slurry polymerization, the kind of solvent is also one of importance factors which can influence the polymerization behaviors [25]. Indeed, literature data regarding α -olefin homopolymerization reports that the polarity of solvent remarkably affects the catalytic activities [26] and, in some case, also the microstructure of polymer [27-30].

In the previous studies, a unique catalyst called “constrained geometry catalyst” (CGC) using half-sandwich titanocenes, have been found that they can afford to give highly activity and incorporate a large amount of α -olefin in to copolymer [1,31]. It revealed that [*t*-BuNSiMe₂Flu]TiMe₂ complex was employed to polymerize propylene, norbornene and ethylene [32-36]. Several papers reported that [*t*-BuNSiMe₂Flu]TiMe₂ catalyst was suitable for the propylene polymerization in various polymerization conditions due to effect of activators and solvents used. They found that the kind of activators and the polarity of solvents played important roles on the catalytic activities and microstructure of polymer as well [29,30,37,38]. A few papers, however, reported on the copolymerization of ethylene with α -olefins [39,40] and only one that reported the supported system [41].

In this present research, the ethylene/1-octene copolymerization using three supports such as SiO_2 , TiO_2 and $\text{SiO}_2\text{-TiO}_2$ mixed oxide supported-MMAO with titanocene catalyst was investigated and compared with homogeneous system. The supports and catalyst precursors were prepared, characterized and investigated for the effect of supports on the catalyst activity and properties of copolymers. Moreover, the roles of solvent effect were also investigated.

The objective of this investigation was to study and characterize effects of various supports and solvent mediums on the catalyst activity and properties of polymers during ethylene and ethylene/1-octene polymerization with titanocene catalyst. The supports such as SiO₂, TiO₂ and SiO₂-TiO₂ mixed oxide were impregnated with the dMMAO as cocatalyst. These supports and supported-MMAOs (catalyst precursors) were also investigated to make better understanding about polymerization results.

This thesis was divided into five chapters. Chapter I involved an overview of the use of metallocene catalyst for the polyolefin industry. In Chapter II, knowledge and open literature dealing with metallocene catalysis for olefin polymerization were presented. The literature review was accentuated metallocene catalyst system used for polymerization of ethylene and ethylene with α -olefins. The properties and microstructure of polymer were also depended on major parameters, for example, comonomer effect and supports or solvents types. The experimental procedure as well as the instrument and techniques used for characterizing the resulting polymers were described in Chapter III.

In Chapter IV, the results on ethylene and ethylene/1-octene polymerization with the different supports and solvents were presented. Effects of various supports and solvent mediums in ethylene/1-octene, comonomer impact on nature of active site on the catalyst content in the copolymer were included. Effect of system between homopolymer and copolymer causing any changes in the polymer properties was also discussed. The characteristics of the supports and catalyst precursors using X-ray diffraction (XRD), raman spectroscopy, scanning electron microscopy (SEM), energy dispersive X-ray spectrometer (EDX), X-ray photoelectron spectroscopy (XPS), and thermogravimetric analysis (TGA) and obtained polymers using gel permeation chromatography (GPC), differential scanning calorimetry (DSC) and ¹³C nuclear magnetic resonance (¹³C NMR) were also included.

Finally, conclusions of this work and some recommendations for future research work were provided in Chapter V.

CHAPTER II

LITERATURE REVIEWS

2.1 Polyolefin Catalysts

Polyolefins can be produced with free radical initiators, Phillips type catalysts, Ziegler-Natta catalysts and metallocene catalysts. Ziegler-Natta catalysts have been most widely used because of their broad range of application. However, Ziegler-Natta catalysts provide polymers having broad molecular weight distribution (MWD) and uncontrollable polymer microstructure due to multiple active sites formed [8].

Metallocene catalysts show in contrast to Ziegler-Natta systems, only one type of active site (single-site catalysts), which produces polymers with narrow molecular weight distribution and chemical composition distribution. The structural change of metallocene catalysts can possible to control polymer microstructure, comonomer incorporations and stereoregularity [42]. These catalysts brought the way to expand possibilities of new olefin polymerization and good property of the resulting polyolefins [9].

2.1.1 Metallocene Catalysts

One of the greatest challenges in organometallic complex is to synthesize the metallocene complex and apply for new polymerization technology with transition group IV metals. Metallocene complexes are become an important class of polymerization catalyst in the research and industrial area since it have many advantage in polymerization such as [43],

1. The homogeneous nature of catalysts provides the active sites that have the great number of activity in olefin polymerization. Comparison to conventional Ziegler-Natta catalyst or Philips catalyst, it was found that metallocene complex gave the higher activity about 100 times.

2. Metallocene catalysts have ability to control the stereoregularity (isotactic, atactic, syndiotactic and hemitactic polypropylene) of the polymers produced from prochiral olefins, such as propylene

3. According from the narrow molecular weight distribution of polymer about 1-2, we can call metallocene catalyst as single site catalysts.

4. Their potential for producing polyolefin with regularly distributed short and long chain branches in the polymer chain. These parameters determine the properties of new materials for applications i.e. LLDPE and thus generate new markets.

5. Heterogeneous catalyst provide the different active sites than those in solution and can have an enormous effect on catalyst activity and the properties of the produced polyolefins in term of molecular weights, branching and stereospecificity.

2.1.2 Structure of Metallocene Catalysts

Metallocene catalysts are the organometallic coordination compounds in which one or two π -carbocyclic ligands such as cyclopentadienyl ring, substituted cyclopentadienyl ring, or derivative of cyclopentadienyl ring (such as fluorenyl and indenyl etc.) are bonded to central transition metal atom. The cyclopentadienyl ring of metallocene singly bonded to the ring-metal bond is not centered on any one of the five carbon atoms in the ring but equally on all of them [44]. The typical structure of a metallocene catalyst is represented by **Figure 2.1** where M is the group 4B, 5B, or 6B transition metal, normally group 4B (Ti, Zr and Hf); A is an optional bridging atom usually Si or C atom; R is a σ -homoleptic hydrocarbyl such as H, alkyl, or other hydrocarbon groups; and X is chlorine or other halogens from group 7A or an alkyl group. The cyclopentadienyl ligands, halides and σ -homoleptic hydrocarbyl represent the three classes of ligands of the metallocene catalysts and variation of, and/or substitutions within some of these ligands could result in variation of the catalytic activity, polymer stereoregularity, and average molecular mass. In case of metallocene catalyst, which have only one π -carbocyclic ligand with a hetero atom that is attached to the bridging atom.



Figure 2.1 Typical chemical structure of a metallocene catalyst

Compositions and types of metallocene have several varieties. When the two cyclopentadienyl (Cp) rings on either side of the transition metal are unbridged, the metallocene is non-stereorigid and it is characterized by C_{2v} - symmetry. The Cp_2M ($M = \text{metal}$) fragment is bent back with the centroid-metal-centroid angle θ about 140° due to the interaction with the other two σ bonding ligands [45]. When the Cp rings are bridged (two Cp rings arranged in the chiral array and connected together with chemical bonds by a bridging group), the stereorigid metallocene, called ansa-metallocene, could be characterized by either a C_1 , C_2 or C_s symmetry depending upon the substitutions on two Cp rings and the structure of the bridging unit as schematically illustrated [44] in the **Figure 2.2**.

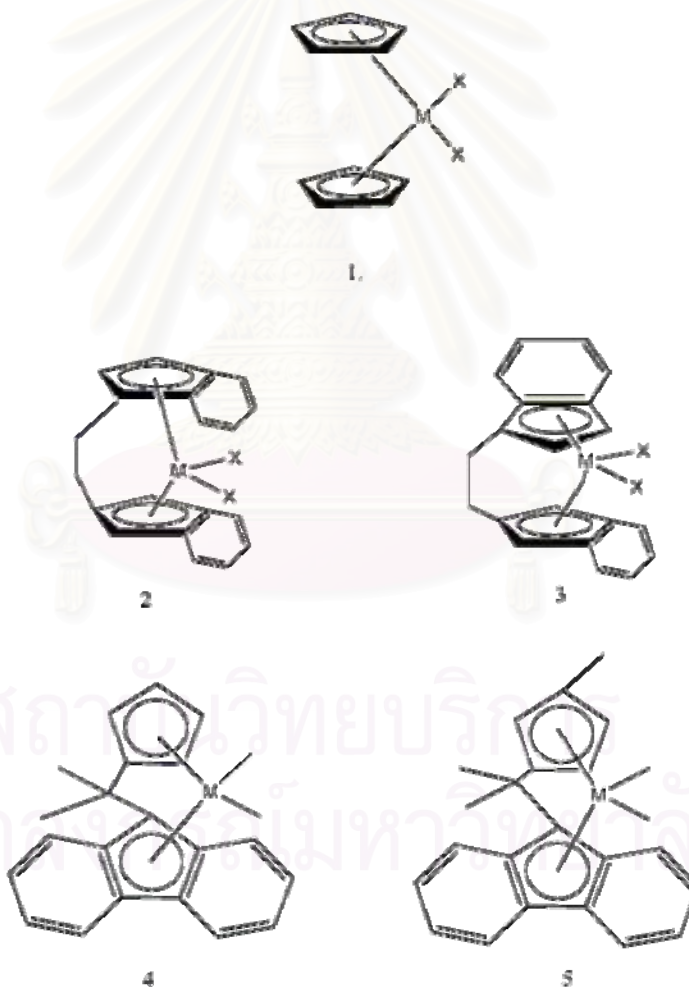


Figure 2.2 Schematic representations of metallocene symmetry (Type 1: C_{2v} -symmetric, Type 2: C_2 -Symmetric, Type 3 and Type 4: C_s -symmetric, Type 5: C_1 -symmetric)

2.1.3 Cocatalysts

Aluminoxane, especially methylaluminoxane (MAO) plays the very important role to activate metallocene catalyst. Before the MAO was discovered, in Ziegler-Natta catalyst alkylaluminumchloride was used to activate Cp_2TiCl_2 but it exhibited the very poor activity. Using of MAO as cocatalyst can promote the productivity of polymerization by several order of magnitude. Otherwise using of MAO, the other aluminoxanes such as ethylaluminoxane (EAO) or isobuthylaluminoxane (iBAO) or modified methylaluminoxane was employed to use as cocatalyst too. (Structure of MAO, EAO, iBAO and MMAO was shown in **Figure 2.3**)

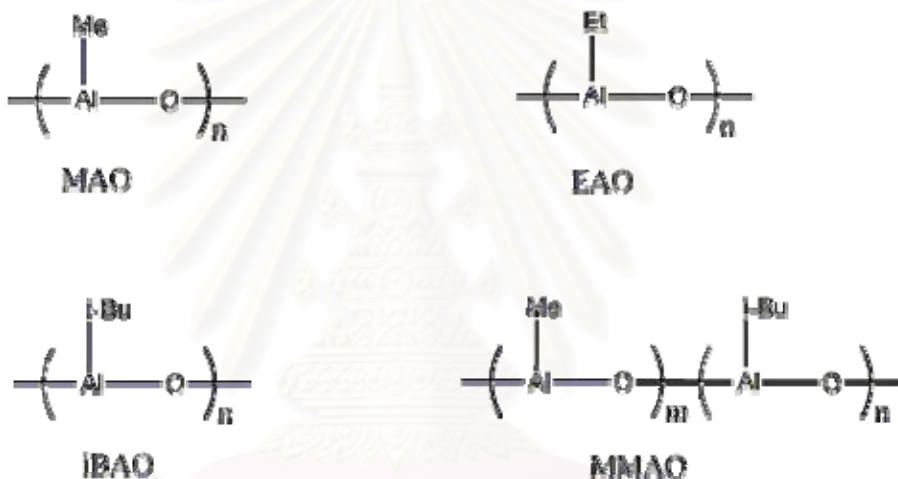
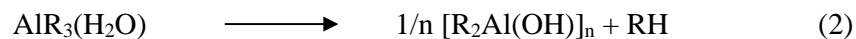


Figure 2.3 Several kinds of MAO

A metallocene catalyst precursor can be activated with organoalumoxanes, especially methylaluminoxane (MAO), which affords highly active catalysts for polymerization ethylene, propylene, and higher α -olefins when combined with group 4 metallocene. MAO is a compound in which aluminum and oxygen atoms are arranged alternately and free valences are saturated by methyl substitutions. It is prepared by carefully controlled partial hydrolysis of trimethylaluminum (TMA) and according to investigations [46-48]. The hydrolysis of AlR_3 ($\text{R} = \text{Me}, \text{Et}, \text{iBu}$) has been shown to proceed via the formation of an alkylaluminum water complex shown in Equation 1 [49], which subsequently eliminates an alkane to form a dialkylaluminum hydroxide complex as shown in Equation 2. This result rapidly associates to give dimers or larger oligomers in solution.



The structure of MAO consists mainly of units of the basic structure $[\text{Al}_4\text{O}_3\text{Me}_6]_4$, which contains four aluminum, three oxygen atoms and six methyl groups. Although very extensive research has been carried out in both academia and industry, the exact composition and structure of MAO are still not entirely clear or well understood.

The proposed structures for MAO in the open literature [50] shown in **Figure 2.4** include: (1) one-dimensional linear chains, (2) cyclic rings, which contain three-coordinate Al centers, (3) two-dimensional structures, and (4) three-dimensional clusters is based on structural similarities with *tert*-butylaluminoxanes, which form isolable and X-ray crystallographically characterizable cage structures (5) [47].

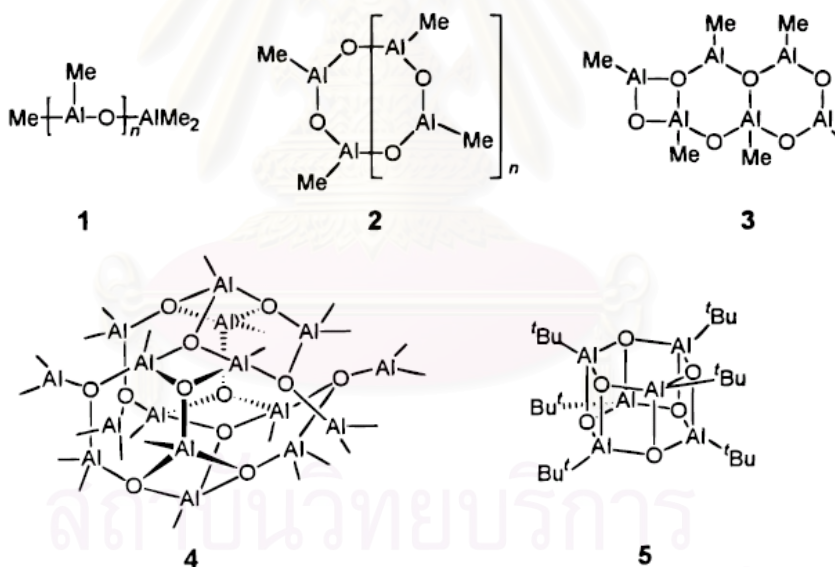
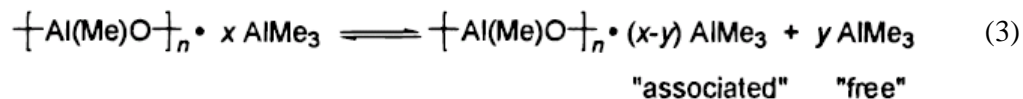


Figure 2.4 The general proposed structure of MAO

Depending on the nature of the hydrated salt (the H_2O source) used for the MAO synthesis and the exact MAO synthetic reaction conditions; MAO-activated metallocenes may exhibit widely differing activities in olefin polymerization. The MAO structure can hardly be elucidated directly because of the multiple equilibria present in MAO solutions, and residual trimethylaluminum in MAO solutions appears

to participate in equilibria that interconvert various MAO oligomers [51]. There are two types of TMA present in typical MAO solutions: “free” TMA and “associated” TMA shown in Equation 3.



Cryoscopy MAO molecular weight decrease after AlMe₃ addition according to a linear relationship, which is caused by disproportionate reactions [52]. However, recent in-situ FTIR spectroscopy investigations do not indicate any obvious reaction between TMA and MAO. Nevertheless, in light of its complicated, unresolved structural features, MAO is usually represented for the sake of simplicity as having linear chain or cyclic ring structures [-Al(Me)-O-]_n, containing three-coordinate aluminum centers [50].

However, conventional MAO has very low solubility in aliphatic solvents as well as poor storage stability in solution. To solve these limits, MAO can be modified. Commercial modified methylaluminoxanes (MMAO), which prepared by controlled hydrolysis of mixture of trimethylaluminum and triisobutylaluminum, exhibit improved solution storage stability and improved solubility in aliphatic solvents and can be produced at lower cost while providing good polymerization efficiency [50].

Recently, the modification by evacuated MAO was studied. Dried methylaluminoxane (MAO) which was free of Me₃Al, was more active than the standard MAO system, resulting in a steady polymerization rate and giving higher M_w polypropylenes. Additive effects of trialkylaluminum on the dried MAO system showed that the polymer yield was increased by the addition of *i*-Bu₃Al and Oct₃Al and decrease by Me₃Al and Et₃Al [37].

Cam and Giannini [53] investigated the role of TMA present in MAO by a direct analysis of Cp₂ZrCl₂/MAO solution in toluene-d₈ using ¹H-NMR. Their observation indicated that TMA might be the major alkylating agent and that MAO acted mainly as a polarization agent. However, in general it is believed that MAO is the key cocatalyst in polymerizations involving metallocene catalysts. The role of MAO included 1) alkylation of metallocene, thus forming catalyst active species, 2)

scavenging impurities, 3) stabilizing the cationic center by ion-pair interaction and 4) preventing bimetallic deactivation of the active species.

Ethylene/ α -olefins copolymers with bimodal CCD were produced with homogeneous Cp_2ZrCl_2 with different cocatalysts such as MAO and mixture of TEA/borate or TIBA/borate [54]. It seemed that the active species generated with different cocatalysts have different activities and produce polymers with different molecular weights.

Hagimoto et al. [55] have investigated the relationship between the supporting effects of MMAO in the living polymerization of propylene, and investigated the additive effect of trialkylaluminiums in the $[\text{ArN}(\text{CH}_2)_3\text{NAr}]\text{TiMe}_2$ metaloxide-supported MMAO systems. It was found that the activity and the molecular weight values in the presence of trialkylaluminiums were slightly smaller than that of the corresponding MMAO/ SiO_2 system due to the induction period. Because of a small amount of trialkylaluminium hindered the initiation reaction.

On the one hand, not only the aluminoxane has effect to the polymerization behavior but the trialkylaluminum has the influence too. Shiono, T. et al. [38] have studied on the effect of trialkylaluminum type to the characteristic of polymerization. For example, the addition of Oct_3Al and Et_3Al increased the propagation rate of living polymerization with $[t\text{-BuNSiMe}_2\text{Flu}]\text{TiMe}_2 / \text{B}(\text{C}_6\text{F}_5)_3$ system at $-50\text{ }^\circ\text{C}$.

2.1.4 Polymerization Mechanism

The mechanisms for olefin polymerization by metallocene-aluminoxane system have been picked up to investigate in several experiment and theoretical study [56-58]. This study has shown that the Cossee mechanism of polymerization is indeed viable for metallocene catalysts. It is also still one of the most generally accepted polymerization mechanism (**Figure 2.5**) [59]. In the cationic metallocene species, the metal atom is coordinated with the π -ligands and alkyl group (growing polymer chain). During polymerization, the monomer coordinates with a highly electrophilic and coordinatively unsaturated cationic complex. It is followed by insertion of a monomer in the metal-carbon bond to produce a polymer chain. The migration of the polymer chain and the formation of the metal-carbon bond occur in concert through a

four center transition state. These results in a new vacant coordination site which was originally occupied by the polymer chain. These processes involving shifting of the growing chain to the position previously occupied by a coordinated monomer continue until termination of polymer chain.

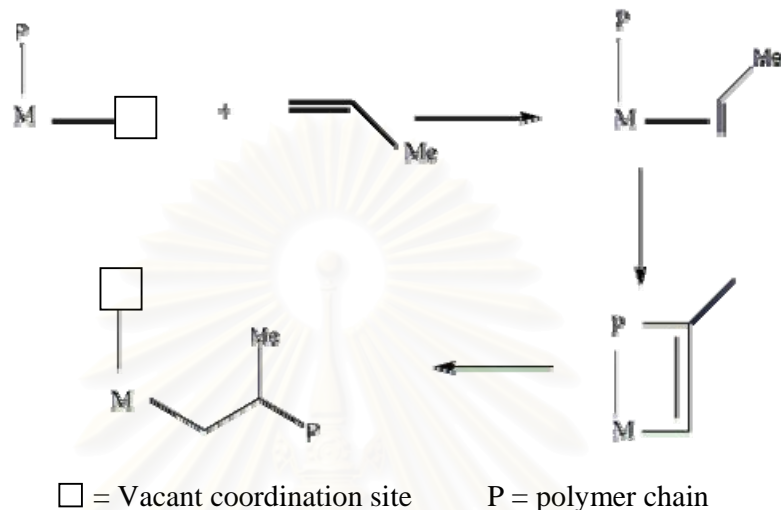


Figure 2.5 Cossee mechanisms for Ziegler-Natta olefin polymerization

2.1.5 Chain Transfer Mechanism

Chain transfer and chain termination reactions can have tremendous influences on the nature of the polymer. In metallocene-catalyzed olefin polymerization, the termination reaction of polymer chain can occur due to many reasons [44] such as chain transfer to β -H elimination, chain transfer to β -Me elimination, chain transfer to aluminum, chain transfer to monomer and chain transfer to hydrogen [60] were demonstrated in **Figure 2.6-2.10** respectively. All of the mechanisms proposed above are dependent on the nature of the metallocene, aluminoxane, and the polymerization conditions. Resconi et al. [61] studied the contribution of various chain transfer processes in the propylene polymerization reaction due to the different metallocenes and reaction conditions. They reported that metallocene catalyst and activator used in each system have the different characteristic of behavior in polymerization. The chain transfer reaction depended on the metallocene catalyst, aluminoxane and polymerization condition employed to the system in propylene polymerization.

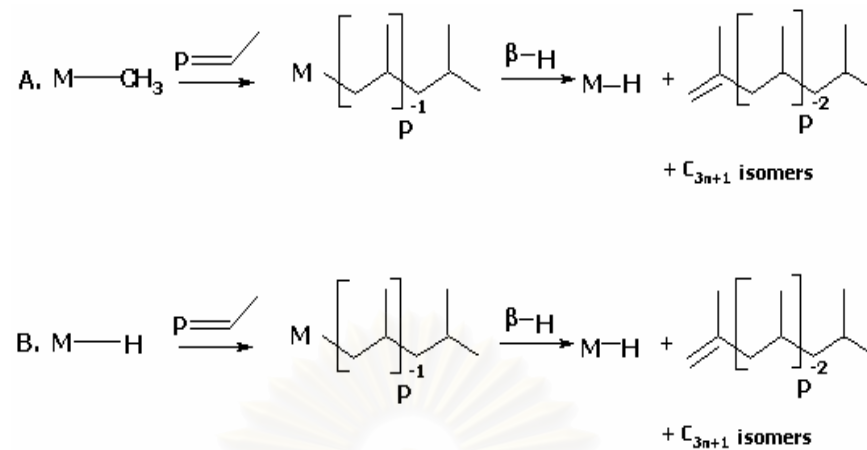


Figure 2.6 Chain transfer via β -H elimination

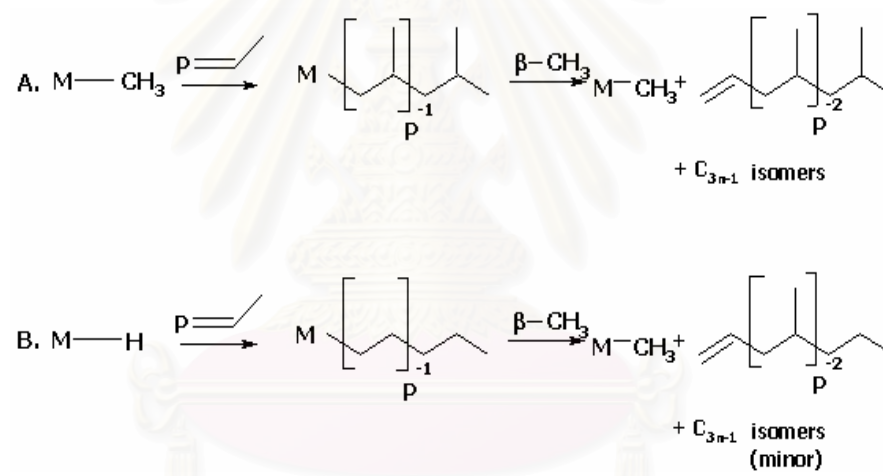


Figure 2.7 Chain transfer via β -CH₃ elimination

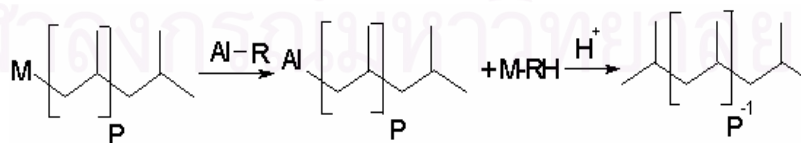


Figure 2.8 Chain transfer to aluminum

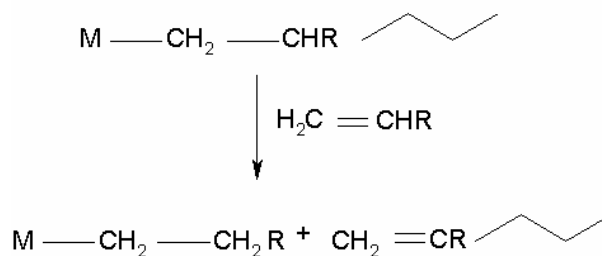


Figure 2.9 Chain transfer to monomer

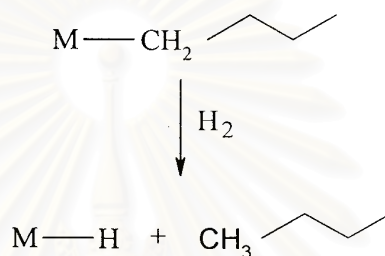
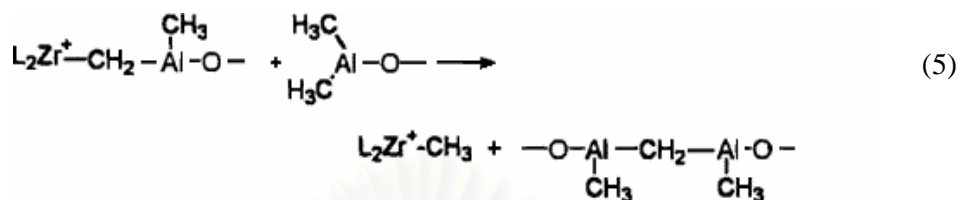
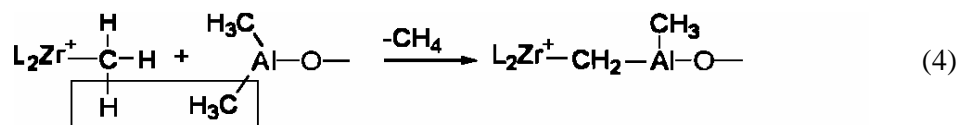


Figure 2.10 Chain transfer to hydrogen

2.1.6 Catalyst Deactivation

Some metallocene catalyst systems exhibit the gradually decreased rate of polymerization due to the catalyst deactivation of active species with metallocene/MAO system. An important deactivation process for MAO-activated catalytic systems is α -hydrogen transfer, which leads to the production of methane [62]. The methane production is much more rapid with MAO than with less Lewis acidic TMA. The deactivation of the metallocenium alkyl + MAO might be attributed to the formation of inactive species with Zr-CH₂-Al or Zr-CH₂-Zr structures in Equation 4. Although these inactive species can be reactivated by a transmetallation reaction with MAO and lost Al-CH₂-Al structure at excess MAO, forming L₂Zr(CH₃)⁺ and Al-CH₂-Al structures in Equation 5.



Kaminsky et al. [63] proposed one mechanism of deactivation of active species with a M-CH₂-Al (**Figure 2.11**). However these inactive species can be reactivated by transmetalation reaction with MAO and lost Al-CH₂-Al structure at high concentration of anion MAO as MAO is consumed during the polymerization by side reactions, by impurity, by chain transfer and by recreating active sites. The regeneration of active sites will decrease at lower concentration of MAO but it cannot compensate to the loss of active site in polymerization process, thus a polymerization rate will gradually decrease.

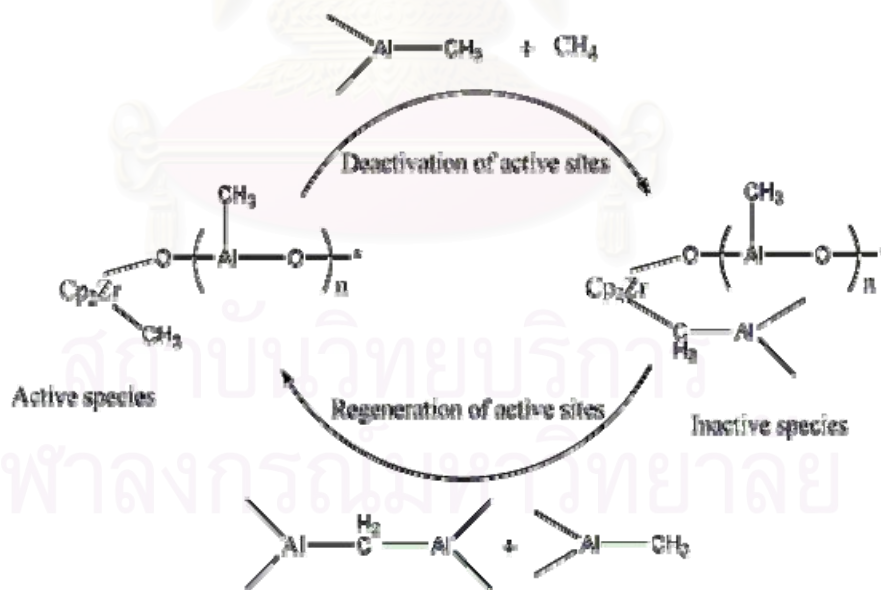


Figure 2.11 Mechanism showing the deactivation of active center for Cp₂ZrCl₂-MAO catalyst system

Moreover, Mulhaupt et al. [64] proposed another type of reaction of deactivation of metallocene catalyst, which is fast and second-order relative to the active site concentration. In this model the deactivation rate was faster than the activation rate of active species in second order relatively in the $\text{Cp}_2\text{ZrCl}_2/\text{MAO}$ system. Deactivations of active species occur after the active species was fully activated. The Mulhaupt deactivation model was shown in **Figure 2.12**.

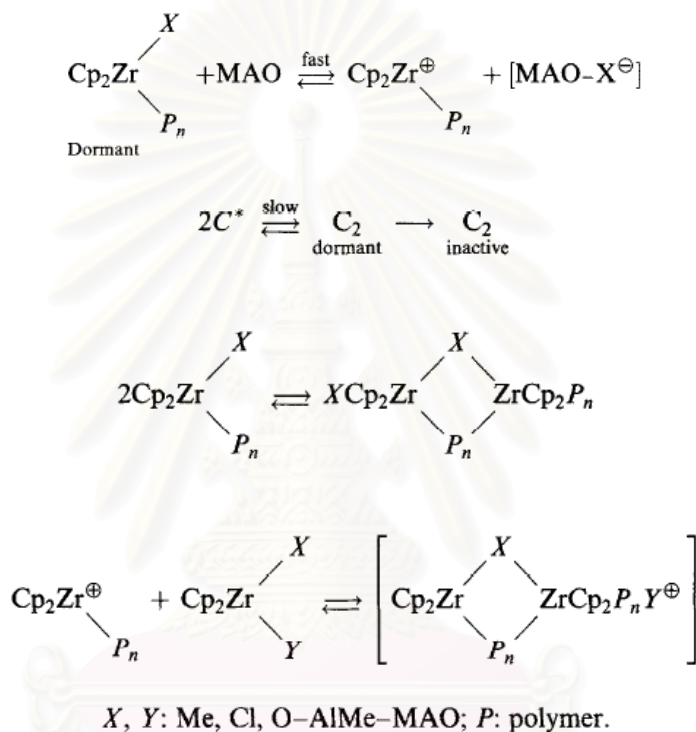


Figure 2.12 Mechanism of reversible second-order deactivation

2.2 Heterogeneous System

In polyolefin production is currently achieved by slurry- and gas-phase polymerization processes, which require the polymerization catalysts to be anchored on solid supports. Although supported catalysts (heterogeneous) are generally less active than non-supported catalysts (homogeneous), they can be practically used for the existing gas phase and slurry polymerization processes. Without using a heterogeneous system, high bulk density and narrow size distribution of polymer particles cannot be achieved [50]. The advantages of supported catalytic include improved polymer morphology, avoiding reactor fouling, lower Al/metal mole ratios

required to obtain the maximum activities in some cases the elimination of the use of MAO, and improved stability of the catalyst due to much slower deactivation by bimolecular catalyst interactions. Therefore, developing heterogeneous metallocene catalysts, that still have all the advantages of homogeneous systems, became one of the main research objectives of applied metallocene catalysis.

In order to heterogenize metallocenes, the most commonly employ an innocuous carrier for catalysts such as silica (SiO_2), alumina (Al_2O_3) and magnesium chloride (MgCl_2). And many supporting materials have been on the research are zeolite, nanocomposite material or other inorganic or organic support.

2.2.1 Supported Metallocene Catalyst Methods

In the case of carriers like silica or other inorganic compounds with OH group on the surface, the resulting catalyst displayed very poor activities even combined with MAO. The reaction of metallocene complexes with the Si-OH groups might cause the decomposition of active species. Such decomposition could be suppressed by fixing MAO on the silica surface and then reacting with metallocenes. Therefore, silica must be pretreated before the interaction with metallocene, to reduce the OH concentration and to prepare an adequate surface for metallocene adsorption and reaction in a non-deactivating way [65].

Different methods for the heterogenization of metallocene can be divided into five methods according to Kaminsky and Strubel [66]. These methods produce catalysts with distinct activities, comonomer reactivity ratios, and stereospecificities. The supporting methods are illustrated in **Figure 2.13**.

(1) Initial adsorption of MAO on the support with subsequent addition of metallocenes in a second step (indirect heterogenization) is the used method in this study.

(2) A variation of method one is the heterogenization of a prereacted solution of metallocene alkyl with $[\text{C}(\text{C}_6\text{H}_5)_3][\text{B}(\text{C}_6\text{F}_5)_4]$ on a SiO_2/MAO carrier.

(3) A mixture of the metallocene and MAO is adsorbed on the support. In this case, the prealkylation time plays an important role.

(4) Another possibility is adsorption and immobilization of the metallocene on the support and then, after addition of MAO (covalent bonding on the

support), the use of this catalytic system in the polymerization process; this results in totally different polymerization behavior than in the analogous homogeneous system.

(5) The metallocene can be bonded directly to the support by a spacer and an anchor group (direct heterogenization).

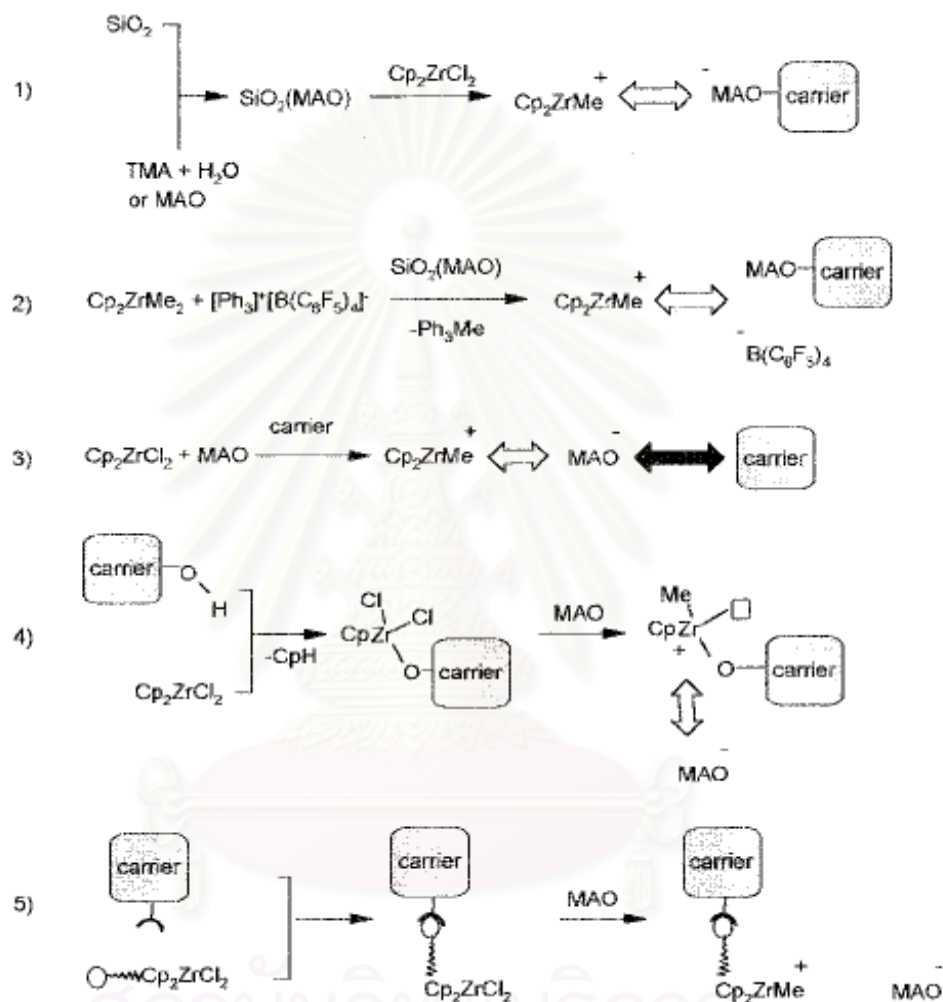


Figure 2.13 Supporting methods of metallocene catalyst

The polymers produced with catalysts supported according to methods (1) to (3) in **Figure 2.13** are similar to the polymers obtained with the homogeneous system. MAO is fixed on the silica carrier by covalent bonding; the nature of fixation of the metallocene is still in discussion, probably the bonding is of ionic nature. However, the most promising method of supporting is indirect heterogenization (1) as the chemical nature of the metallocene is changed. The polymers obtained by the

method of indirect heterogenization are very similar to those obtained by the homogeneous system. Each metallocene on the support forms an active center and the starting point for the growth of a polymer chain. As the active sites on the surface of each catalyst grain are identical, all chains grow uniformly resulting in polymers narrow molar mass distribution [1].

2.2.2 Effect of Supported Methods

Collins et al. [67] reported that $\text{Et}(\text{Ind})_2\text{ZrCl}_2$, when supported on partially dehydrated silica, reacted with surface hydroxyl groups during adsorption to form inactive catalyst precursors and free ligands (**Figure 2.14**). Therefore, the activity is lower compared to the case of using dehydrated silica. For the case of alumina, the activity of catalyst supported on dehydrated alumina is lower than the one supported on partially dehydrated alumina. The high Lewis acidity of aluminum sites on dehydrated alumina facilitates the formation of Al-Cl bonds and Zr-O bonded species when the metallocene compound is adsorbed on these sites. However, the metal sites in this case remain inactive even after MAO addition.

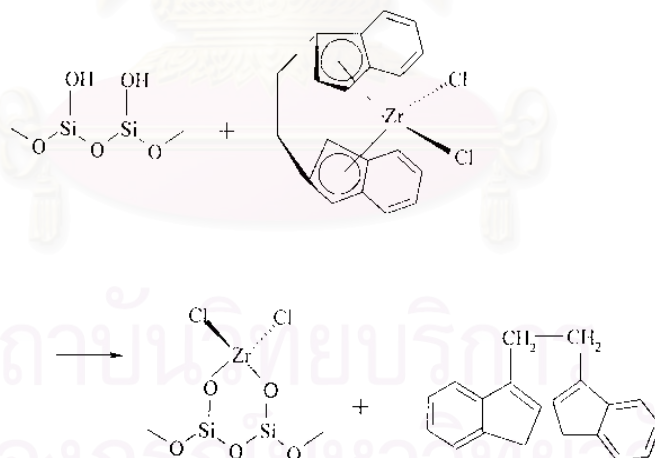


Figure 2.14 Structure of $\text{Et}(\text{Ind})_2\text{ZrCl}_2$ supported on silica

When silica is pretreated with MAO, the supporting mechanism is different. The zirconocene is complexed to MAO supported on silica, which will

make the catalyst similarly to a homogeneous system. The polymers produced in this way have lower molecular weights.

Hiatky and Upton [68] reported that supporting of the aluminum-alkyl free catalysts can form 2 complexes as shown in **Figure 2.15**, (a) deactivation through coordination of Lewis- basic surface oxides to the electrophilic metal center or (b) reaction of the ionic complex with residual surface hydroxyl groups.

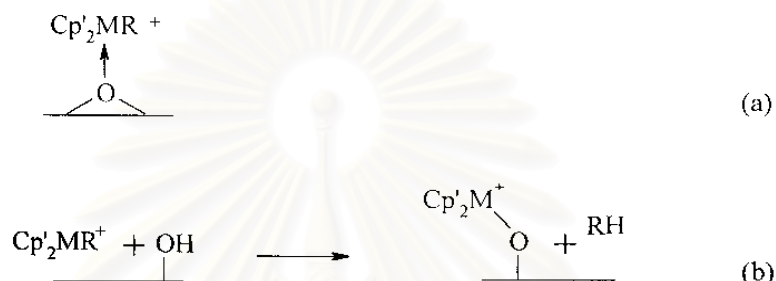


Figure 2.15 Effect of surface hydroxyl groups on ionic metallocene catalysts

However, highly active supported ionic metallocene catalysts for olefin polymerization can be prepared by pretreating the support with scavenger. It is assumed that pretreatment of the support with a scavenger serves to activate the support and compatibilize it with the ionic metallocene complex.

Lee et al. [69] used TMA pretreated-silica as the support for metallocene catalysts. The activity of supported catalysts showed dependency to H_2O content in silica, H_2O/TMA ratio, metallocene, and cocatalyst. The supported catalyst was also able to polymerize ethylene in the absence of MAO when common alkyl aluminum was used as the cocatalyst.

Harrison et al. [70] compared a variety of silica and alumina supports with different degrees of surface hydroxylation as the supports. It was shown that as the concentration of OH groups on the surface of the support increased, more MAO could be impregnated and thus catalyst with more metallocene content could be produced. The most obvious benefit of supported catalyst with more metallocene was increased activities compared to catalysts with lower concentration of surface hydroxyl groups (increased activities both in $kg\ PE/mol\ Zr/hr$ and $kg\ PE/g\ support/h$). However, at high polymerization temperatures, leaching of catalyst from the support was observed.

In lower polymerization temperatures, leaching was less significant, however, the morphology and bulk density of the polymer formed were still unsuitable for use in gas-phase polymerization.

Hagimoto et al. [55] investigated the relationship between the supporting effects of MMAO and compared the effects of supported MMAOs using alumina (Al_2O_3), magnesia (MgO) and silica gel (SiO_2) in propylene polymerization with $[\text{ArN}(\text{CH}_2)_3\text{NAr}]\text{TiMe}_2$. They found that propagation rate (k_p) value and the MWD value strongly depended on the metal oxide employed as a support. (k_p : $\text{SiO}_2 > \text{Al}_2\text{O}_3 > \text{MgO} \approx \text{homogeneous}$, MWD: $\text{MgO} > \text{Al}_2\text{O}_3 > \text{SiO}_2 > \text{homogeneous}$)

Soga et al. [71] described a method to support zirconocenes more rigidly on SiO_2 . The supporting steps are as follows: 1) Silica was treated with SiCl_4 to substitute the OH groups with chlorine atoms. 2) The resulting silica was filtered and washed with tetrahydrofuran (THF). 3) The solid was re-suspended in THF and a lithium salt of indene, dissolved in THF, was added drop-wise. 4) The resulting solid was filtered and washed again with THF. And to re-suspended solid in THF, $\text{ZrCl}_4 \cdot 2\text{THF}$ dissolved in THF was added. The final solid part was separated by filtration, washed with THF and diethyl ether, and dried under vacuum. The supported catalyst produced in this way showed higher isospecificity than the corresponding homogenous system for propylene polymerization. MAO or ordinary alkylaluminums were used as cocatalysts. The yield was higher when MAO was used as the cocatalyst, but the molecular weight of the polypropylene was half of the molecular weight obtained when TIBA was used as the cocatalyst (3.4×10^5 g/mol and 7.2×10^5 g/mol, respectively). **Figure 2.16** shows the structure of the silica supported metallocenes.

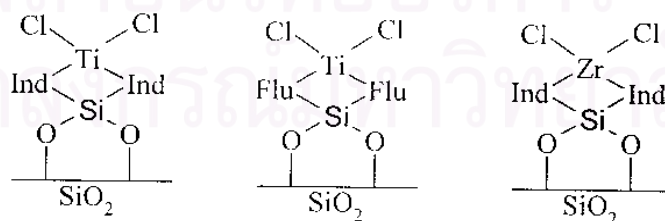


Figure 2.16 Structure of some silica supported metallocene catalysts

Liskola et al. [72] treated the surface of partially dehydroxylated silica with a silane coupling agents, $\text{Cp}(\text{CH}_2)_3\text{Si}(\text{OCH}_2\text{CH}_3)_3$, and then immobilized CpZrCl_3 onto cyclopentadienyl surface formed on the silica to obtain a highly active catalyst (**Figure 2.17**) for ethylene polymerization in the presence of MAO. Depending on the calcination temperature and the modification methods, the catalysts show different activities and produced polymers with different molecular weights. In general, when compared to homogeneous Cp_2ZrCl_2 systems, all the supported catalysts showed lower activities, but the polymers produced had higher molecular weights. In this study, when compared to homogeneous Cp_2ZrCl_2 systems, the activities of the supported catalysts were similar but molecular weights of polymer produced were lower and depended on the silica surface modification method used. The polydispersity index of the polymers ranged from 2.2 to 2.8.

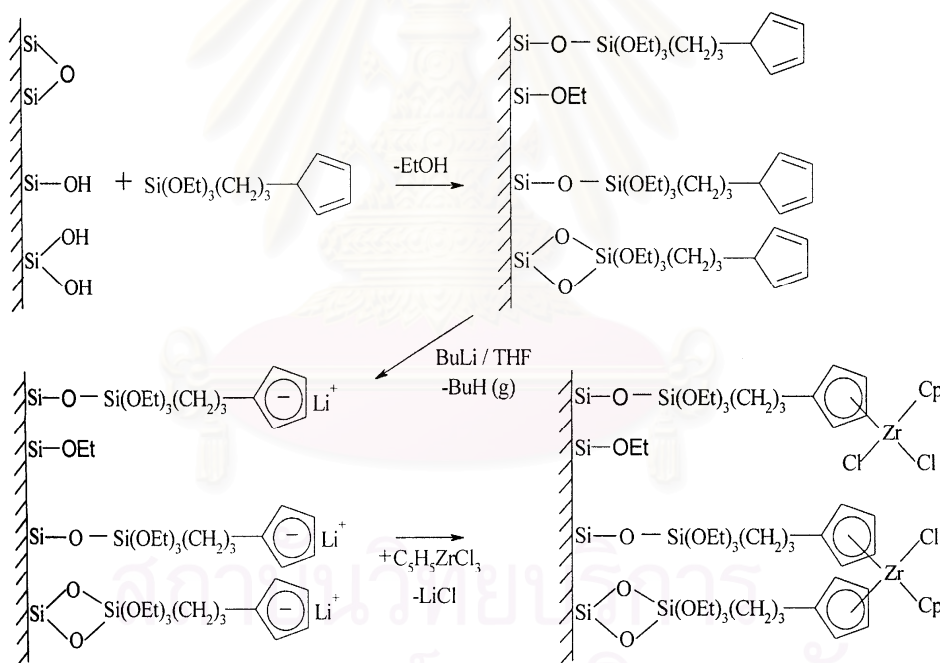


Figure 2.17 Modification of silica with $\text{Cp}(\text{CH}_2)_3\text{Si}(\text{OCH}_2\text{CH}_3)_3$ and preparation of supported metallocene catalysts

Lee et al. [73] used spacer molecules in supporting metallocene catalysts onto silica to eliminate the steric hindrance near the active site caused by the silica surface (**Figure 2.18**). By distancing the active site from the silica surface, higher

catalytic activities but lower polymer molecular weights were obtained in comparison with analogous silica-supported catalysts without spacer between silica and CpIndZrCl_2

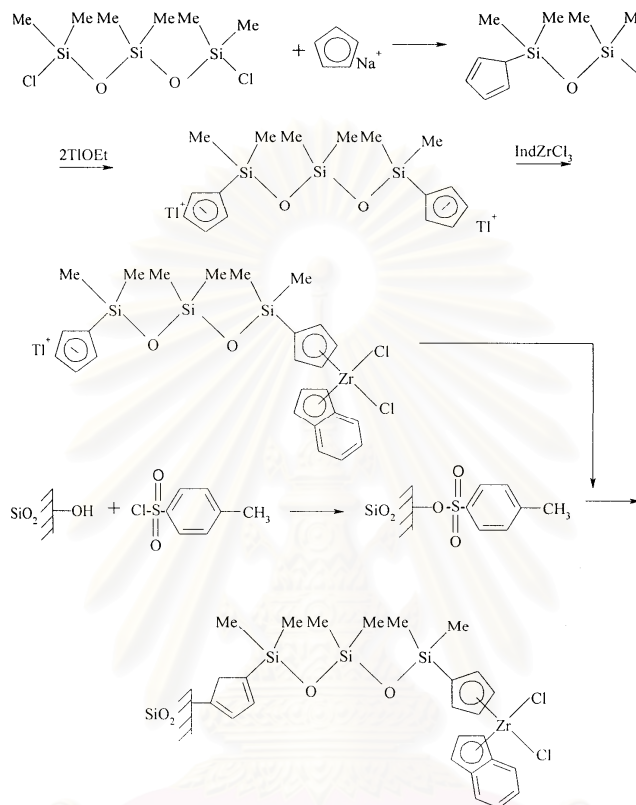


Figure 2.18 Mechanism for supporting metallocene catalysts on silica using spacer molecules

2.3 The Parameters Affecting Catalyst Activity and Polymer Characteristic

In general, the catalyst activity and the characteristic of polymer such as, molecular weight, molecular weight distribution, stereoregularity, dyad distribution, triad distribution and monomer insertion depend on the polymerization parameters. The major parameters in this experiment can be classified in three categories: (1) comonomer, (2) supported types, and (3) solvent medium in experiment.

2.3.1 Comonomer Effect

The enhancement of the rate in copolymerization of ethylene with α -olefins has been observed in both heterogeneous and homogeneous catalytic systems. Introducing small amounts of α -olefins, such as propylene and 1-hexene, may increase the activity by 50-100% in ethylene polymerization with $\text{Cp}_2\text{ZrCl}_2/\text{MAO}$ catalyst [59]. The comonomer can be affected the overall crystallinity, melting point, softening range, transparency and also structural, thermochemical, and rheological properties of the formed polymer. Copolymers can also be used to enhance mechanical properties by improving the miscibility in polymer blending [74].

This comonomer effect is sometimes linked to the reduction of diffusion limitations by producing a lower crystallinity polymer or to the activation of catalytic sites by the comonomer. The polymer molecular weight often decreases with comonomer addition, possibly because of a transfer to comonomer reactions. Heterogeneous polymerization tends to be less sensitive to changes in the aluminum/transition metal ratio. Chain transfer to aluminum is also favored at high aluminum concentrations. This increase in chain transfer would presumably produce a lower molecular weight polymer. In addition, some researchers observed the decrease, and some observed no change in the molecular weight with increasing aluminum concentration [75].

Copolymer based on ethylene with different incorporation of 1-hexene, 1-octene, and 1-decene were investigated by Quijada et al. [24]. The type and the concentration of the comonomer in the feed do not have a strong influence on the catalytic activity of the system, but the presence of the comonomer increases the activity compared with that in the absence of it. From ^{13}C -NMR it was found that the size of the lateral chain influences the percentage of comonomer incorporated, 1-hexene being the highest one incorporated. The molecular weight of the copolymers obtained was found to be dependent on the comonomer concentration in the feed, showing that there is a transfer reaction with the comonomer. The polydispersity (M_w/M_n) of the copolymers is rather narrow and dependent on the concentration of the comonomer incorporation.

In addition, Soares et al. [76] studied copolymerization of ethylene and 1-hexene with an in-situ supported metallocene catalysts. Copolymer was produced

with alkylaluminum activator and effect on MWD and SCBD was examined. They found that TMA exhibited the highest activity while TEA and TIBA had significantly lower activities. Molecular weight distributions of copolymers produced by using the different activator types were unimodal and narrow, however, short chain branching distributions were very different. Each activator exhibited unique comonomer incorporation characteristics that can produce bimodal SCBD with the use of a single activator. They used individual and mixed activator system for controlling the SCBDs of the resulting copolymers while maintaining narrow MWDs.

The ethylene polymerization rate of the copolymerization reaction with the catalyst system $\text{SiO}_2/\text{MAO}/\text{rac-Me}_2\text{Si} [2\text{-Me-4-Ph-Ind}]_2\text{ZrCl}_2$ was studied by Fink et al. [77]. The temperature was varied from 40 °C to 57 °C. Small amount of hexene in the reaction solution increased the polymerization rate. The extent of the "comonomer effect" depended on the polymerization temperature. At 57 °C the maximum activity of the ethylene/hexene copolymerization was 8 times higher than the homopolymerization under the same conditions. At 40 °C the highest reaction rate for the copolymerization is only 5 times higher than that for the ethylene homopolymerization. For the polymer properties of the ethylene/ α -olefin copolymerization, the molecular weights of the polymers decreased with increasing comonomer incorporation. Ethylene/hexene copolymers produced by a metallocene catalyst also have the same melting point and glass transition temperature.

Series of ethylene copolymerization with 1-hexene or 1-hexadecene over four different siloxy-substituted ansa-metallocene/methylaluminoxane (MAO) catalyst systems were studied by Seppala et al. [78]. Metallocene catalysts $\text{rac-Et}[2\text{-}(t\text{-BuMe}_2\text{SiO})\text{Ind}]_2\text{ZrCl}_2$ (1), $\text{rac-Et}[1\text{-}(t\text{-BuMe}_2\text{SiO})\text{Ind}]_2\text{ZrCl}_2$ (2), $\text{rac-Et}[2\text{-}(i\text{-Pr}_3\text{SiO})\text{Ind}]_2\text{ZrCl}_2$ (3) and $\text{rac-Et}[1\text{-}(i\text{-Pr}_3\text{SiO})\text{Ind}]_2\text{ZrCl}_2$ (4) were used. The effects of minor changes in the catalyst structure, more precisely changes in the ligand substitution pattern were studied. They found that series of polymerization with siloxy-substituted bis(indenyl) ansa-metallocene are highly active catalyst precursors for ethylene- α -olefins copolymerizations. The comonomer response of all four catalyst precursors was good. Under the same conditions the order of copolymerization ability of the catalyst was $\text{rac-Et}[2\text{-}(i\text{-Pr}_3\text{SiO})\text{Ind}]_2\text{ZrCl}_2 > \text{rac-Et}[2\text{-}(t\text{-BuMe}_2\text{SiO})\text{Ind}]_2\text{ZrCl}_2$ and $\text{rac-Et}[1\text{-}(i\text{-Pr}_3\text{SiO})\text{Ind}]_2\text{ZrCl}_2 > \text{rac-Et}[1\text{-}(t\text{-BuMe}_2\text{SiO})\text{Ind}]_2\text{ZrCl}_2$. These catalysts are able to produce high molecular weight copolymers.

2.3.2 Supporting Effect

The major advantage of supported catalytic system is the desired polymer morphology and avoiding reactor fouling with finely dispersed swelling polymers. In the contrary, this system still has several disadvantages too. The catalytic activities for supported metallocene are usually lower than that of non-supported systems due to the formation of inactive species between catalyst and support. Moreover, formation of different active species, deactivation of catalyst during supporting procedure and mass transfer resistance may contribute to decreased catalyst activity [62]. The nature of the active sites affects the polymer morphology, catalyst stability and activity, and the characteristics of the polymer produced. However, structure and chemistry of the active sites in supported catalysts are not clearly understood.

Steinmetz et al. [79] examined the particle growth of polypropylene made with a supported metallocene catalyst using scanning electron microscopy (SEM). They noticed formation of a polymer layer only on the outer surface of catalyst particles during the initial induction period. As the polymerization continued, the whole particle was filled with polymer. Particle fragmentation pattern depended on the type of supported metallocene.

Soga and Kaminaka [80] compared copolymerizations (ethylene/propylene, ethylene/1-hexene, and propylene/1-hexene) with $\text{Et}(\text{H}_4\text{Ind})_2\text{ZrCl}_2$ supported on SiO_2 , Al_2O_3 or MgCl_2 . Broadness of MWD was found to be related to the combination of support types and types of monomers. The effect of silica and magnesium supports on copolymerization characteristics was also investigated by Nowlin et al. [81]. Their results indicated that comonomer incorporation was significantly affected by the way that support was treated based on the reactivity ratio estimation calculated with simplified Finemann Ross method. However, it should be noted that Finemann Ross method could be misleading due to linear estimation of nonlinear system.

Marques et al. [82] investigated copolymerization of ethylene and 1-octene by using the homogeneous catalyst system based on $\text{Et}(\text{Flu})_2\text{ZrCl}_2/\text{MAO}$. A study was performed to compare this system with that of $\text{Cp}_2\text{ZrCl}_2/\text{MAO}$. The influence of different support materials for the Cp_2ZrCl_2 was also evaluated, using silica, MgCl_2 , and the zeolite sodic mordenite NaM. The copolymer produced by the $\text{Et}(\text{Ind})_2\text{ZrCl}_2/\text{MAO}$ system showed higher molecular weight and narrower molecular

weight distribution, compared with that produced by $\text{Cp}_2\text{ZrCl}_2/\text{MAO}$ system. Because of the extremely congested environment of the fluorenyl rings surrounding the transition metal, which hinders the beta hydrogen interaction, and therefore, the chain transference. Moreover, the most active catalyst was the one supported on SiO_2 , whereas the zeolite sodic mordenite support resulted in a catalyst that produced copolymer with higher molecular weight and narrower molecular weight distribution. Both homogeneous catalytic systems showed the comonomer effect, considering that a significant increase was observed in the activity with the addition of a larger comonomer in the reaction medium.

The effect of different catalyst support treatments in the 1-hexene/ethylene copolymerization with supported metallocene catalyst was investigated by Soares et al. [83]. The catalysts in the study were supported catalysts containing SiO_2 , commercial MAO supported on silica (SMAO) and MAO pretreated silica (MAO/silica) with Cp_2HfCl_2 , $\text{Et}(\text{Ind})_2\text{HfCl}_2$, Cp_2ZrCl_2 and $\text{Et}(\text{Ind})_2\text{ZrCl}_2$. All the investigated supported catalysts showed good activities for the ethylene polymerization (400-3000 kg polymer/mol metal.h). Non-bridged catalysts tend to produce polymers with higher molecular weight when supported on to SMAO and narrow polydispersity. The polymer produced with Cp_2HfCl_2 supported on silica has only a single low crystallinity peak. On the other hand, Cp_2HfCl_2 supported on SMAO and MAO/silica produced ethylene/1-hexene copolymers having bimodal CCDs. For the case of Cp_2ZrCl_2 and $\text{Et}(\text{Ind})_2\text{ZrCl}_2$, only unimodal CCDs were obtained. It seems that silica-MAO-metallocene and silica-metallocene site differ slightly in their ability to incorporate comonomer into the growing polymer chain, but not enough to form bimodals CCDs.

Looveren et al. [84] studied methylalumoxane (MAO)-MCM-41 as support in the co-oligomerization of ethene and propene with $[\text{C}_2\text{H}_4(\text{Ind})_2\text{Zr}(\text{CH}_3)_2]$. They were found that the MAO-MCM-41 was catalytically more active than the corresponding silica-based MAO derivative or the homogeneous system.

Jongsomjit et al. [85] were investigated role of titania in $\text{TiO}_2\text{-SiO}_2$ mixed oxides-supported metallocene catalyst during ethylene/1-octene copolymerization. This study showed enhanced activities of ethylene/1-octene copolymerization via $\text{TiO}_2\text{-SiO}_2$ mixed oxides-supported MAO with a zirconocene catalyst. It was proposed that titania was decorated on silica surface and acted as a spacer to anchor

MAO to the silica support resulting in less steric hindrance and less interaction on the support surface.

2.3.3 Solvent Medium Effect

Olefins polymerization in slurry phase is important to accompany with the solvent medium. Each kind of solvent has own characteristic, such as polarity, dielectric constant or molecular structure, etc. Solvent affects catalyst activities in two ways: (1) changing the monomer concentration since solubility of monomer depends on solvent; and (2) the solvation effect in the formation of active centers and the polymerization processes [59]. When toluene was used as solvent in ethylene polymerization with CpZrCl₂/MAO catalyst, all of the Zr formed active centers and the propagation rate constant k_p , was 1700 (mol.s)⁻¹ at $T_p = 30$ °C, [Al]/[Zr] = 500 and [C₂H₄] = 0.12 M. While using *n*-decane as solvent under the same polymerization conditions except [C₂H₄] = 0.092 M, only 60% of Zr became catalytically active and $k_p = 300$ (mol.s)⁻¹ and the activity dropped to one-tenth of that in toluene.

Forlini et al. [28,86] have reported the effect of solvent medium to the propylene/1-hexene polymerization with ethylene-bis-(indenyl)zirconium dichloride /MAO system. According to this study, the dielectric constant value of the solvent medium had large effect to the productivity of polymerization. On the other hand polymer compositions are similar. Evidently, activity and selectivity versus the more hindered comonomer are governed by the different factors: the solvent polarity, which as the enormous effect on activity has in fact the negligible effect on comonomer compositions.

The exceptional activity improvement due to the polar solvent is well known, which was accounted for by the fact that the increase of the dielectric constant should enhance the ionic dissociation. The shift of the equilibrium reaction versus the ionic solvent separated active species leads to a wider active center population and explains the high activity observed.

However, the solvent polarity also has the nucleophilic nature of solvent which could compete more with the α -olefins than with propylene, in the coordinate to the active site, due to steric reason.

Nishii et al. [29,30] have investigated on the solvent effect to the stereospecificity in propylene polymerization by the [*t*-BuNSiMe₂Flu]TiMe₂-based catalyst systems with dried-aluminoxane as cocatalyst at 0 °C. This study exhibited that if heptane was chosen to be a solvent medium, the obtain polypropylene gave the syndiotactic polypropylene. On the contrary, chlorobenzene as polymerization medium gave the atactic polypropylene. Furthermore, either heptane or chlorobenzene produces the living nature of polymerization. Thus, block syndiotactic-atactic polypropylene could be produced from this system.

Intaragamjon et al. [39] were investigated on the solvent effects on the catalytic behaviors of [*t*-BuNSiMe₂Flu]TiMe₂ complex during ethylene/1-hexene (EH) copolymerization. At 70 °C, it was found that with using toluene as the polymerization medium, activity was the highest followed by with heptane and chlorobenzene. No activity was observed when dichloromethane was employed. It revealed that activities of polymerization strongly depended on the solvent medium used regarding to its dielectric constant value (ϵ).

According to these researches, the monomer insertion behaviors depend on the solvent polarity including the dielectric constant value.



สถาบันวิทยบริการ
จุฬาลงกรณ์มหาวิทยาลัย

CHAPTER III

EXPERIMENTAL

3.1 Objectives of the Thesis

1. To investigate the roles of SiO_2 , $\text{SiO}_2\text{-TiO}_2$ and TiO_2 supports in homogeneous and heterogeneous titanocene system on ethylene polymerization and ethylene/1-octene copolymerization behaviors.

2. To study the influence of solvents in homogeneous and heterogeneous titanocene system on the catalytic activity and polymer properties during ethylene based polymerization and copolymerization.

3.2 Scopes of the Thesis

1. Preparation of supports such as SiO_2 , $\text{SiO}_2\text{-TiO}_2$ and TiO_2 by impregnation with the dried modified methylaluminoxane (dMMAO).

2. Study and characterization for the effects of supports with titanocene catalyst on catalytic and polymer properties during ethylene and ethylene/1-octene polymerization.

3. Study and characterization for the effects of solvent mediums with titanocene catalyst on catalytic and polymer properties during ethylene and ethylene/1-octene polymerization.

3.3 Research Methodology

Research Methodology of flow diagram is show in **Figure 3.1**.

All reactions were conducted under argon atmosphere using Schlenk techniques and glove box.

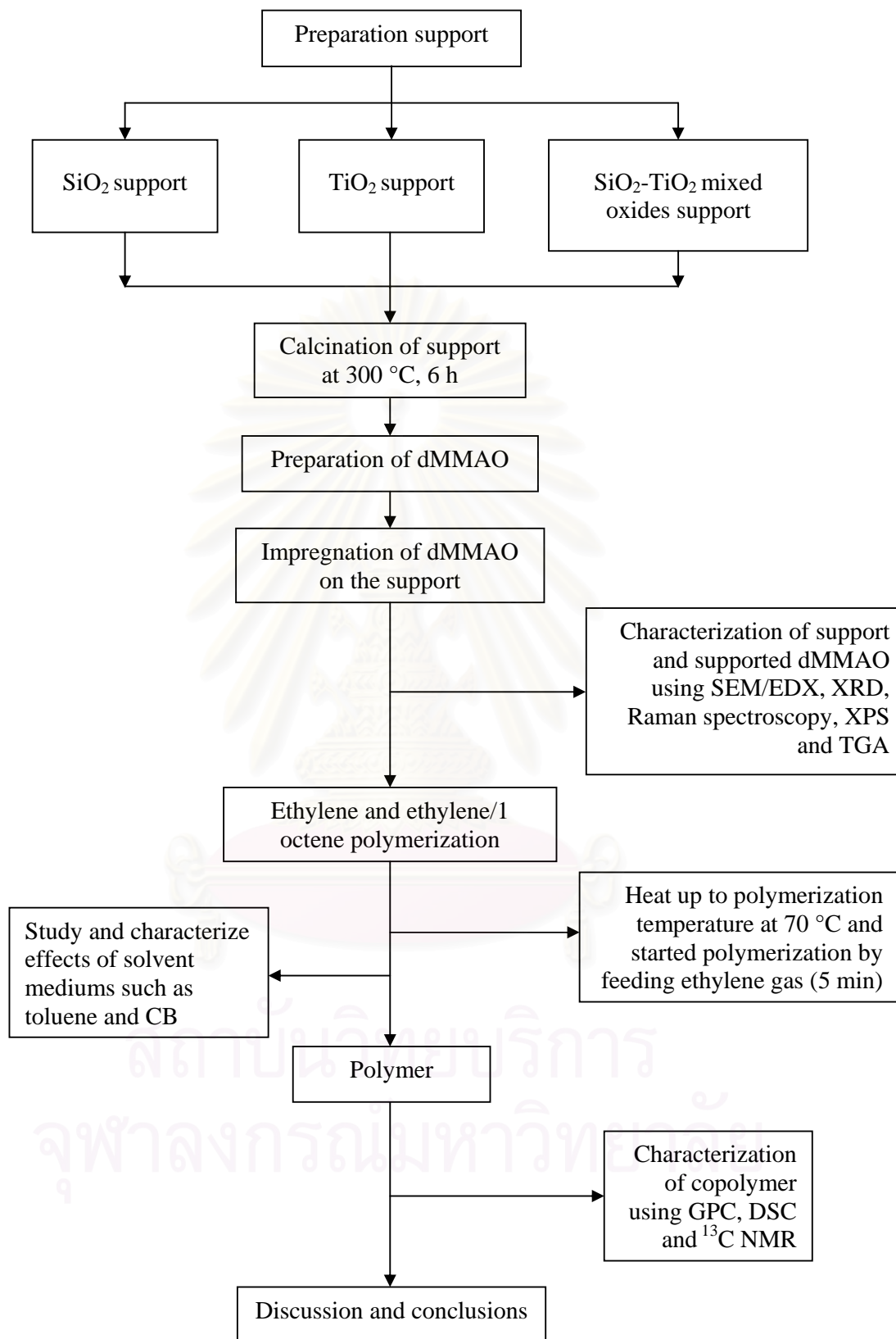


Figure 3.1 Flow diagram of research methodology

3.4 Experimental

3.4.1. Chemicals

The chemicals used in these experiments were analytical grade, but only major materials are specified as follows:

1. *tert*-Butyl amido silyl dimethyl fluorenyl titanium dimethyl (*[t*-BuNMe₂SiFlu]TiMe₂) catalyst was prepared according to the literature [40].
2. Ethylene gas (99.96%) was deviated from National Petrochemical Co., Ltd., Thailand and used as received.
3. 1-Hexane (95%) was donated from Shell (Public) Company, Inc. and purified by distilling over sodium under argon atmosphere before use.
4. 1-Heptane ($\geq 97\%$) was purchased from Fluka Chemie A.G. Switzerland and purified by distilling over sodium under argon atmosphere before used.
5. Chlorobenzene was purchased from Fluka Chemie, A.G., Switzerland and purified by distilling over sodium under argon atmosphere before used.
6. Toluene was deviated from EXXON Chemical Ltd., Thailand. This solvent was dried over dehydrated CaCl₂ and distilled over sodium/benzophenone under argon atmosphere before use.
7. 1-Octene (98%) was purchased from Aldrich Chemical Company, Inc. and purified by distilling over calciumhydride under argon atmosphere before used.
8. Modified methylaluminoxane (MMAO) 1.86 M in toluene was donated from Tosoh Akso, Japan and used without further purification.
9. Silica gel from Fuji Silysia Chemical Ltd., Japan (Cariact P-10, surface area 281 m²/g) was calcined at 300 °C for 6 hours under vacuum.
10. Titanium (IV) oxide power (99.8 %, pure anatase, surface area 70 m²/g) was purchased from Aldrich Chemical Company, Inc. was calcined at 300 °C for 6 hours under vacuum.
11. Hydrochloric acid (Fuming 36.7%) was supplied from Sigma and used as received.
12. Methanol (Commercial grade) was purchased from SR lab and used as received.
13. Sodium (99%) was purchased from Aldrich Chemical Company, Inc. and used as received.

14. Benzophenone (99%) was purchased from Fluka Chemie A.G. Switzerland and used as received.

15. Calciumhydride (99%) was purchased from Fluka Chemie A.G. Switzerland and used as received.

16. Ultra high purity argon gas (99.999%) was purchased from Thai Industrial Gas Co., Ltd., and further purified by passing through columns packed with molecular sieve 3A, BASF Catalyst R3-11G, sodium hydroxide (NaOH) and phosphorus pentaoxide (P_2O_5) to remove traces of oxygen and moisture.

3.4.2 Equipments

Due to the metallocene system is extremely sensitive to the oxygen and moisture. Thus, the special equipments were required to handle while the preparation and polymerization process. For example, glove box: equipped with the oxygen and moisture protection system was used to produce the inert atmosphere. Schlenk techniques (Vacuum and Purge with inert gas) are the others set of the equipment used to handle air-sensitive product.

3.4.2.1 Cooling system

The cooling system was in the solvent distillation in order to condense the freshly evaporated solvent.

3.4.2.2 Inert gas supply

The inert gas (argon) was passed through columns of BASF catalyst R3-11G as oxygen scavenger, molecular sieve 3×10^{-10} m to remove moisture. The BASF catalyst was regenerated by treatment with hydrogen at 300 °C overnight before flowing the argon gas through all the above columns. The inert gas supply system is shown in **Figure 3.2**.

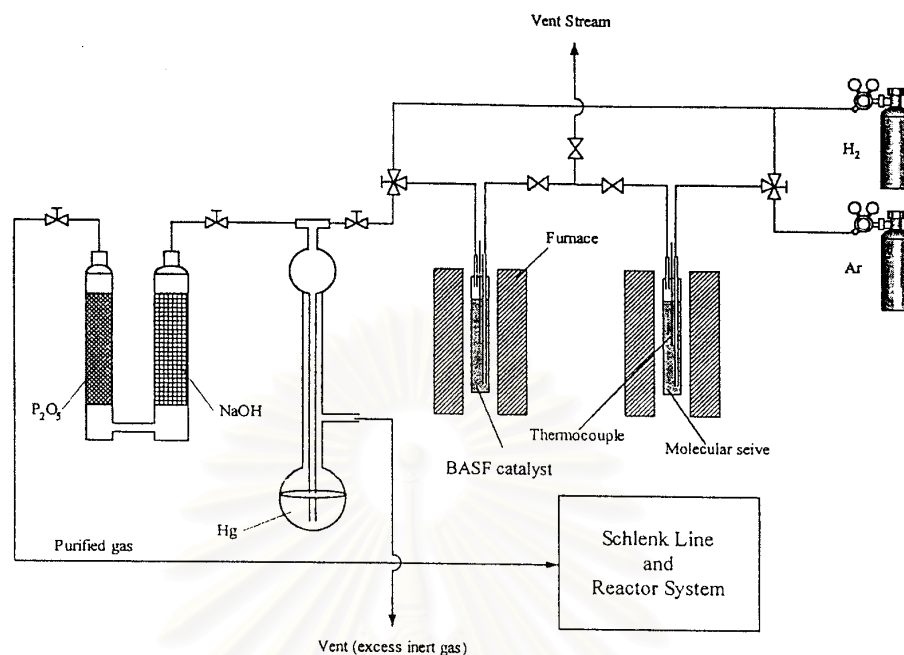


Figure 3.2 Inert gas supply system

3.4.2.3 Magnetic stirrer and heater

The magnetic stirrer and heater model RTC basis from IKA Labortechnik were used.

3.4.2.4 Reactor

A 100 ml glass flask connected with 3-ways valve was used as the copolymerization reactor for atmospheric pressure system and a 100 ml stainless steel autoclave was used as the copolymerization reactor for high pressure systems.

3.4.2.5 Schlenk line

Schlenk line consists of vacuum and argon lines. The vacuum line was equipped with the solvent trap and vacuum pump, respectively. The argon line was connected with the trap and the mercury bubbler that was a manometer tube and contains enough mercury to provide a seal from the atmosphere when argon line was evacuated. The schlenk line was shown in **Figure 3.3**.

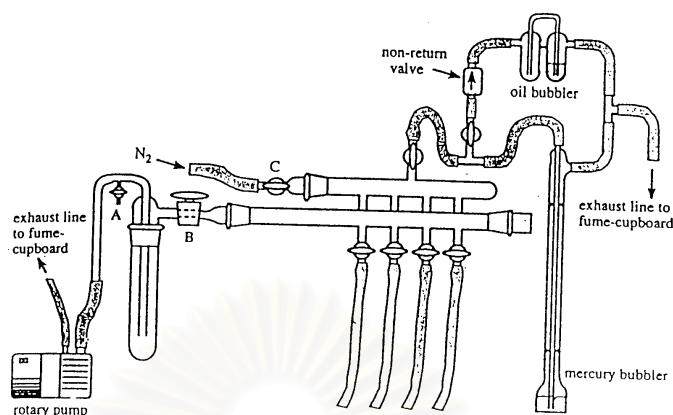


Figure 3.3 Schlenk line

3.4.2.6 Schlenk tube

A tube with a ground glass joint and side arm, which was three-way glass valve as shown in **Figure 3.4**. Sizes of schlenk tubes were 50, 100 and 200 ml used to prepare catalyst precursor and store materials which were sensitive to oxygen and moisture.



Figure 3.4 Schlenk tube

3.4.2.7 Vacuum pump

The vacuum pump model 195 from Labconco Corporation was used. A pressure of 10^{-1} to 10^{-3} mmHg was adequate for the vacuum supply to the vacuum line in the schlenk line.

3.4.2.8 Polymerization line

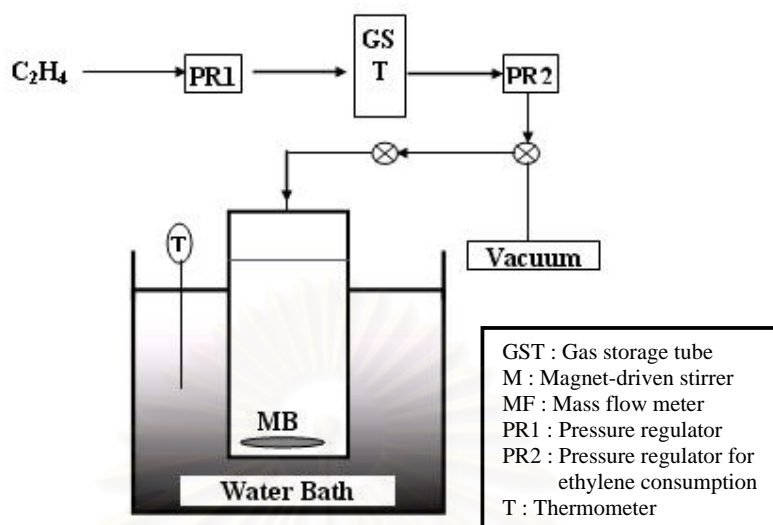


Figure 3.5 Diagram of system in slurry phase polymerization

3.4.3 Catalyst Synthesis

3.4.3.1 Synthesis of *t*-BuNHSiMe₂Flu

Firstly, the solution of fluorene (11.6 g, 70mmol) in diethylether (120 ml) was added n-butyllithium (1 equivalent to fluorene) at 0 °C within 1 hr and stirred for 3 hours and room temperature. After that the solution was evacuated to give Li(C₁₃H₉). Transfer the slurry solution to another flask that contain dichlorodimethylsilane (40 ml) soluble in hexane (100 ml) at -78 °C, and stirred for overnight. The suspensions liquid was removed the excess silane compound in vacuum. After adding hexane and stir the solution, the not soluble solid was precipitate and the solvent was decanted. From the decanted solution we remove the solvent in vacuum again to obtain 9-chlorodimethylsilyl-fluorene (16.2 g, 62 mmol) as off-white solid.

Secondly, the solution of 9-chlorodimethylsilyl-fluorene (9.2 g, 36 mmol) in THF (100 ml) was added *t*-Butylamine (6 g, 76 mmol) at 0 °C, and stirred overnight at room temperature. Solution was evacuated, washed with THF and decanted solvent was evacuated again to give *t*-BuNHSiMe₂Flu as yellow-orange oil.

3.4.3.2 Synthesis of [*t*-BuNMe₂SiFlu]TiMe₂

Stirring the ligand *t*-BuNHSiMe₂Flu (1.56 g, 5.28 mmol) in Et₂O (100 ml) solution that was added Methyllithium 4 equivalents slowly for 5 hours. And transfer

this solution to another flask that contain the TiCl_4 (1 eq.) in pentane (100 ml) solution. The resulting solution was stirred overnight at room temperature. After that, the solution was evacuated, washed, and stirred with hexane (130 ml). The decanted hexane solution was concentrate and cooled overnight at $-30\text{ }^\circ\text{C}$ to recrystallize and give the yellow-orange crystal as $[\textit{t}\text{-BuNMe}_2\text{SiFlu}]\text{TiMe}_2$ catalyst.

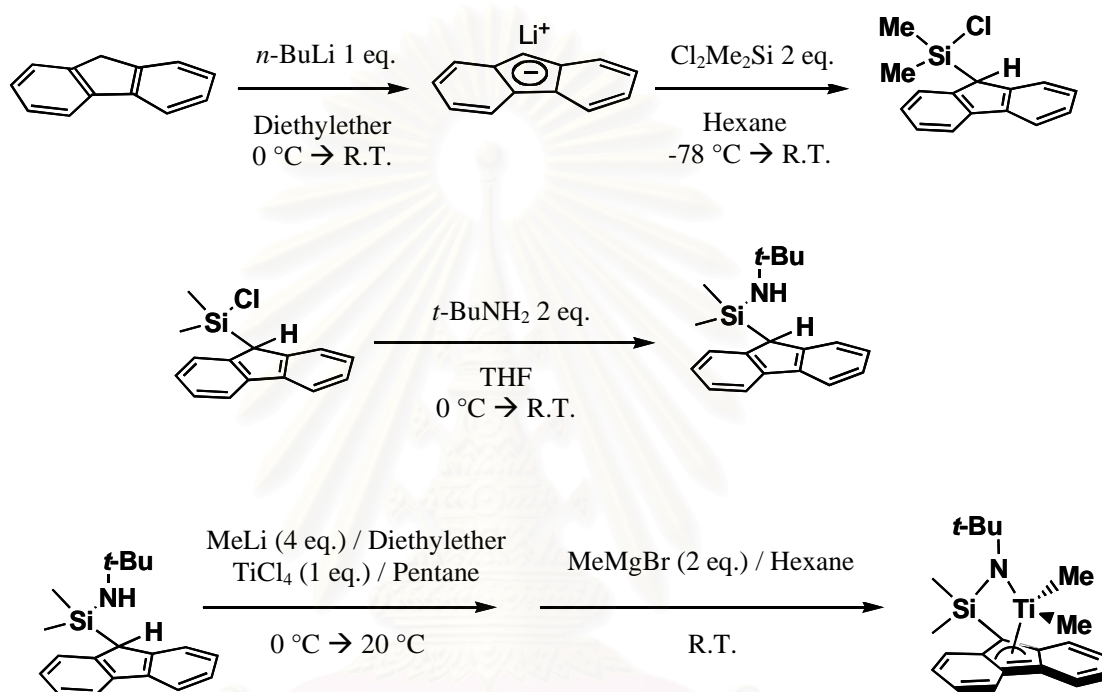


Figure 3.6 Synthetic pathway of $[\textit{t}\text{-BuNSiMe}_2\text{Flu}]\text{TiMe}_2$

3.4.4 Supporting Procedure

3.4.4.1 Preparation of Mixed oxides

1 g of $\text{SiO}_2\text{-TiO}_2$ (4:1 by weight) was impregnated by grinding and dispersing in toluene (ca. 20 ml). The mixture was stirred for 30 min and washed 5 times with toluene, followed by drying in vacuum at room temperature to obtain the mixed $\text{SiO}_2\text{-TiO}_2$ oxide support.

3.4.4.2 Preparation of dMMAO

100 ml of MMAO solution in toluene was evacuated at room temperature and washed with toluene (100 ml) for 3 times to remove the impurity. Then continue

to wash with heptane (100 ml) for 4 times to remove TMA and TIBA in MMAO to give dMMAO as white solid.

3.4.4.3 Preparation of Supported dMMAO

SiO₂, SiO₂-TiO₂ and TiO₂ support were heated under vacuum at 300 °C for 6 hours. 20 g of calcined silica in 250 ml of toluene was reacted with the desired amount of dMMAO (15 g) in toluene solution (100 ml) at room temperature for 30 minutes. The solid part was separated and washed 7 times with 150 ml of hexane, followed by drying in vacuum at room temperature to obtain silica-supported dMMAO (SiO₂/dMMAO). Similarly, silica-titania mixed oxide-supported dMMAO (SiO₂-TiO₂/dMMAO) and titania-supported dMMAO (TiO₂/dMMAO) were prepared according to the method as described above.

3.4.5 Ethylene and Ethylene/1-Octene Polymerization Procedures

Ethylene and 1-octene copolymerization reaction were carried out in a 100 ml semi-batch stainless steel autoclave reactor equipped with magnetic stirrer. The autoclave and magnetic bar were dried in oven at 110 °C for 30 minutes and vacuumed-purged with argon in glove box before use in polymerization. First, the desired amount of the supported dMMAO and the solvent such as heptane, toluene and chlorobenzene (to make a total volume of 30 ml) were introduced into the reactor. Then adding the 1 ml (10 μmol) of [*t*-BuNMe₂SiFlu]TiMe₂ catalyst in toluene solution to make the $[Al]_{MMAO}/[Ti]_{cat.} = 400$. The reactor was then immersed in liquid nitrogen. After that, 0.024 mol of 1-octene was injected into the reactor. The reactor was frozen in liquid nitrogen and evacuated to remove the argon. The reactor was adjusted to the polymerization temperatures at 70°C. By feeding ethylene into the reactor, the polymerization was started. The ethylene pressure and reactor temperature were kept constant during the polymerization (pressure in reactor = 50 psi). Polymerization was conducted for 5 min. Then, terminated with acidic methanol and stirred for 30 min. The polymer obtained was precipitated. Finally, filtrate and the obtain polymer was dried at room temperature. Similarly, ethylene polymerization was prepared according to the procedure described above but did not add 1-octene into the process.

3.4.6 Characterization Method of Supports and supported dMMAO

3.4.6.1 X-ray diffraction (XRD)

XRD was performed to determine the bulk crystalline phases of supports. It was conducted using a SIEMENS D-5000 X-ray diffract meter with $\text{CuK}\alpha$ ($\lambda = 1.54439 \text{ \AA}$). The spectra were scanned at a rate of $2.4^\circ/\text{min}$ in the range $2\theta = 20\text{-}80^\circ$.

3.4.6.2 Raman spectroscopy

Raman spectroscopy was performed to determine the bulk crystalline phases of supports. The Raman spectra of the supports were collected by projecting a continuous wave YAG laser of neodymium (Nd) red (810 nm) through the samples at room temperature. A scanning range of $100\text{-}1000 \text{ cm}^{-1}$ with a resolution of 2 cm^{-1} was applied.

3.4.6.3 Scanning electron microscopy (SEM) and energy dispersive X-ray spectroscopy (EDX)

SEM and EDX were used to determine the support morphologies and elemental distribution throughout the support granules, respectively. The SEM of JEOL mode JSM-6400 was applied. EDX was performed using Link Isis series 300 program.

3.4.6.4 X-ray photoelectron spectroscopy (XPS)

XPS was used to determine the binding energies (BE) and the amount of Al on support surfaces. It was carried out using the Shimazu AMICUS with VISION 2-control software. Spectra were recorded at room temperature in high-resolution mode (0.1 eV step, 23.5 eV pass energy) for Al 2p core-level region. The samples were mounted on an adhesive carbon tape as pellets. The energies reference for Ag metal (368.0 eV for $3d_{5/2}$) was used for this study.

3.4.6.5 Thermogravimetric analysis (TGA)

TGA was performed to determine the interaction force of the supported dMMAO. It was conducted using TA Instruments SDT Q 600 analyzer. The samples of 10-20 mg and a temperature ramping from 25 to 600 °C at $2^\circ\text{C}/\text{min}$ were used in the operation. The carrier gas was N_2 UHP.

3.4.7 Characterization Method of Polymer

3.4.7.1 Gel permeation chromatography (GPC)

The molecular weight and molecular weight distribution of polymer was determined using GPC (PL-GPC-220). Samples were prepared having approximately concentration of 1 to 2 mg/ml in trichlorobenzene (mobile phase) by using the sample preparation unit (PL-SP 260) with filtration system at a temperature of 150 °C. The dissolved and filtered samples were transferred into the GPC instrument at 150 °C. The calibration was conducted using the universal calibration curve based on narrow polystyrene standards.

3.4.7.2 Differential scanning calorimetry (DSC)

The melting temperature of polymer products was determined with thermal analysis measurement. It was performed using a Perkin-Elmer DSC P7 calorimeter. The DSC measurements reported here were recorded during the second heating/cooling cycle with the rate of 20 °C/min. This procedure ensured that the previous thermal history was erased and provided comparable conditions for all samples. Approximately, 10 mg of sample was used for DSC measurement at a time.

3.4.7.3 ^{13}C NMR spectroscopy (^{13}C NMR)

^{13}C NMR spectroscopy was used to determine the α -olefin incorporation and copolymer microstructure. Chemical shift were referenced internally to the CDCl_3 and calculated according to the method described by Randall [87]. Sample solution was prepared by dissolving 50 mg of copolymer in 1,2,4-trichlorobenzene and benzene- d_6 . ^{13}C NMR spectra were taken at 60 °C using BRUKER AVANCE II 400 operating at 100 MHz with an acquisition time of 1.5 s and a delay time of 4 s.

CHAPTER IV

RESULTS AND DISCUSSION

The purpose of this study is to investigate and characterize effects of various supports and solvent mediums on the catalyst activity and properties of polymers during ethylene and ethylene/1-octene polymerization with the titanocene catalyst. The supports and supported-MMAOs (catalyst precursors) were also investigated to make better understanding about polymerization results.

4.1 Characterization of supports and supported dMMAOs

4.1.1 Characterization of supports with X-ray diffraction (XRD)

The various supports such as silica, titania, and mixed silica-titania were characterized before impregnation with dMMAO. It was observed that the pure silica exhibited a broad XRD peak as seen typically for the conventional amorphous silica. Similar to silica, the XRD patterns for pure titania indicated only the characteristics peaks of anatase titania at 25° (major), 37°, 48°, 55°, 56°, 62°, 71°, and 75°. XRD patterns of the mixed silica-titania revealed the combination of silica and titania being present as mentioned above. The XRD patterns of these supports are shown in **Figure 4.1**.

สถาบันวิทยบริการ
จุฬาลงกรณ์มหาวิทยาลัย

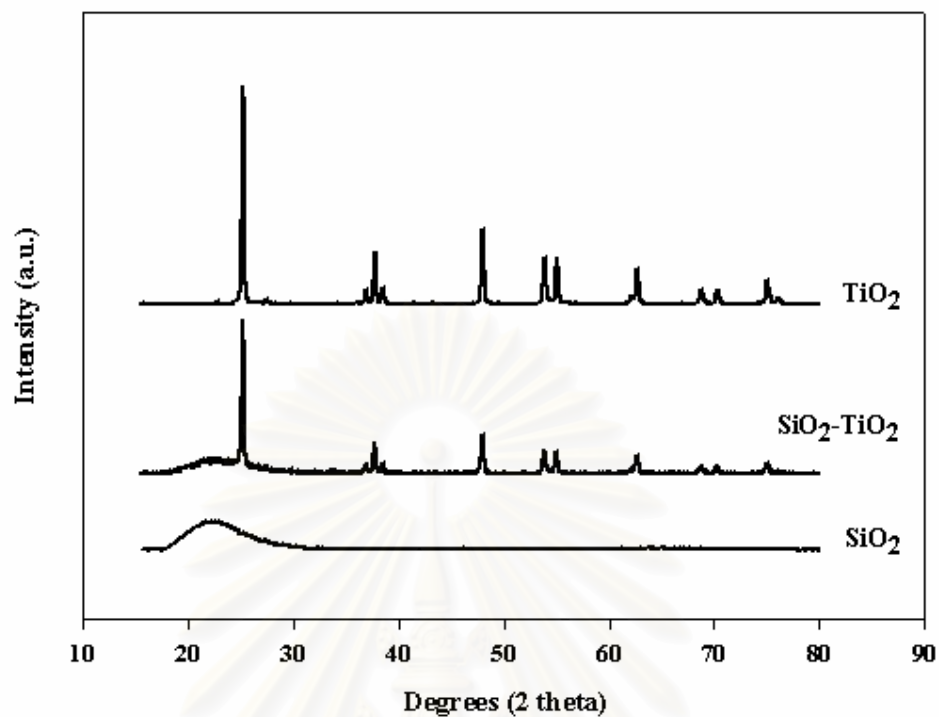


Figure 4.1 XRD patterns of various supports prior to impregnation with dMMAO

4.1.2 Characterization of supports with Raman spectroscopy

Raman spectra of the supports before impregnation with dMMAO are shown in **Figure 4.2**. It was found that the titania support exhibited the Raman bands at 639, 516, and 397 cm^{-1} for titania in its anatase form as seen from our previous work [88,89] whereas silica was the Raman insensitive upon the scanning range applied.

สถาบันวิทยบริการ
จุฬาลงกรณ์มหาวิทยาลัย

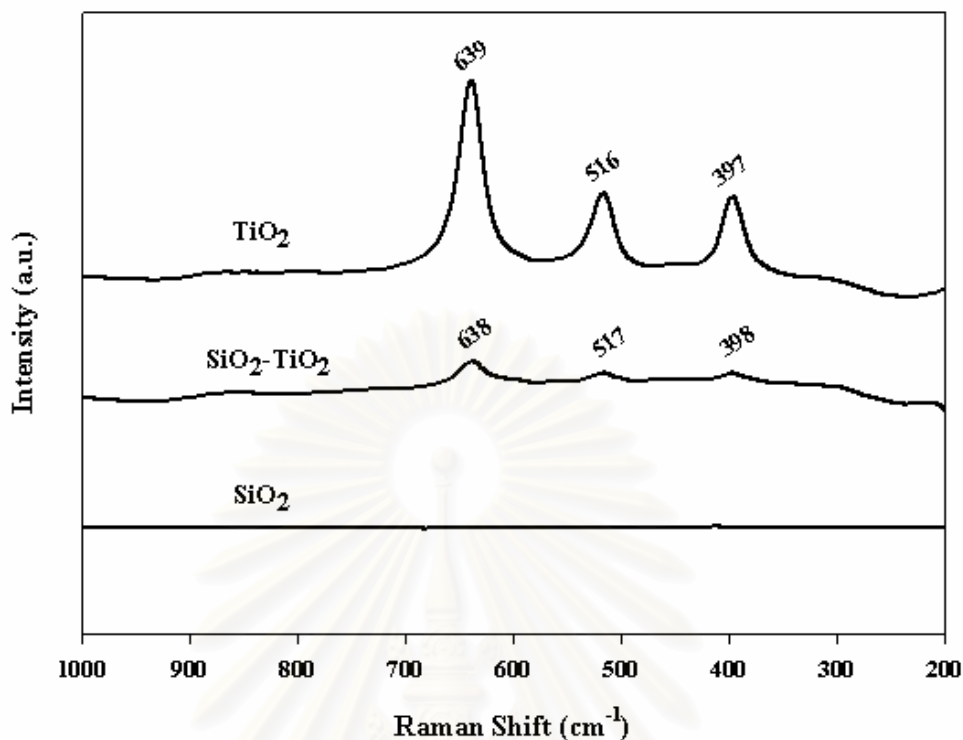


Figure 4.2 Raman spectra of various supports prior to impregnation with dMMAO

4.1.3 Characterization of supports and supported dMMAO with scanning electron microscopy (SEM) and energy dispersive X-ray spectroscopy (EDX)

EDX and SEM were performed to determine the content of $[Al]_{dMMAO}$, the elemental distributions and the morphologies of supports. After impregnation of supports with dMMAO, the $[Al]_{dMMAO}$ content was measured using EDX. The amounts of $[Al]_{dMMAO}$ in various supports are listed in **Table 4.1**.

Table 4.1 The content of $[Al]_{dMMAO}$ on various supports

Cocatalyst	$[Al]_{dMMAO}$ (%mass)
dMMAO/SiO ₂	12.56
dMMAO/SiO ₂ -TiO ₂	14.69
dMMAO/TiO ₂	18.56

The typical measurement curve for the quantitative analysis using EDX is shown in **Figure 4.3**. It can be seen that the amount of $[Al]_{dMMAO}$ in various

supports were varied due to the adsorption ability of each support. It revealed that titania exhibited the highest amount of $[Al]_{dMMAO}$ being present among other supports probably due to its strong interaction. On the other hand, increased amount of $[Al]_{dMMAO}$ can be observed with the presence of titania as also seen in the mixed silica-titania compared with that in the pure silica. Besides the content of $[Al]_{dMMAO}$ in supports, one should consider the distribution of $[Al]_{dMMAO}$ in the supports. The elemental distribution was also performed using EDX mapping on the external surface. The support morphology and the $[Al]_{dMMAO}$ distribution in the various supports are shown in **Figure 4.4**. As seen, all samples exhibited good distribution of Al without any changes in the support morphology.

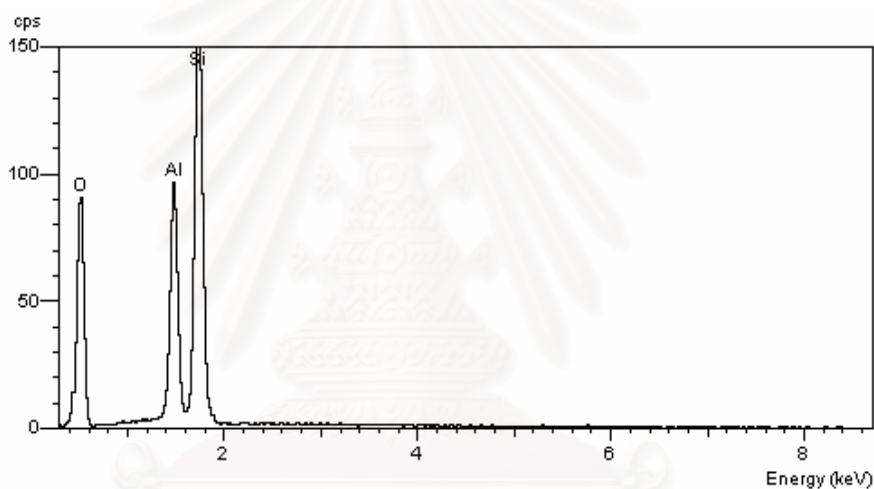


Figure 4.3 A typical spectrum of the supported dMMAO from EDX analysis used to measure the average $[Al]_{dMMAO}$ concentration on various supports

สถาบันวิทยบริการ
จุฬาลงกรณ์มหาวิทยาลัย

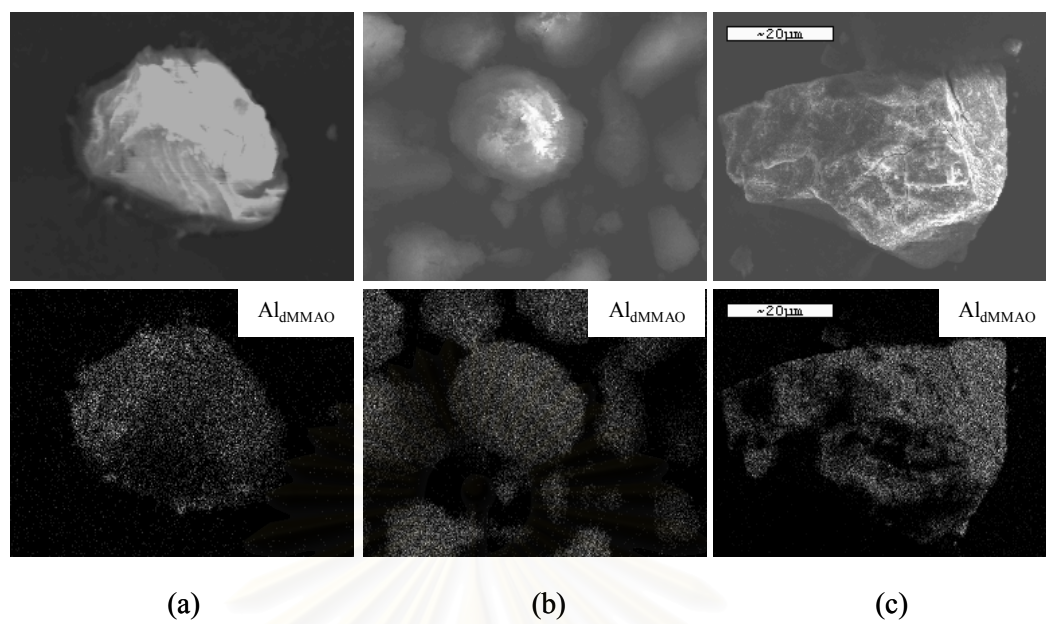


Figure 4.4 SEM/EDX mapping for Al distributions on (a) SiO_2 , (b) $\text{SiO}_2\text{-TiO}_2$, and (c) TiO_2 supports

4.1.4 Characterization of supports and supported dMMAO with X-ray photoelectron spectroscopy (XPS)

In order to give a better understanding on species present on supports, the XPS study of the dMMAO on various supports was conducted. The binding energy (BE) of Al 2p core-level of $[\text{Al}]_{\text{dMMAO}}$ was measured. The typical XPS profile of Al 2p on various supports is shown in **Figure 4.5** indicating the BE of 74.6-74.8 eV. These values were also in accordance with the MMAO present on the silica support as reported by Hagimoto et al. [90]. This was suggested that no significant change in the oxidation state of $[\text{Al}]_{\text{dMMAO}}$ upon the various support employed.

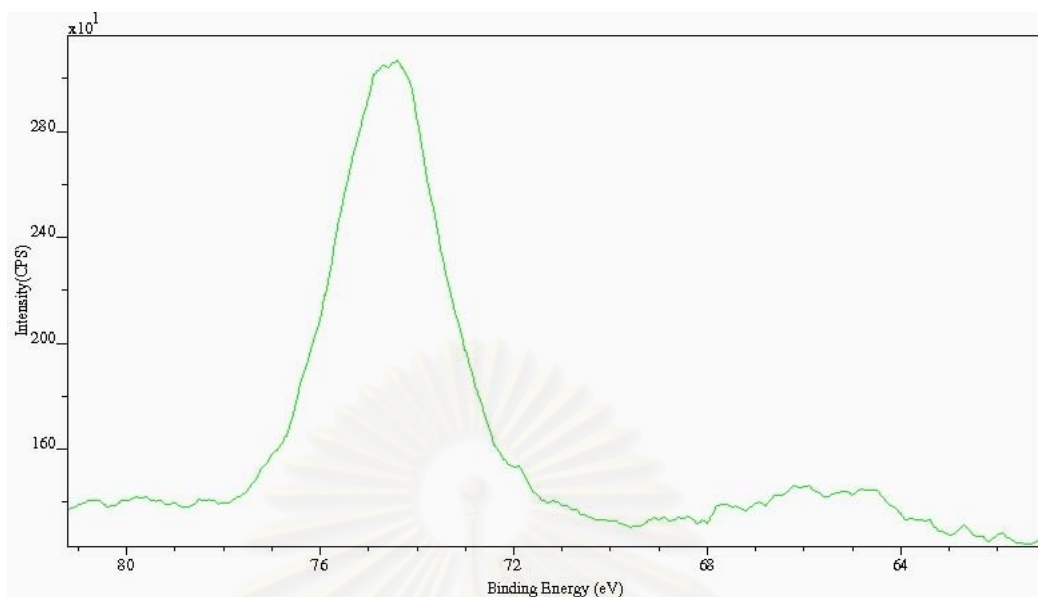


Figure 4.5 A typical XPS spectrum of Al 2p core-level of dMMAO and dMMAO on various supports

The surface concentrations of Al 2p measured by XPS were also shown in **Table 4.2**. Considering the various supports employed, the surface concentrations of Al 2p were in the order of $\text{TiO}_2 > \text{SiO}_2\text{-TiO}_2 > \text{SiO}_2$ as seen from the bulk using EDX. It was obvious that the TiO_2 support contained the highest amount of surface Al 2p due to strong interaction. The presence of TiO_2 in the mixed $\text{SiO}_2\text{-TiO}_2$ also enhanced the interaction of dMMAO due to the synergistic effect arising from TiO_2 .

Table 4.2 XPS data of Al 2p core-level of cocatalysts

Cocatalyst	BE (eV) for Al^{3+}	Amount of Al^{3+} at surface (%mass)
dMMAO	74.7	28.5
dMMAO/ SiO_2	74.6	25.0
dMMAO/ $\text{SiO}_2\text{-TiO}_2$	74.8	25.6
dMMAO/ TiO_2	74.7	27.1

4.1.5 Characterization of supports and supported dMMAO with Thermogravimetric analysis (TGA)

In this study, dMMAO was dispersed by impregnation onto the various supports. The degree of interaction between the support and the cocatalyst (dMMAO) can be determined by the TGA measurement. The TGA provide information on the degree of interaction for the dMMAO bound to the support in terms of weight loss and removal temperature. The TGA profiles of $[Al]_{dMMAO}$ on various supports are shown in **Figure 4.6** indicating the similar profiles for various supports. It was observed that the weight loss of $[Al]_{dMMAO}$ present on various supports were in the order of SiO_2 (22%) > SiO_2-TiO_2 (21%) > TiO_2 (19%). The species having strong interaction with the support was removed at ca. 265, 269 and 315 °C for SiO_2 , SiO_2-TiO_2 and TiO_2 , respectively. This indicated that $[Al]_{dMMAO}$ present on TiO_2 had the strongest interaction.

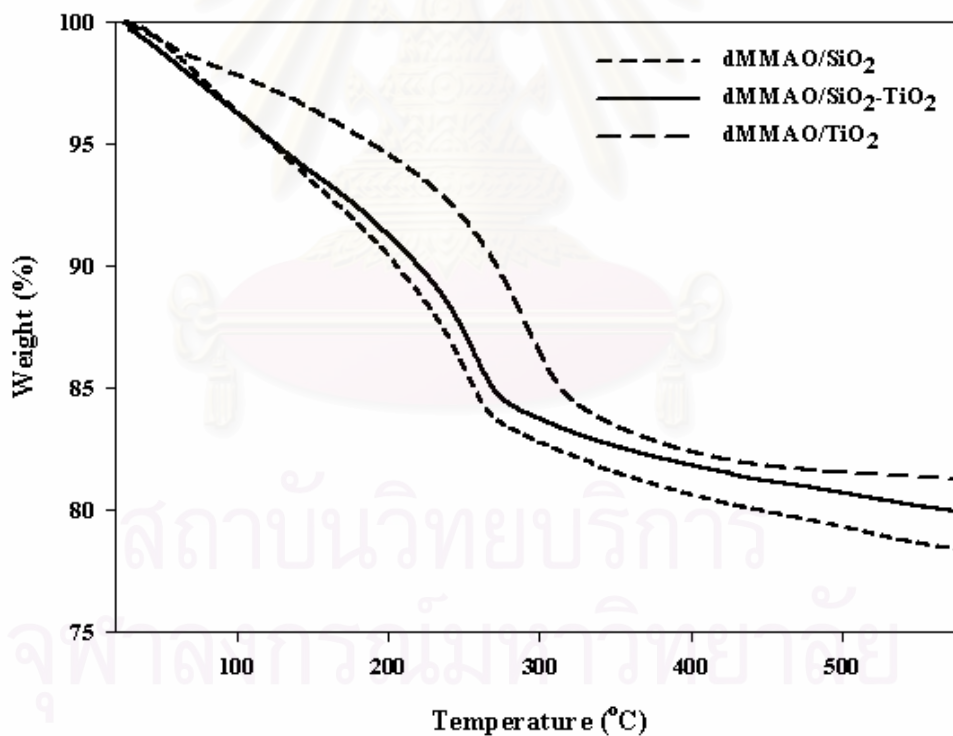


Figure 4.6 TGA profiles of supported dMMAO on various supports

4.2 Characteristics and catalytic properties of ethylene/1-octene copolymerization

The various supports (SiO_2 , $\text{SiO}_2\text{-TiO}_2$, and TiO_2) after impregnation with dMMAO (dMMAO/SiO_2 , $\text{dMMAO/SiO}_2\text{-TiO}_2$, and dMMAO/TiO_2) were used and investigated for catalytic activities. The ethylene/1-octene copolymerization via various supported dMMAO with $[t\text{-BuNSiMe}_2\text{Flu}]\text{TiMe}_2$ was performed in order to determine the characteristics and catalytic properties of copolymer influenced by the various supports and solvents mediums. Dried modified methylaluminoxane (dMMAO) was used as cocatalyst which the molar ratio of $\text{Al}_{[\text{dMMAO}]/\text{Ti}}$ was 400. The copolymerization were performed in toluene and chlorobenzene (CB) solvent at $70\text{ }^\circ\text{C}$ using 5 min feeding ethylene (pressure in reactor = 50 psi), 3.8 ml of 1-octene and titanium concentration $10 \times 10^{-6}\text{ M}$ with total solution volume of 30 ml.

4.2.1 The effect of various supports and solvent mediums on the catalytic activity

For comparative studies, the catalytic activities towards the copolymerization of ethylene/1-octene upon various supports were measured. The polymerization activities of the homogeneous system and various supports employed in toluene are shown in **Table 4.3**. It can be observed that the polymerization activities were in the order of homogeneous system > $\text{SiO}_2\text{-TiO}_2$ > SiO_2 > TiO_2 . As known, the supported system exhibited lower activity than the homogeneous one due to the supporting effect. This should be due to a loss of active species by support interaction and/or steric hindrance arising from the support. Considering only the supported system, the $\text{SiO}_2\text{-TiO}_2$ rendered the highest activity among the other supports. In fact, the presence of TiO_2 in SiO_2 can result in decreased interaction between the cocatalyst and SiO_2 supports. It was reported that TiO_2 may acted as a spacer group to anchor MAO to the SiO_2 support resulting in less steric hindrance and less interaction on the support surface as seen for the zirconocene/MAO system as well [85]. Hence, the similar effect was consistently observed for the titanocene/dMMAO system. It should be mentioned that the lowest polymerization activity obtained for the TiO_2 support was due to the strong support interaction [91]. In order to give a better understanding on species present on supports, the XPS study of the dMMAO on various supports was conducted. The typical XPS profile of Al 2p

on various supports was shown in **Figure 4.6**. This was suggested that no significant change in the oxidation state of $[Al]_{dMMAO}$ upon the various supports employed. As a matter of fact, the differences in polymerization activities observed on various supports were not caused by any changes of the surface species. The BE of Al 2p core-level of $[Al]_{dMMAO}$ and the surface concentrations of Al 2p on various supports as also seen in **Table 4.2**. On the other hand, changes in activity upon various supports were mainly attributed to both the amounts of $[Al]_{dMMAO}$ present and its interaction with the support. Considering the various supports employed, the surface concentrations of Al 2p were in the order of $TiO_2 > SiO_2-TiO_2 > SiO_2$ as seen from the bulk using EDX. It was obvious that the TiO_2 support contained the highest amount of surface Al 2p due to strong interaction resulting in less leaching of dMMAO during the preparation. The presence of TiO_2 in the mixed SiO_2-TiO_2 also enhanced the interaction of dMMAO due to the synergistic effect arising from TiO_2 . Based on, the surface concentrations of Al 2p, one might argue that with TiO_2 support, the polymerization activity should be the highest since it apparently had the highest concentration of Al 2p. However, based on our results, the polymerization activity using the TiO_2 was the lowest. This indicated that besides the surface concentration of $[Al]_{dMMAO}$, the interaction between the $[Al]_{dMMAO}$ and support was substantially important. In fact, the strong interaction of species with TiO_2 or other supports employed in this study was referred to the interaction between the support and the cocatalyst (dMMAO). Based on this study, dMMAO was dispersed by impregnation onto the support prior to polymerization. In order to give a better understanding, the interaction of support and dMMAO can be proposed based on the review paper by Severn et al. [92]. They revealed that the connection of the support and cocatalyst occurred via the $O_{support} \sim Al_{cocatalyst}$ linkage. The stronger interaction can result in being more difficult for the dMMAO bound to the support to react with the Ti-complex during activation process leading to lower catalytic activity for polymerization. As mentioned, the TiO_2 support is known to have a strong interaction with species being present on it. The TGA measurement was performed to proof the interaction between the $[Al]_{dMMAO}$ and various supports. The profiles of $[Al]_{dMMAO}$ on various supports as seen in **Figure 4.7**. This result indicated that $[Al]_{dMMAO}$ present on TiO_2 had the strongest interaction, thus, lowest polymerization activity observed. However, in the case of SiO_2-TiO_2 support, although it had stronger interaction than that of SiO_2 , it exhibited higher polymerization interaction due to higher concentration of $[Al]_{dMMAO}$

at surface as mentioned above. Besides, the presence of TiO_2 in SiO_2 as a spacer group was also counted for higher activity.

Table 4.3 Copolymerization^a activity

System	Solvent	Yield (g)	Activity (kg of Polymer/mol Ti.h)
Homogeneous	Toluene	3.25	3897
SiO_2 support		2.49	2984
SiO_2 - TiO_2 support		2.61	3131
TiO_2 support		2.33	2795
Homogeneous	CB	3.23	3871
SiO_2 support		1.68 ^b	10095
SiO_2 - TiO_2 support		2.69 ^c	12127
TiO_2 support		2.53	3032

^a Polymerization condition: $\text{Ti} = 10 \mu\text{mol}$, $\text{Al/Ti} = 400$, $\text{Temp} = 70 \text{ }^\circ\text{C}$, $\text{Time} = 5 \text{ min}$, 50 psi of ethylene pressure was applied.

^b Polymerization time = 1 min

^c Polymerization time = 1.5 min

In order to investigate the solvent effect on this polymerization system. The solvent having different dielectric constant values (ϵ) such as chlorobenzene (CB) was employed for the corresponding polymerization system. The dielectric constant is in order of $\text{CB} (5.68) > \text{toluene} (2.38)$ [93]. The polymerization activity results in CB are also shown in **Table 4.3**. It can be observed that there was no significant change regarding to activity for the homogeneous system when changing the solvent medium. However, the dramatic increase in activity was apparently found in the supported system especially with SiO_2 and SiO_2 - TiO_2 supports when CB was employed as the solvent medium. It indicated that the polymerization activities substantially increased with SiO_2 and SiO_2 - TiO_2 supports in CB almost 4 times higher compared with those in toluene. The activity for TiO_2 support in CB only slightly increased compared to that in toluene. It can be proposed that the different solvents can possibly alter the nature of catalyst in two ways; (i) changing the interaction between the support and cocatalyst and/or (ii) changing the form of active species i.e., active ion-pair and solvent-separated ion-pair as seen in the homogeneous system as reported by Nishii et

al. [29] and Intaragamjon et al. [39]. It is worth noting that the dramatic increases in polymerization activities in CB compared to those in toluene can be perhaps attributed to increased propagation rate presuming that the $[Al]_{dMMAO}$ species present on SiO_2 and SiO_2-TiO_2 supports were similar by means of the XPS measurement. Nishii et al. [29] investigated the propylene polymerization using the Ti complex in various solvents having different dielectric constants value in homogeneous system. They reported that the high polarity of solvent resulted in increased activity due to the increased propagation rate. It revealed that the enhancement of the separation of the active metal cation and the MMAO-derived anion in the polar solvent occurred. It should be also noted that there was no solvent effect observed with the support having the strong interaction such as TiO_2 as seen in **Table 4.3**.

4.2.2 The effect of various supports and solvent mediums on the molecular weight of copolymers

The molecular weight based on weight average (M_w) and based on number average (M_n), and molecular weight distribution (MWD) of polymers obtained by GPC are shown in **Table 4.4** and GPC curves of the copolymers are also shown in **Appendix A**.

Table 4.4 Copolymer characterization

System	Solvent	GPC Analysis (g/mol)			T_m^a
		$M_w (10^4)$	$M_n (10^4)$	MWD	
Homogeneous	Toluene	13.43	4.95	2.7	- ^b
SiO_2		36.37	13.80	2.6	-
SiO_2-TiO_2		36.60	16.02	2.3	-
TiO_2		6.91	4.25	1.6	-
Homogeneous	CB	27.24	8.11	3.4	-
SiO_2		50.98	26.52	1.9	-
SiO_2-TiO_2		37.86	9.64	4.0	-
TiO_2		18.16	6.50	2.8	-

^a Melting temperature was measured by DSC analysis

^b Value not be detected from the measurement

Considering polymerization in toluene, the supported system (except for TiO₂ support) gave the higher M_w than that of the homogeneous system, however, without any significant changes in MWD. It was suggested that using TiO₂ apparently promoted the chain transfer reaction consequently resulting in lower M_w. The effect of TiO₂ support on the zirconocene/MAO system was also reported by Jongsomjit et al. [85]. However, it was obvious that the titanocene/dMMAO system gives much higher M_w. It can be observed that polymerization in CB exhibited higher M_w than those in toluene without a significant change in MWD. The increased M_w in CB can be attributed to the solvent-separated ion-pair active species occurred which allowed inserting more monomers into the growing chain. Thus, the solvent-separated ion-pair can provide the high activity while also enhancing the insertion of monomer to the growing chain.

4.2.3 The effect of various supports and solvent mediums on the microstructure of copolymers

¹³C NMR spectroscopy was used to determine comonomer incorporation and polymer microstructure. The quantitative analysis of triad distribution for all copolymers was conducted on the basic assignment of the ¹³C NMR spectra of ethylene/1-octene (EO) copolymer according to the method of Randall [87]. The triad distribution of all copolymers is shown in **Table 4.5**. The ¹³C NMR spectra of the copolymer are also shown in **Appendix B**.

Table 4.5 Triad distribution and %octene incorporation of copolymer obtained from ^{13}C NMR

System	Solvent	OOO	EOO	EOE	EEE	OEE	OEO	%Octene incorporation
Homogeneous	Toluene	0.107	0.481	0.096	0.184	0.015	0.117	68
SiO ₂		0.295	0.436	0.067	0.102	0.012	0.087	80
SiO ₂ -TiO ₂		0.140	0.487	0.082	0.181	0.011	0.098	71
TiO ₂		0.027	0.415	0.140	0.125	0.133	0.160	58
Homogeneous	CB	0.223	0.558	0.045	0.102	0.010	0.062	83
SiO ₂		0.498	0.162	0.085	0.247	0.008	0.000	75
SiO ₂ -TiO ₂		0.610	0.346	0.000	0.014	0.030	0.000	96
TiO ₂		0.268	0.442	0.054	0.093	0.009	0.134	76

It can be observed that the incorporation of 1-octene increased with the CB system for the homogeneous system, the SiO₂-TiO₂, and TiO₂-supported systems. This indicated that the solvent-separated ion-pair obtained from CB exhibited less steric hindrance, then enhancing the insertion of 1-octene in the growing polymer. However, for the SiO₂-supported system, a slight decrease in 1-octene incorporation was found when CB was employed. This was probably due to the inhibition arising from more steric hindrance in SiO₂-supported system. Nishii et al. [29] also investigated the effect of Ti-complex on the syndiospecificity of polypropylene in the homogeneous system. They reported that the presence of the solvent-separated ion-pair allowed the growing chain to migrate between the two enantiomeric ligand sites on the Ti cation without monomer insertion. However, with the contact ion-pair obtained from the non-polar solvent, the migration of the growing chain was not allowed. Based on their work, it can be concluded that migration of the growing chain in different solvent mediums was the main factor for controlling the stereospecificity of polymer. However, in the present work, the copolymerization of ethylene/1-octene was conducted on both homogeneous and supported catalytic systems. Based on the ^{13}C NMR results, it can be observed that the microstructure of polymer was similar in regardless of solvents employed. Therefore, the migration of the growing chain did not occurred when compared to the corresponding propylene polymerization system. Considering the triad distribution, it revealed that the

polymers obtained from both solvent mediums were block polymer ($r_{E,RO} > 1$) indicating the large amounts of triblock (OOO) for the CB system and diblock (EEO) for the toluene system as seen in **Table 4.5**.

4.2.4 The effect of various supports and solvent mediums on the thermal properties of copolymers

The DSC was performed to measure the thermal properties of polymers. The melting temperatures (T_m) of copolymer were shown in **Table 4.4**. DSC curves of the copolymer are also shown in **Appendix C**. It revealed that no melting temperature was found indicating non-crystalline polymer produced in this specified polymerization system. The non-crystalline polymers were attributed to the high degree of 1-octene insertion, which can be confirmed by ^{13}C NMR.

4.3 Comparative study of ethylene and ethylene/1-octene polymerization

The various supports (SiO_2 , $\text{SiO}_2\text{-TiO}_2$, and TiO_2) after impregnation with dMMAO (dMMAO/ SiO_2 , dMMAO/ $\text{SiO}_2\text{-TiO}_2$, and dMMAO/ TiO_2) were used and investigated for catalytic activities. The ethylene (E) and ethylene/1-octene (EO) polymerization via various supported dMMAOs with $[t\text{-BuNSiMe}_2\text{Flu}]\text{TiMe}_2$ were performed in order to determine the characteristics and catalytic properties of polymer influenced by the various supports and solvents mediums. Dried modified methylaluminoxane (dMMAO) was used as cocatalyst which the molar ratio of $\text{Al}_{[\text{dMMAO}]}/\text{Ti}$ was 400. The polymerization were performed in toluene and CB solvent at $70\text{ }^\circ\text{C}$ using 5 min feeding ethylene (pressure in reactor = 50 psi), 3.8 ml of 1-octene and titanium concentration $10 \times 10^{-6}\text{ M}$ with total solution volume of 30 ml.

4.3.1 The effect of various supports and solvent mediums on the catalytic activity

The catalytic activities towards the ethylene polymerization upon various supports were measured. The polymerization activities of the homogeneous system and various supports employed in toluene and CB are shown in **Table 4.6**. For ethylene polymerization in toluene, it indicated that the activities of the supported system were also lower than the homogeneous one due to the supporting effect.

Considering the supported system, the slightly difference in the polymerization activities was apparently found.

For ethylene polymerization in CB, there was the same trend in activities. The activities for supported system only slightly increased compared to that in toluene. However, it was found that the activities in homogeneous system decreased when CB was employed as the solvent medium. Intaragamjon et al. [39] also investigated the solvent effect of titanocene/MMAO system on ethylene/1-hexene copolymerization. Based on the possible reaction of the contact ion-pair model, they reported that the polarity of solvent greatly affects the polymerization activity where the high polarity of solvent gives high activity until the ion-pair becomes fully separated. Therefore, in homogeneous system, it was concluded that too high dielectric constant value of solvent resulted in low activity due to it required the complexation energy to generate the fully separated ion-pair active species. It should be also noted that there was no solvent effect observed with the support in this system. In all cases, there was no activities for 1-octene polymerization at this specified polymerization condition.

For comparative study of ethylene and ethylene/1-octene polymerization, the catalytic activities were measured. From **Table 4.6**, it is clearly illustrated that the activities of polymerization dramatically increased with the insertion of α -olefin monomer (1-octene). These phenomena are commonly well known as the second comonomer effect in copolymerization behavior [94]. For both polymerization and copolymerization, the homogeneous system exhibited higher activity than supported one. This indicated that the supporting effect resulted in reducing activity. In order to consider the solvent effect on these polymerization systems, polymerization in toluene and CB was employed. For the ethylene/1-octene copolymerization, the dramatic increases in activity were apparently found in the supported system especially with SiO₂ and SiO₂-TiO₂ supports when CB was employed as the solvent medium. There was no significant change regarding to activity for the homogeneous system. While the ethylene polymerization, it exhibited higher activity when toluene was employed as the solvent medium in only the homogeneous system.

Table 4.6 Polymerization^a activity

Polymer	System	Solvent	Yield (g)	Activity (kg of Polymer/mol Ti.h)
E	Homogeneous	Toluene	0.36 ^b	904
E	SiO ₂		0.25 ^c	594
E	SiO ₂ -TiO ₂		0.16 ^d	518
E	TiO ₂		0.15 ^e	434
E	Homogeneous	CB	0.66	790
E	SiO ₂		0.56	677
E	SiO ₂ -TiO ₂		0.46	549
E	TiO ₂		0.45	542
EO	Homogeneous	Toluene	3.25	3897
EO	SiO ₂		2.49	2984
EO	SiO ₂ -TiO ₂		2.61	3131
EO	TiO ₂		2.33	2795
EO	Homogeneous	CB	3.23	3871
EO	SiO ₂		1.68 ^f	10095
EO	SiO ₂ -TiO ₂		2.69 ^g	12127
EO	TiO ₂		2.53	3032

^a Polymerization condition: Ti = 10 μmol, Al/Ti = 400, Temp = 70 °C, Time = 5 min, 50 psi of ethylene pressure was applied.

^b Polymerization time = 2.4 min

^c Polymerization time = 2.5 min

^d Polymerization time = 1.8 min

^e Polymerization time = 2.1 min

^f Polymerization time = 1 min

^g Polymerization time = 1.5 min

4.3.2 The effect of various supports and solvent mediums on the molecular weight of polymers

The molecular weight based on weight average (M_w) and based on number average (M_n), and molecular weight distribution (MWD) of polymers obtained by GPC are shown in **Table 4.7** and GPC curves of the polymers are also shown in **Appendix A**.

Table 4.7 Polymer characterization

Polymer	System	Solvent	GPC Analysis (g/mol)		
			$M_w (10^4)$	$M_n (10^4)$	MWD
E	Homogeneous	Toluene	31.90	2.17	14.7
E	SiO ₂		59.10	6.72	8.8
E	SiO ₂ -TiO ₂		42.18	12.86	3.3
E	TiO ₂		24.34	1.06	23.0
E	Homogeneous	CB	24.85	2.53	9.8
E	SiO ₂		46.61	7.81	6.0
E	SiO ₂ -TiO ₂		31.45	5.22	6.0
E	TiO ₂		27.20	3.28	8.3
EO	Homogeneous	Toluene	13.43	4.95	2.7
EO	SiO ₂		36.37	13.80	2.6
EO	SiO ₂ -TiO ₂		36.60	16.02	2.3
EO	TiO ₂		6.91	4.25	1.6
EO	Homogeneous	CB	27.24	8.11	3.4
EO	SiO ₂		50.98	26.52	1.9
EO	SiO ₂ -TiO ₂		37.86	9.64	4.0
EO	TiO ₂		18.16	6.50	2.8

Considering ethylene polymerization in toluene, the supported system (except for TiO₂ support) gave the higher M_w than that of the homogeneous system, and gave narrower MWD. It was suggested that using TiO₂ apparently promoted the chain transfer reaction consequently resulting in lower M_w . The effect of TiO₂ support on the zirconocene/MAO system was also reported by Jongsomjit et al. [85]. However, it was obvious that the titanocene/dMMAO system gives much higher M_w . For ethylene polymerization in CB, the similar trend as seen in toluene was observed. It can be found that ethylene polymerization in CB exhibited narrower MWD than those in toluene (except for SiO₂-TiO₂ support) without a significant change in M_w . This indicated that the SiO₂-TiO₂ supported system in toluene solvent gave the narrower MWD due to higher propagation rate observing from higher M_n . However, it can be concluded that changing of solvent medium slightly affected the M_w of polymer in the ethylene polymerization system.

For ethylene/1-octene copolymerization, it was observed that this copolymerization gave narrower MWD than that ethylene polymerization, and gave higher M_n and M_w . This indicated that the copolymerization exhibited higher propagation rate than the ethylene polymerization.

4.3.3 The effect of various supports and solvent mediums on the thermal properties of polymers

The DSC was performed to measure the thermal properties of polymers. The melting temperatures (T_m) of polymer were evaluated and shown in **Table 4.8**. DSC curves of the polymer are also shown in **Appendix C**.

Table 4.8 Melting temperature and %crystallinity of polymer produced

Polymer	System	Solvent	T_m (°C)	Crystallinity (%) ^a
E	Homogeneous	Toluene	124	14
E	SiO ₂		119	6
E	SiO ₂ -TiO ₂		121	5
E	TiO ₂		122	22
E	Homogeneous	CB	124	18
E	SiO ₂		121	18
E	SiO ₂ -TiO ₂		122	16
E	TiO ₂		120	26
EO	Homogeneous	Toluene	- ^b	- ^c
EO	SiO ₂		-	-
EO	SiO ₂ -TiO ₂		-	-
EO	TiO ₂		-	-
EO	Homogeneous	CB	-	-
EO	SiO ₂		-	-
EO	SiO ₂ -TiO ₂		-	-
EO	TiO ₂		-	-

^a Calculated from heat of crystalline formation based on HDPE

^b Value not be detected from the measurement

^c Cannot be calculated without T_m

It can be observed that for ethylene polymerization the T_m ranged between 119 to 124 °C. It indicated that there was no significant change in T_m . The highest crystallinity was observed in TiO_2 supported system. In general, T_m is proportional to the crystallinity of polymer. This was suggested that using the solvent having high dielectric constant value apparently resulted in increased crystallinity of polymer. However, considering the copolymerization of ethylene/1-octene, no T_m was observed in all systems. The non-crystalline polymers obtained were attributed to the high degree of 1-octene insertion as mentioned before.



สถาบันวิทยบริการ
จุฬาลงกรณ์มหาวิทยาลัย

CHAPTER V

CONCLUSIONS AND RECOMMENDATION

5.1 Conclusions

In summary, for ethylene/1-octene copolymerization, the activities of the supported system were lower than the homogeneous one due to the supporting effect. In the supported system, the SiO₂-TiO₂-supported dMMAO with Ti-complex exhibited the highest activity towards ethylene/1-octene copolymerization in different solvent mediums due to decreased support interaction and steric hindrance. The lowest polymerization activity obtained for the TiO₂ support was due to the strong support interaction. In particular, the dramatic increase in catalytic activity can be achieved using the high dielectric constant solvent medium such as chlorobenzene (CB). It can be proposed that the different solvents can possibly alter the nature of catalyst in two ways; (i) changing the interaction between the support and cocatalyst and/or (ii) changing the form of active species i.e, active ion-pair and solvent-separated ion-pair as seen in the homogeneous system. However, there was no significant change in the observed activity upon the different solvent mediums in the homogeneous system. The presence of CB also resulted in high M_w of polymer. In all cases, the block copolymer was obtained along with high insertion of 1-octene. All obtained polymer also were the non-crystalline polymer.

The ethylene/1-octene copolymerization gave higher activities than the ethylene polymerization due to the second comonomer effect in copolymerization behavior. For ethylene polymerization, the activities of the supported system were also lower than the homogeneous one. In the supported system, the slightly difference in the polymerization activities was apparently found. It was found that the activities in homogeneous system decreased when CB was employed as the solvent medium. It was concluded that too high dielectric constant value of solvent resulted in low activity due to the fully separated ion-pair formed. The supported system (except for TiO₂ support) gave the higher M_w than that of the homogeneous system, and gave narrower MWD. It can be concluded that changing of solvent medium did not affect the M_w of polymer in this system. Moreover, it was observed that the ethylene/1-

octene copolymerization gave narrower MWD than that ethylene polymerization, and gave higher M_n and M_w . This indicated that the copolymerization exhibited higher propagation rate than the ethylene polymerization. The T_m of ethylene polymerization ranged between 119 to 124 °C. The TiO_2 supported system gave the highest crystallinity of polymer. The solvent having high dielectric constant value apparently resulted in increased crystallinity of polymer as seen in CB.

5.2 Recommendations

- Investigation of other supports should be further studied.
- Interaction between support and dMMAO under reaction condition should be performed.
- Effect of other cocatalyst i.e. MAO free activators should be investigated.



สถาบันวิทยบริการ
จุฬาลงกรณ์มหาวิทยาลัย

REFERENCES

1. Kaminsky, W. and Laban, A. Metallocene catalysis. **Applied Catalysis A: General** 222 (2001): 47-61.
2. Reybuck, S. E., Meyer, A., and Waymouth, R. M. Copolymerization behavior of unbridged indenyl metallocenes: Substituent effects on the degree of comonomer incorporation. **Macromolecules** 35 (2002): 637-643.
3. Krentsel B. A., Kissin, Y. V., Kleiner V. J., and Stotskaya L. L. **Polymers and Copolymers of Higher α -Olefins**. Cincinnati. Hanser/Gardner Publications, 1997.
4. Bert, K. E., Crossland, R., Ford, H., and Gardner, A. K. Polyethylene. 1933-83. **Proceeding of the Golden Jubilee Conference, The plastic and Rubber Institute, London** (1983): B1.1-B1.31.
5. Breslow, D. S. and Newburg, N. R. Bis-(cyclopentadienyl)-titaniumdichloride-alkylaluminum complexes as catalysts for the polymerization of ethylene. **Journal of American Chemical Society** 79 (1957): 5072-5073.
6. Reichert, K. H. and Meyer, K. R. **Makromolekular Chemistry** 169 (1973): 163-176.
7. Sinn, H. and Kaminsky, W. Ziegler-Natta Catalyst. **Advances in Organometallic Chemistry** 18 (1980): 99-149.
8. Kashiwa, N. and Imuta, J. Recent progress on olefin polymerization catalysts. **Catalysis Surveys from Japan** 1 (1997): 125-142.
9. Santos, J. H. Z. D., Rosa, M. B. D., Krug, C., Stedile, F. C., Haag, M. C., Dupont, J., and Forte, M. D. C. Effects of ethylene polymerization conditions on the activity of SiO₂-supported zirconocene and on polymer properties. **Journal of Polymer Science Part A: Polymer Chemistry** 37 (1999): 1987-1996.
10. Brintzinger, H-H, Fischer, D., Mulhaupt, R., Rieger, B., and Waymouth, R. M. Stereospecific olefin polymerization with chiral metallocene catalysts. **Angewandte Chemie (International Edition in English)** 34 (1995): 1143-1170.
11. Simanke, A. G., Galland, G. B., Freitas, L., Da Jornada, J. A. H., Quijada, R.,

- and Mauler, R. S. Influence of the comonomer content on the thermal and dynamic mechanical properties of metallocene ethylene/1-octene copolymers. **Polymer** 40 (1999): 5489-5495.
12. Xu, X. R., Xu, J. T., Feng, L. X., and Chen, W. Effect of short chain-branching distribution on crystallinity and modulus of metallocene-based ethylene-butene copolymers. **Journal of Applied Polymer Science** 77 (2000): 1709-1715.
 13. Hlatky, G. G. Heterogeneous single-site catalysts for olefin polymerization. **Chemical Review** 100 (2000): 1347-1376.
 14. Dankova, M. and Waymouth, R. M. High comonomer selectivity in ethylene/hexene copolymerization by unbridged indenyl metallocenes. **Macromolecules** 36 (2003): 3815-3820.
 15. Galimberti, M., Piemontesi, F., Mascellani, N., Camurati, I., Fusco, O., and Destro, M. Metallocenes for ethene/propene copolymerizations with high product of reactivity ratios. **Macromolecules** 32 (1999): 7968-7976.
 16. Schneider, M. J., Suhm, J., Mulhaupt, R., Prosenc, M.-H., and Brintzinger, H.-H. Influence of indenyl ligand substitution pattern on metallocene-catalyzed ethene copolymerization with 1-octene. **Macromolecules** 30 (1997): 3164-3168.
 17. Yano, A., Hasegawa, S., Kaneko, T., Sone, M., Sato, M., and Akimoto, A. Ethylene/1-hexene copolymerization with $\text{Ph}_2\text{C}(\text{Cp})(\text{Flu})\text{ZrCl}_2$ derivatives: correlation between ligand structure and copolymerization behavior at high temperature. **Macromolecular Chemistry and Physics** 200 (1999): 1542-1553.
 18. Marques, M., Conte, A., De Resende, F. C., and Chaves, E. G. Copolymerization of ethylene and 1-octene by homogeneous and different supported metallocenic catalysts. **Journal of Applied Polymer** 82 (2001): 724-730.
 19. Jacobs, G., Das, T. K., Zhang, Y., Li, J., Racoillet, G., and Davis, B. H. Fischer-Tropsch synthesis: Support, loading, and promoter effects on the reducibility of cobalt catalysts. **Applied Catalysis A: General** 233 (2002): 263-281.
 20. Quijada, R., Retuert, J., Gurvara, J. L., Rojas, R., Valle, M., Saavedra, P., Palza,

- H., and Galland, G. B. Results coming from homogeneous and supported metallocene catalysts in the homo- and copolymerization of olefins. **Macromolecular Symposia** 189 (2002): 111-125.
21. Ribeiro, M. R., Deffieux, A., and Portela, M. F. Supported metallocene complexes for ethylene and propylene polymerizations: Preparation and activity. **Industrial and Engineering Chemistry Research** 36 (1997): 1224-1237.
 22. Chu, K. J.; Soares, J. B. P. and Penlidis, A. Polymerization mechanism for in situ supported metallocene catalysts. **Journal of Polymer Science Part A: Polymer Chemistry** 38 (2000): 462-468.
 23. Gao, X. and Wachs, I. E. Titania-silica as catalysts: Molecular structural characteristics and physico-chemical properties. **Catalysis Today** 51 (1999): 233-254.
 24. Quijada, R., Galland, G. B., and Mauler, R. S. The influence of the comonomer in the copolymerization of ethylene with α -olefins using $C_2H_4[Ind]_2ZrCl_2$ /methylaluminoxane as catalyst system. **Macromolecular Chemistry and Physics** 197 (1996): 3091-3098.
 25. James, C. V., James, C. W. C., Caddam, N. B., and Richard, A. N. Effect of polarity of the medium on the stereospecific polymerization of propylene by ansa-zirconocene catalyst. **Journal of Polymer Science Part A: Polymer Chemistry** 32 (1994): 2049-2056.
 26. Coevoet, D., Cramail, H., and Deffieux, A. Activation of *rac*-ethylenebis(indenyl)zirconium dichloride with a low amount of methylaluminoxane (MAO) for olefin polymerizations. **Macromolecular Chemistry and Physics** 197 (1996): 885-867.
 27. Yang, S. H., Huh, J., and Jo, W. H. Effect of solvent polarity on the initiation and the propagation of ethylene polymerization with constrained geometry catalyst/MAO catalytic system: A density functional study with the conductor-like screening model. **Macromolecules** 38 (2005): 1402-1409.
 28. Forlini, F., Princi, E., Tritto, I., Sacchi, M. C., and Piemontesi, F. ^{13}C NMR Study of the effect of coordinating solvents on zirconocene-catalyzed propene/1-hexene copolymerization. **Macromolecular Chemistry and Physics** 203 (2002): 645-652.
 29. Nishii, K., Matsumae, T., Dare, E. O., Shiono, T., and Ikeda, T. Effect of

- solvents on living polymerization of propylene with [*t*-BuNSiMe₂Flu] TiMe₂-MMAO catalyst system. **Macromolecular Chemistry and Physics** 205 (2004): 363-369.
30. Nishii, K., Shiono, T., and Ikeda, T. A novel synthetic procedure for stereoblock poly(propylene) with a living polymerization system. **Macromolecular Rapid Communications** 25 (2004): 1029-1032.
 31. Soga, K., Uozumi, T., Nakamura, S., Toneri, T., Teranishi, T., Sano, T., Arai, T., and Shiono, T. Structures of polyethylene and copolymers of ethylene with 1-octene and oligoethylene produced with the Cp(2)ZrCl(2) and [(C(5)Me(4))SiMe(2)N(*t*-Bu)]TiCl₂ catalysts. **Macromolecular Chemistry and Physics** 197 (1996): 4237-4251.
 32. Hasan, T., Nishii, K., Shiono, T., and Ikeda, T. Living polymerization of norbornene via vinyl addition with ansa-fluorenylamidodimethyltitanium complex. **Macromolecules** 35 (2002): 8933-8935.
 33. Nishii, K., Hagihara, H., Ikeda, T., Akita, M., and Shiono, T. Stereospecific polymerization of propylene with group 4 ansa-fluorenylamidodimethyl complexes. **Journal of Organometallic Chemistry** 691 (2006): 193-201.
 34. Nishii, K., Ikeda, T., Akita, M., and Shiono, T. Polymerization of propylene with [*t*-BuNSiMe(2)Ind]TiMe₂-MAO catalyst systems. **Journal of Molecular Catalysis A: Chemical** 231 (2005): 241-246.
 35. Hasan, T., Ikeda, T., and Shiono, T. Random copolymerization of propene and norbornene with ansa-fluorenylamidodimethyltitanium-based catalysts. **Macromolecules** 38 (2005): 1071-1074.
 36. Hasan, T., Ikeda, T., and Shiono, T. Ethene-norbornene copolymer with high norbornene content produced by ansa-fluorenylamidodimethyltitanium complex using a suitable activator. **Macromolecules** 37 (2004): 8503-8509.
 37. Ioku, A., Hasan, T., Shiono, T., and Ikeda, T. Effects of cocatalysts on propene polymerization with [*t*-BuNSiMe₂(CSMe₄)]TiMe₂. **Macromolecular Chemistry and Physics** 203 (2002): 748-755.
 38. Shiono, T., Yoshida, S., Hagihara, H., and Ikeda, T. Additive effects of trialkylaluminum on propene polymerization with (*t*-BuNSiMe(2)Flu) TiMe₂-based catalysts. **Applied Catalysis A: General** 200 (2000): 145-152.

39. Intaragamjon, N., Shiono, T., Jongsomjit, B., and Praserttham, P. Elucidation of solvent effects on the catalytic behaviors for $[t\text{-BuNSiMe}_2\text{Flu}]\text{TiMe}_2$ complex during ethylene/1-hexene copolymerization. **Catalysis Communications** 7 (2006): 721–727.
40. Hagihara, H., Shiono, T., and Ikeda, T. Living polymerization of propane and 1-hexene with the $[t\text{-BuNSiMe}(2)\text{Flu}]\text{TiMe}_2/\text{B}(\text{C}_6\text{F}_5)(3)$ catalyst. **Macromolecules** 31 (1998): 3184-3188.
41. Ioku A, Shiono, T, and Ikeda, T. Supporting effect of methylaluminoxane on propene polymerization with monocyclopentadienylalkyltitanium derivatives. **Applied Catalysis A: General** 226 (2002): 15-22.
42. Sinclair, K. B. and Wilson, R. B. Metallocene catalysis - A revolution in olefin polymerization. **Chemistry & Industry** 7 (1994): 857-862.
43. Helmut, G.A. and Koppl, A. Effect of the nature of metallocene complexes of group IV metals on their performance in catalytic ethylene and propylene polymerization. **Chemical Review** 100 (2000): 1205-1222.
44. Gupta, V. K., Satish, S., and Bhardwaj, I. S. Metallocene complexes of group 4 elements in the polymerization of monoolefins. **Journal of Macromolecular Science - Reviews in Macromolecular Chemistry and Physics** C34, No.3 (1994): 439-514.
45. Pasyankiewicz, S. Aluminoxanes-synthesis, structure, complexes, and reactions. **Polyhedron** 9 (1990): 429-453.
46. Koide, Y., Bott, S. G., and Barron, A. R. Alumoxanes as cocatalysts in the palladium-catalyzed copolymerization of carbon monoxide and ethylene: Genesis of a structure-activity relationship. **Organometallics** 15 (1996): 2213-2226.
47. Sinn, H. Proposals for structure and effect of methylalumoxane bases on mass balances and phase-separation experiments. **Macromolecular Symposia** 97 (1995): 27-52.
48. Ystenes, M., Eilertsen, J. L., Liu, J. K., Ott, M., Rytter, E., and Stovneng, J. A. Experimental and theoretical investigations of the structure of methylaluminoxane (MAO) cocatalysts for olefin polymerization. **Journal of Polymer Science Part A: Polymer Chemistry** 38 (2000): 3106-3127.
49. Mason, M. R., Smith, J. M., Bott, S. G., and Barron, A. R. Hydrolysis of tri-

- tert*-butylaluminum: The first structural characterization of alkylalumoxanes $[(R_2Al)_2O]_n$ and $(RAIO)_n$. **Journal of the American Chemical Society** 115 (1993): 4971-4984.
50. Chen, E. Y. X. and Marks, T. J. Cocatalysts for metal-catalyzed olefin polymerization: Activators, activation processes, and structure-activity relationships. **Chemical Reviews** 100 (2000): 1391-1434.
 51. Giannetti, E., Nicolett, G. M., and Mazzocchi, R. Homogeneous Ziegler-Natta catalyst. II. Ethylene polymerization by IVB transition metal complexes/methyl aluminoxane catalyst systems. **Journal of polymer science Part A-1: Polymer chemistry** 23 (1985): 2117-2134.
 52. Tritto, I., Mealares, C., Sacchi, M. C., and Locatelli, P. Methylaluminoxane: NMR analysis, cryoscopic measurements and cocatalytic ability in ethylene polymerization. **Macromolecular Chemistry and Physics** 198 (1997): 3963-3977.
 53. Cam, D. and Giannini, U. **Makromolekular Chemistry** 193 (1992): 1049-1055.
 54. Katayama, H., Shiraishi, H., Hino, T., Ogane, T., and Imai, A. The effect of aluminum compounds in the copolymerization α -olefins. **Macromolecular Symposia** 97 (1995): 109-118.
 55. Hagimoto, H., Shiono, T., and Ikeda, T. Supporting effects of methylaluminoxane on the living polymerization of propylene with a chelating (diamide) dimethyltitanium complex. **Macromolecular Chemistry and Physics** 205 (2004): 19-26.
 56. Resconi, L., Abis, L., and Francisocono, G. 1-Olefin polymerization at bis(pentamethylcyclopentadienyl)zirconium and -hafnium centers: Enantioface selectivity. **Macromolecules** 25(1992): 6814-6817.
 57. Ciardelli, F., Altomare, A., and Carlini, C. Chiral discrimination in the polymerization of α -olefins by Ziegler-Natta initiator systems. **Progress in Polymer Science** 16(1991): 259-277.
 58. Ewen J. A. Mechanisms of stereochemical control in propylene polymerizations with soluble group 4B metallocene/methylalumoxane catalysts. **Journal of the American Chemical Society** 106(1984): 6355-6364.
 59. Huang, J. and Rempel, G. L. Ziegler-Natta catalysts for olefin polymerization: Mechanistic insights from metallocene systems. **Progress in Polymer Science** 20 (1995): 459-526.

60. Tsutsui, T., Mizuno, A., and Kashiwa, N. Effect of hydrogen on propene polymerization with ethylenebis(1-indenyl)zirconium dichloride and methylalumoxane catalyst system. **Macromolecular Rapid Communications** 11 (1990): 565-570.
61. Resconi, L., Piemontesi, F., Francisocono, G., Abis, L., and Fiorani, T. Olefin polymerization at bis(pentamethylcyclopentadienyl)zirconium and hafnium centers: Chain-transfer mechanisms. **Journal of the American Chemical Society** 114 (1992): 1025-1032.
62. Kaminsky, W. New polymers by metallocene catalysis. **Macromolecular Chemistry and Physics** 197 (1996): 3907-3945.
63. Kaminsky, W., Ahlers, A., and Steiger, R. Stereospecific polymerization by metallocene/aluminoxane catalysts. **Journal of Molecular Catalysis A: Chemical** 74 (1992): 109-119.
64. Fischer, D., Jungling, S., and Mulhaupt, R. Donor- and acceptor-modified metallocene-based homogeneous Ziegler-Natta catalysts **Makromolekular Chemistry Macromolekular Symposia** 66 (1993): 191-202.
65. Ferreira, M. L., Belelli, P. G., Juan, A., and Damiani, D. E. Theoretical and experimental study of the interaction of methylaluminoxane (MAO)-low temperature treated silica: Role of trimethylaluminium (TMA) **Macromolecular Chemistry and Physics** 201 (2000): 1334-1344.
66. Kaminsky, W. and Strübel, C. Gas-phase polymerization of 1,3-butadiene with supported half-sandwich-titanium-complexes. **Macromolecular Chemistry and Physics** 201 (2000): 2519-2531.
67. Collins, S., Kelly, W. M., and Holden, D.A. Polymerization of propylene using supported, chiral, ansa-metallocene catalysts: Production of polypropylene with narrow molecular weight distributions. **Macromolecules** 25 (1992): 1780-1785.
68. Hlatky, G. G. and Upton, D. J. Supported ionic metallocene polymerization catalysts. **Macromolecules** 29 (1996): 8019-8020.
69. Lee, D. H., Shin, S. Y., and Lee, D. H. Ethylene polymerization with metallocene and trimethylaluminum-treated silica. **Macromolecular Symposia** 97 (1995): 195-203.
70. Harrison, D., Coulter, I. M., Wang, S., Nistala, S., Kuntz, B. A., Pigeon, M.,

- Tian, J., and Collins, S. Olefin polymerization using supported metallocene catalysts: Development of high activity catalysts for use in slurry and gas phase ethylene polymerizations. **Journal of Molecular Catalysis A: Chemical** 128 (1998): 65-77.
71. Soga, K., Kim, H. J., and Shiono, T. Highly isospecific SiO₂-supported zirconocene catalyst activated by ordinary alkylaluminiums. **Macromolecular Rapid Communications** 15 (1994): 139-144.
72. Iiskola, E. I., Timonen, S., Pakkanen, T. T., Harkki, O., Lehmus, P., and Seppälä, J. V. Cyclopentadienyl surface as a support for zirconium polyethylene catalysts. **Macromolecules** 30 (1997): 2853-2859.
73. Lee, D., Yoon, K., and Noh, S. Polymerization of ethylene by using zirconocene catalyst anchored on silica with trisiloxane and pentamethylene spacers. **Macromolecular Rapid Communications** 18 (1997): 427-431.
74. Albano, C., Sánchez, G., and Ismayel, A. Influence of a copolymer on the mechanical properties of a blend of PP and recycled and non-recycled HDPE. **Polymer Bulletin** 41 (1998): 91-98.
75. Shan, C. L. P., Soares, J. B. P., and Penlidis, A. Ethylene/1-octene copolymerization studies with in situ supported metallocene catalysts: Effect of polymerization parameters on the catalyst activity and polymer microstructure. **Journal of Polymer Science Part A: Polymer Chemistry** 40 (2002): 4426-4451.
76. Shan, C. L. P., Chu, K. J., Soares, J., and Penlidis, A. Using alkylaluminium activators to tailor short chain branching distributions of ethylene/1-hexene copolymers produced with in-situ supported metallocene catalysts. **Macromolecular Chemistry and Physics** 201 (2000): 2195-2202.
77. Przybyła, C., Tesche, B., and Fink, G. Ethylene hexene copolymerization with the heterogeneous catalyst system SiO₂/MAO/*rac*-Me₂Si[2-Me-4-Ph-Ind](2)ZrCl₂: The filter effect. **Macromolecular Rapid Communications** 20 (1999): 328-332.
78. Härkki, O., Lehmus, P., Leino, R., Luttikhedde, H. J. G., Näsman, J. H., and Seppälä, J. V. Copolymerization of ethylene with 1-hexene or 1-hexadecene over siloxy-substituted metallocene catalysts.

- Macromolecular Chemistry and Physics** 200 (1999): 1561-1565.
79. Steinmetz, B., Tesche, B., Przybyla, C., Zechlin, J., and Fink, G. Polypropylene growth on silica-supported metallocene catalysts: A microscopic study to explain kinetic behavior especially in early polymerization stages. **Acta Polymerica** 48 (1997): 392-399.
80. Soga, K. and Kaminaka, M. **Makromolekulare Chemie Rapid Communications** 13 (1992): 221-224.
81. Nowlin, T. E., Kissin, Y. V., and Wagner, K. P. High activity Ziegler-Natta catalysts for the preparation of ethylene copolymers. **Journal of Polymer Science Part A: Polymer Chemistry** 26 (1988): 755-764.
82. De Fatima V., Marques, M., Conte, A., De Resende, F. C., and Chaves, E. G. Copolymerization of ethylene and 1-octene by homogeneous and different supported metallocenic catalysts. **Journal of Applied Polymer Science** 82 (2001): 724-730.
83. Kim, J. D. and Soares, J. B. P. Copolymerization of ethylene and 1-hexene with supported metallocene catalysts: Effect of support treatment. **Macromolecular Rapid Communications** 20 (1999): 347-350.
84. Looveren, L. K. V., Geysen, D. F., Vercruyssen, K. A., Wouters, B. H., Grobet, P. J., and Jacobs, P. A. Methylalumoxane MCM-41 as Support in the Co-Oligomerization of Ethene and Propene with [$\{C_2H_4(1\text{-indenyl})_2\}Zr(CH_3)_2$]. **Angewandte Chemie (International Edition in English)** 37 (1998): 517-520.
85. Jongsomjit, B., Ngamposri, S., and Praserthdam, P. Role of titania in TiO_2 - SiO_2 mixed oxides-supported metallocene catalyst during ethylene/1-octene copolymerization. **Catalysis Letters** 100 (2005): 139-146.
86. Forlini, F., Tritto, I., Locatelli, P., Sacchi, M.C., and Piemontesi, F. ^{13}C NMR studies of zirconocene-catalyzed propylene/1-hexene copolymers: In-depth investigation of the effect of solvent polarity. **Macromolecular Chemistry and Physics** 201 (2000): 401-408.
87. Randall, J. C. A review of high resolution liquid ^{13}C nuclear magnetic resonance characterization of ethylene-based polymers. **Journal of Macromolecular Science, Reviews in Macromolecular Chemistry and Physics** C29 (1989): 201.
88. Jongsomjit, B., Sakdamnusun, C., Goodwin, Jr., J.G., and Praserthdam, P.

- Co-support compound formation in titania-supported cobalt catalyst. **Catalysis Letters** 94 (2004) 209-215.
89. Jongsomjit, B., Wongsalee, T., and Praserttham, P. Catalytic behaviors of mixed TiO₂-SiO₂-supported cobalt Fischer-Tropsch catalysts for carbon monoxide hydrogenation. **Materials Chemistry and Physics** 97 (2006): 343-350.
90. Hagimoto H., Shiono, T., and Ikeda, T. Supporting effects of methylaluminumoxane on the living polymerization of propylene with a chelating (diamide)dimethyltitanium complex. **Macromolecular Chemistry and Physics** 205 (2004): 19-26.
91. Riva, R., Miessner, H., Vitali, R., and Piero, G. D. Metal-support interaction in Co/SiO₂ and Co/TiO₂. **Applied Catalysis A: General** 196 (2000): 111-123.
92. Severn, J. R., Chadwick, J. C., Duchateau, R., and Friederichs, N. "Bound but not gagged" - Immobilizing single-site α -olefin polymerization catalysts. **Chemical Reviews** 105 (2005): 4073-4147.
93. Kleinschmidt, R., Griebenow, Y., and Fink, G. Stereospecific propylene polymerization using half-sandwich metallocene/MAO systems: A mechanistic insight. **Journal of Molecular Catalysis A: Chemical** 157 (2000): 83-90.
94. Forlini, F., Fan, Z. Q., Tritto, I., and Locatelli, P. Metallocene-catalyzed propene/1-hexene copolymerization: Influence of amount and bulkiness of cocatalyst and of solvent polarity. **Macromolecular Chemistry and Physics** 198 (1997): 2397-2408.
95. Liu, S., Yu, G., and Huang, B. Polymerization of ethylene by zirconocene-B(C₆F₅)₃ catalysts with aluminum compounds. **Journal of Applied Polymer Science** 66 (1997): 1715-1720.



APPENDICES

สถาบันวิทยบริการ
จุฬาลงกรณ์มหาวิทยาลัย



APPENDIX A
(Gel Permeation Chromatography)

สถาบันวิทยบริการ
จุฬาลงกรณ์มหาวิทยาลัย

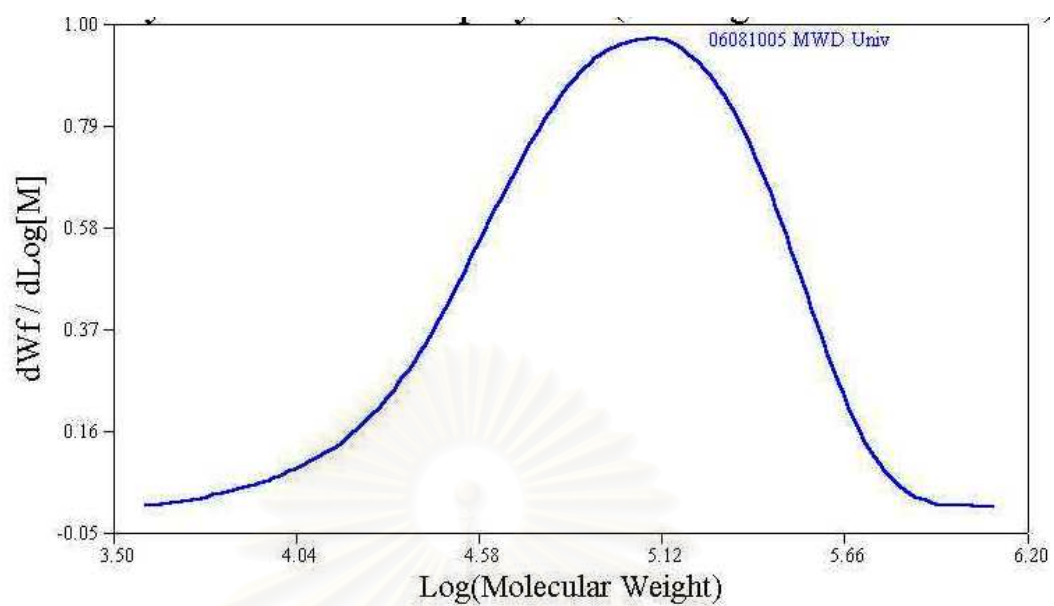


Figure A-1. GPC curve of ethylene/1-octene copolymer produce with homogeneous in toluene

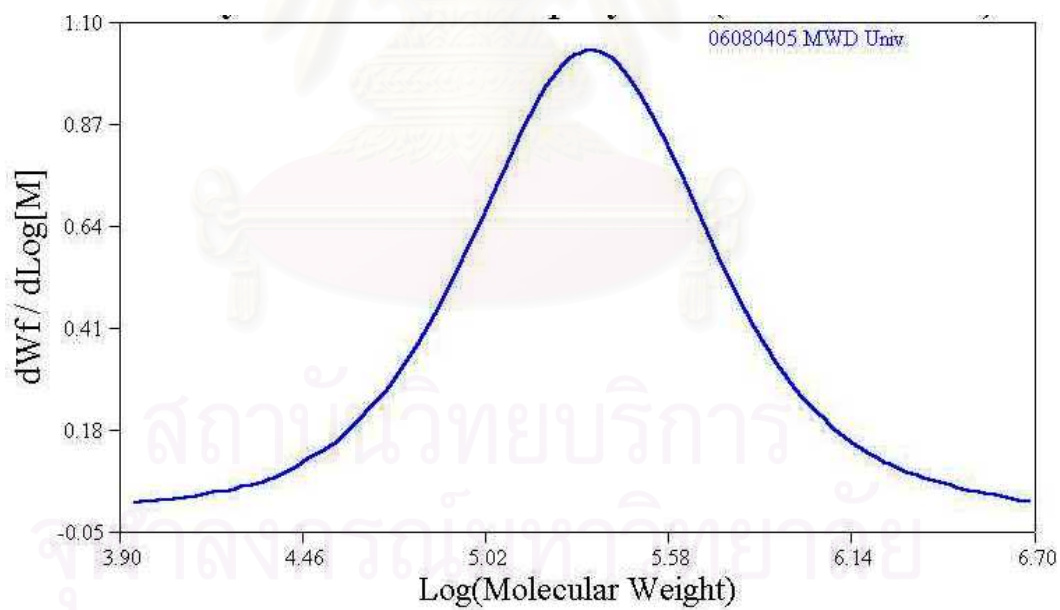


Figure A-2. GPC curve of ethylene/1-octene copolymer produce with SiO_2 in toluene

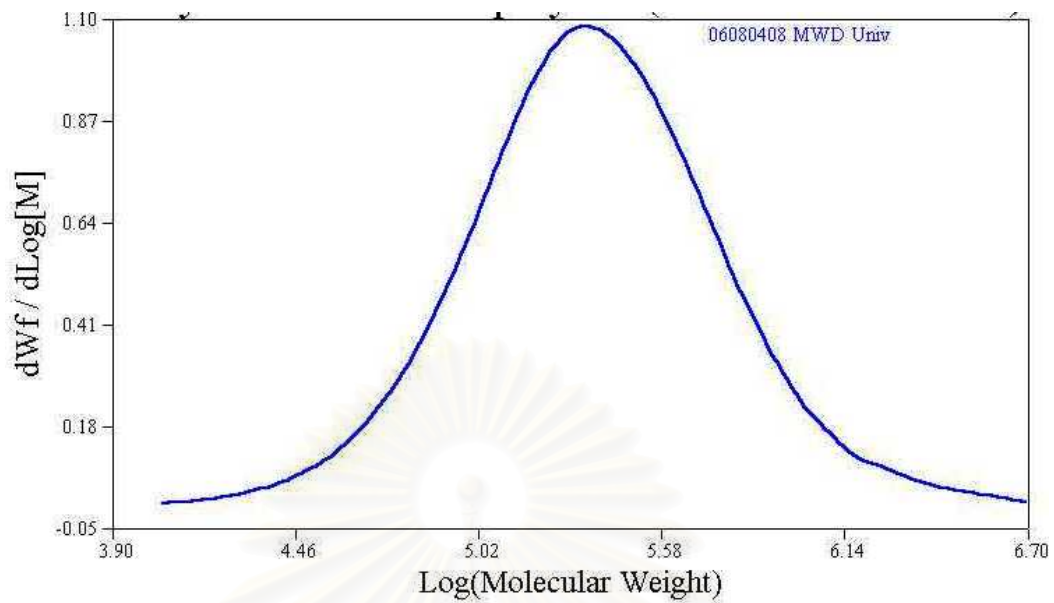


Figure A-3. GPC curve of ethylene/1-octene copolymer produce with SiO_2-TiO_2 in toluene

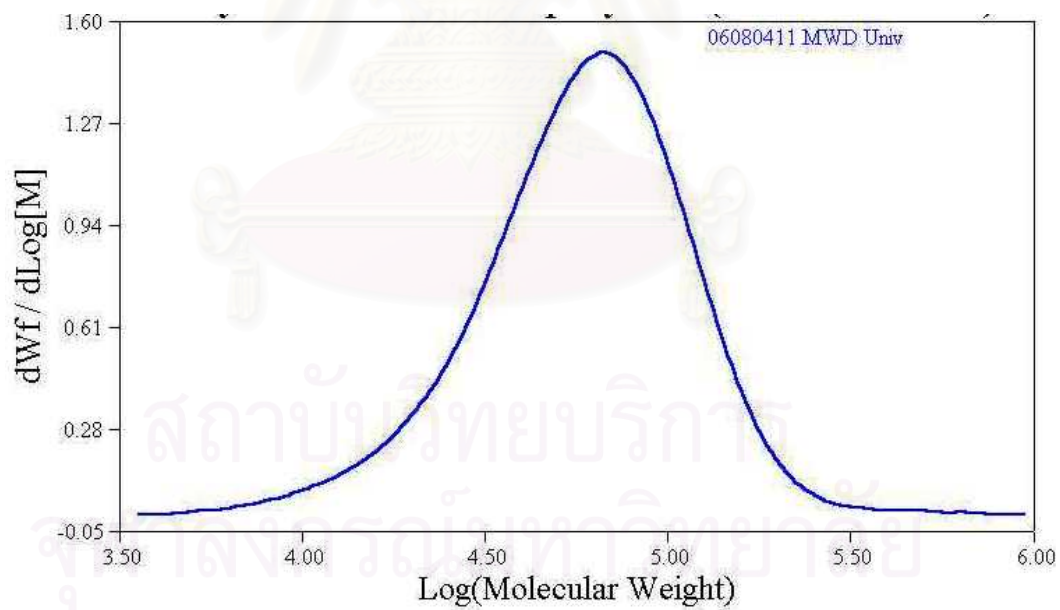


Figure A-4. GPC curve of ethylene/1-octene copolymer produce with TiO_2 in toluene

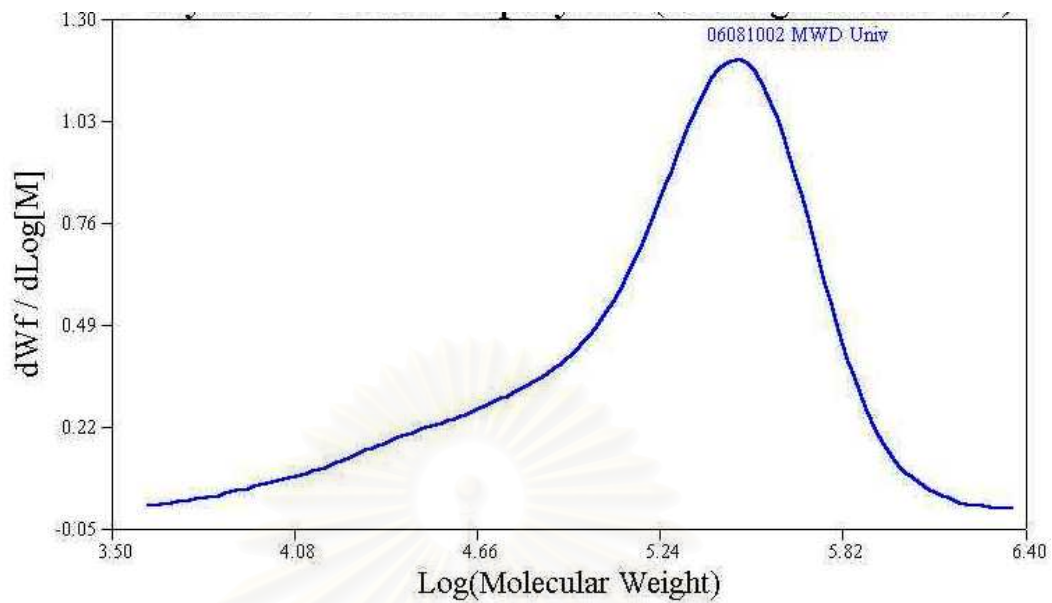


Figure A-5. GPC curve of ethylene/1-octene copolymer produce with homogeneous in chlorobenzene

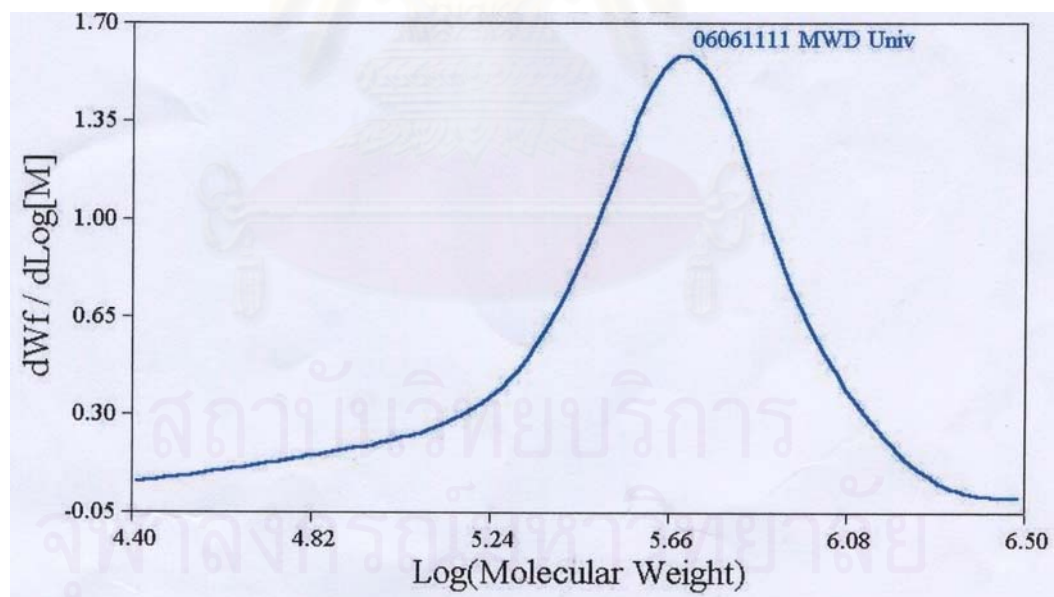


Figure A-6. GPC curve of ethylene/1-octene copolymer produce with SiO_2 in chlorobenzene

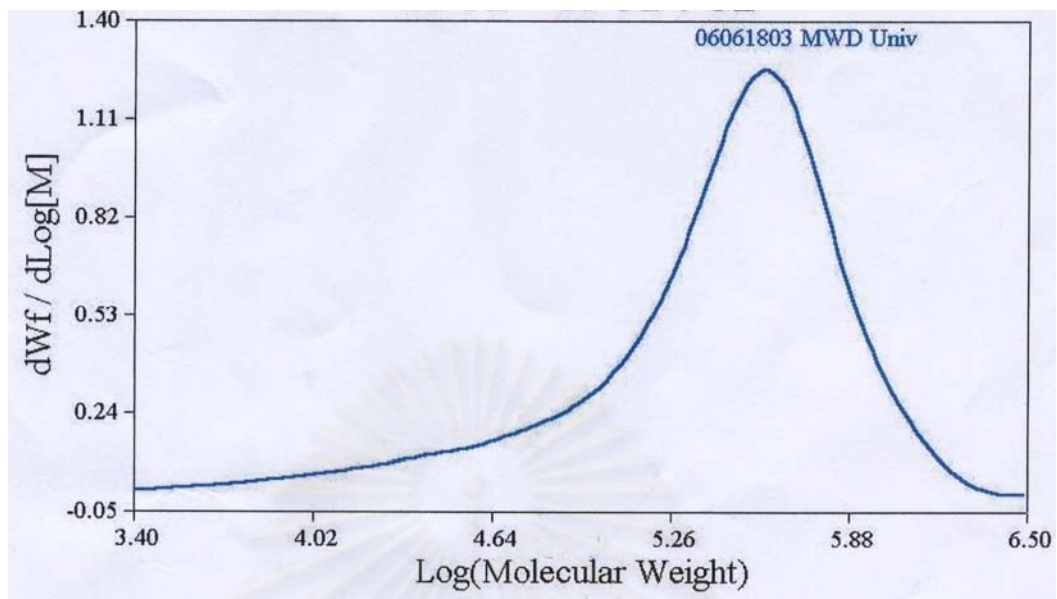


Figure A-7. GPC curve of ethylene/1-octene copolymer produce with SiO_2-TiO_2 in chlorobenzene

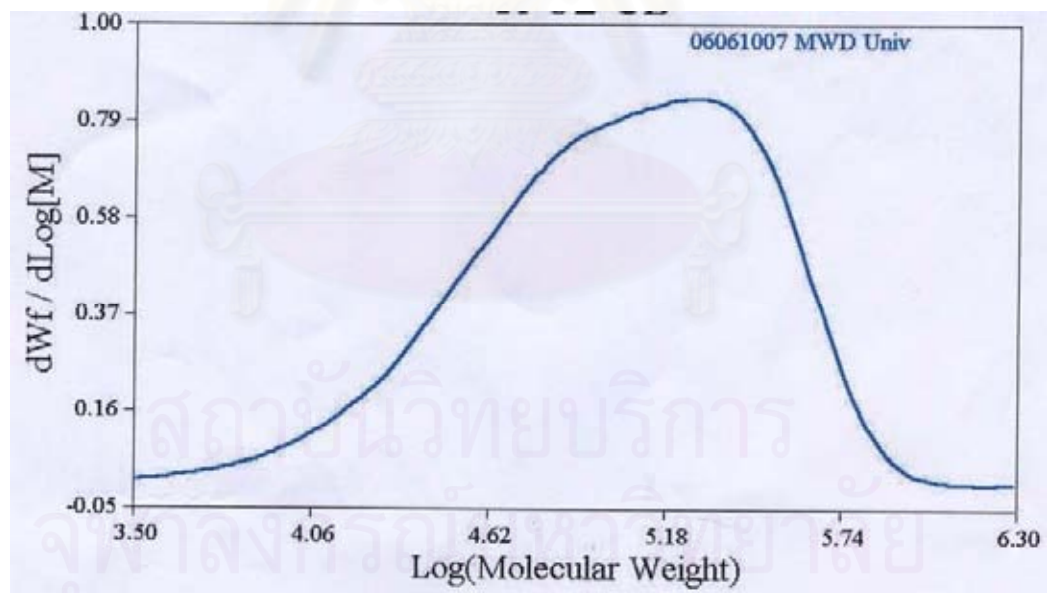


Figure A-8. GPC curve of ethylene/1-octene copolymer produce with TiO_2 in chlorobenzene

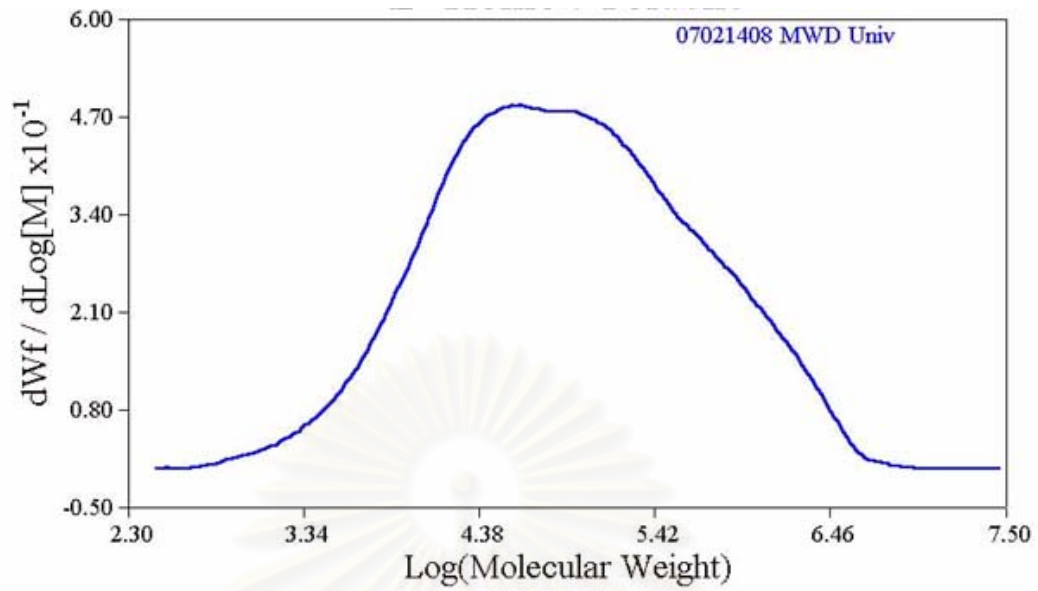


Figure A-9. GPC curve of polyethylene produce with homogeneous in toluene

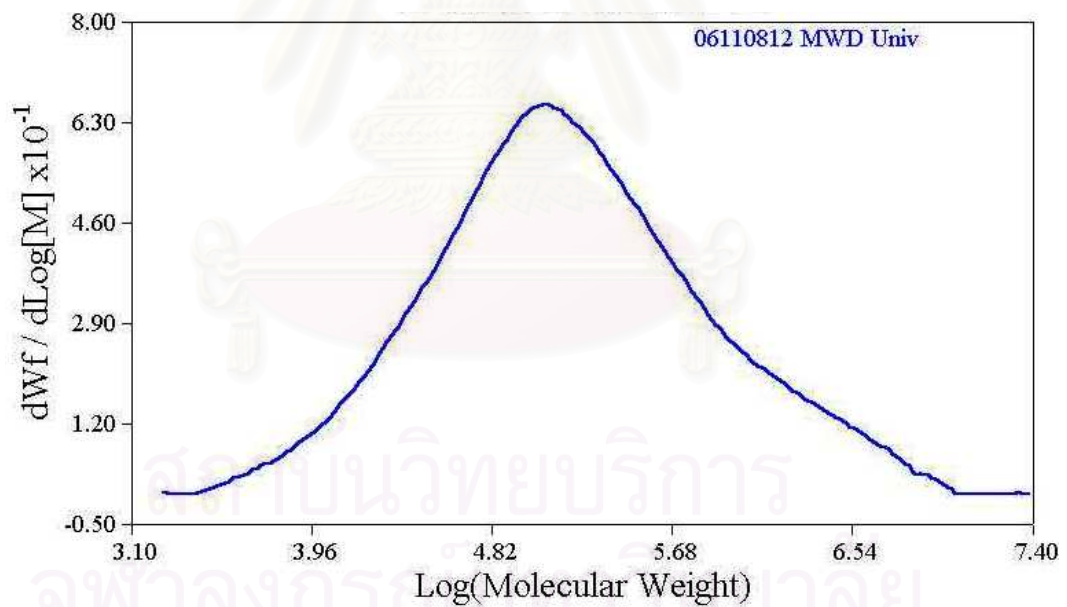


Figure A-10. GPC curve of polyethylene produce with SiO₂ in toluene

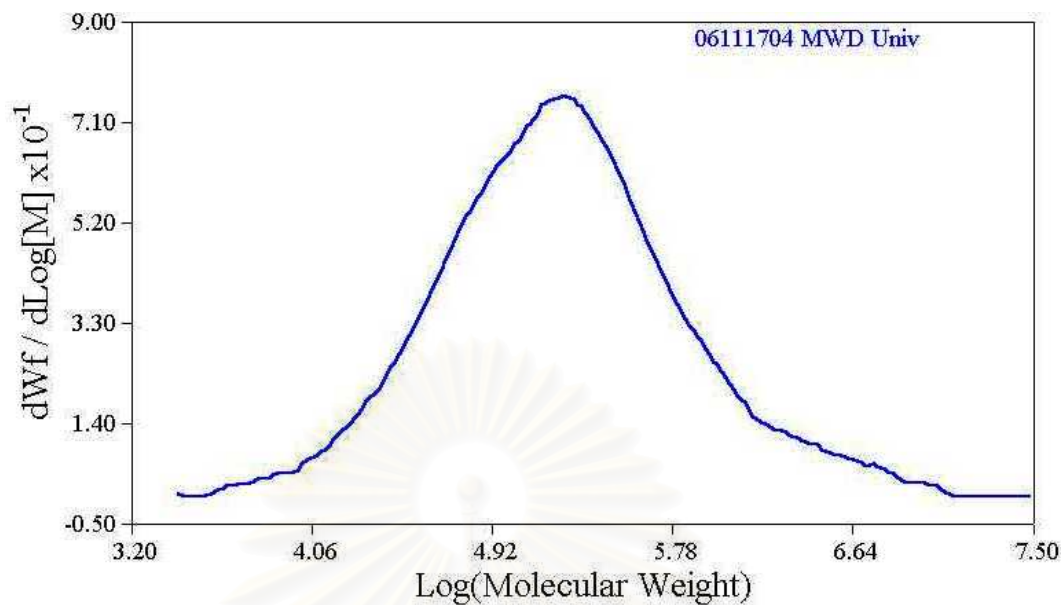


Figure A-11. GPC curve of polyethylene produce with $\text{SiO}_2\text{-TiO}_2$ in toluene

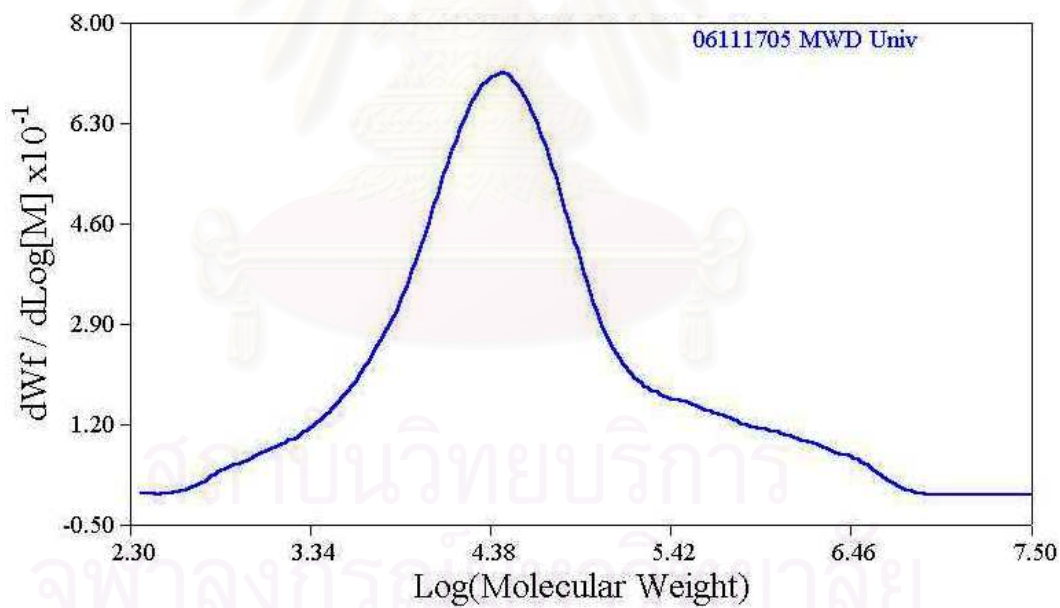


Figure A-12. GPC curve of polyethylene produce with TiO_2 in toluene

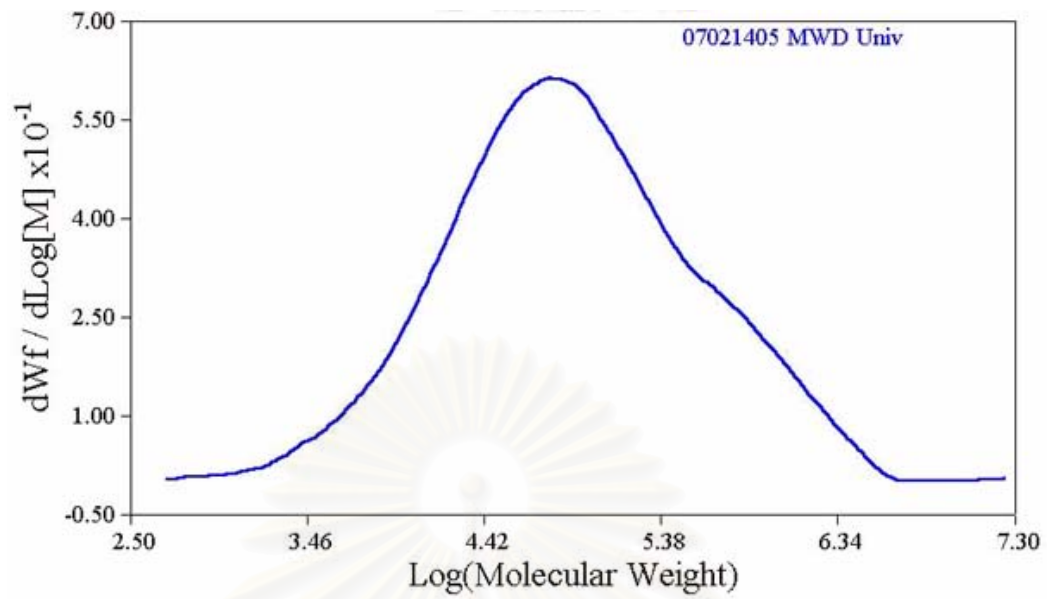


Figure A-13. GPC curve of polyethylene produce with homogeneous in chlorobenzene

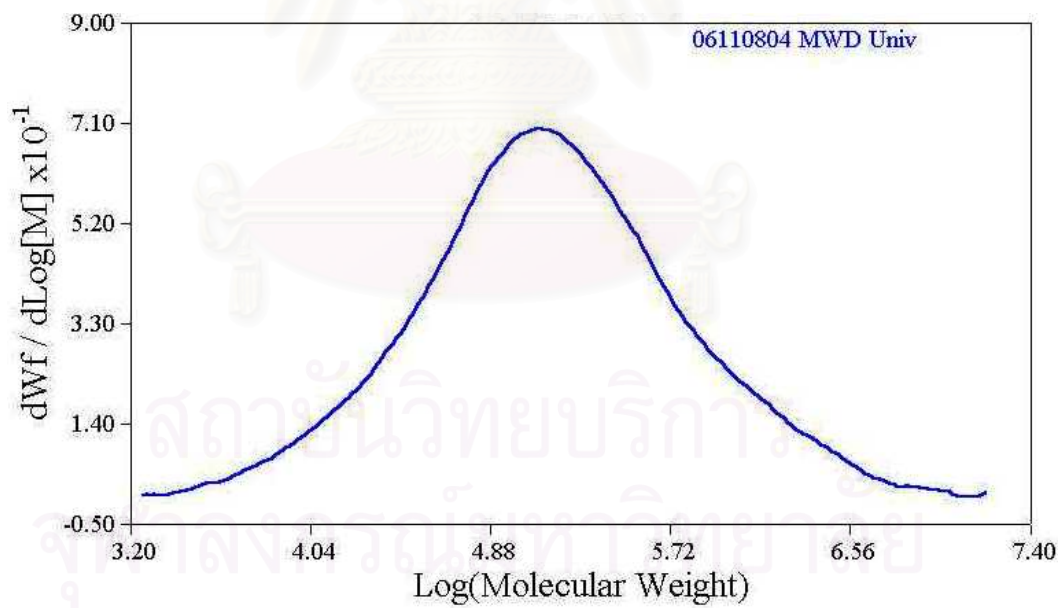


Figure A-14. GPC curve of polyethylene produce with SiO_2 in chlorobenzene

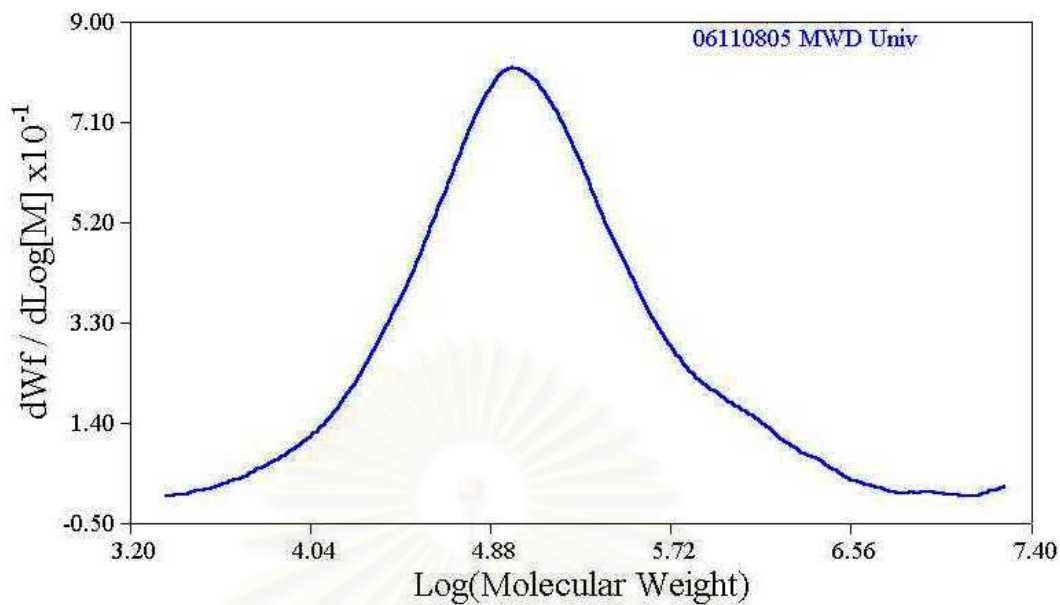


Figure A-15. GPC curve of polyethylene produce with SiO₂-TiO₂ in chlorobenzene

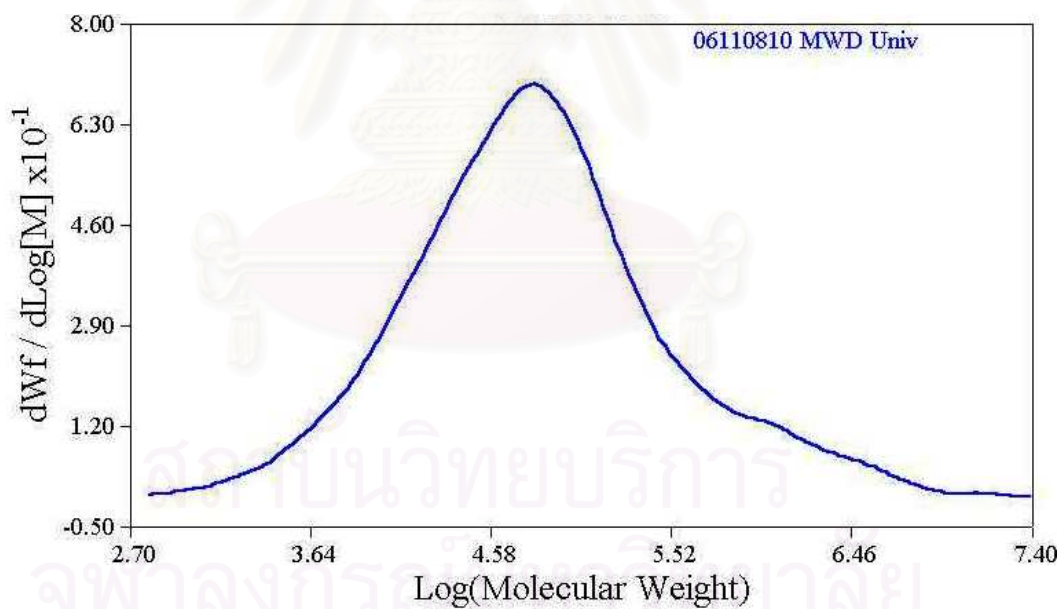
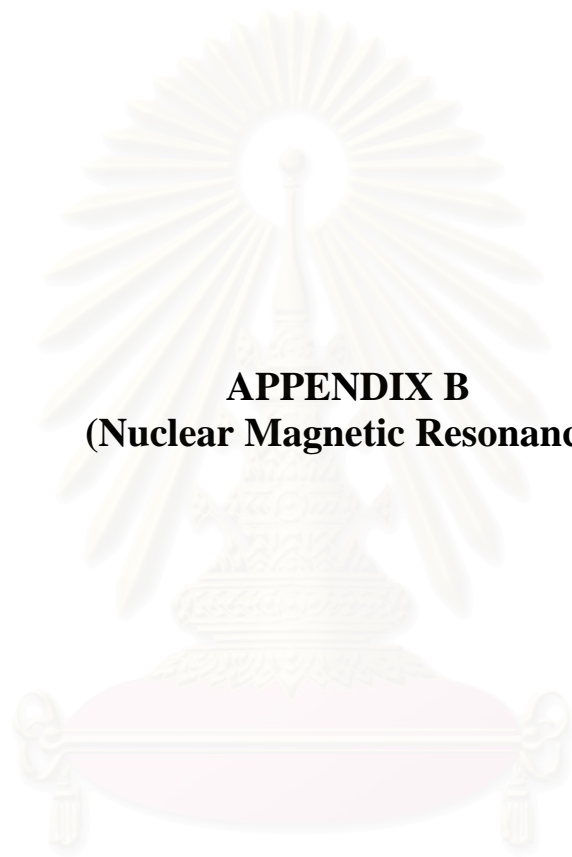


Figure A-16. GPC curve of polyethylene produce with TiO₂ in chlorobenzene



APPENDIX B
(Nuclear Magnetic Resonance)

สถาบันวิทยบริการ
จุฬาลงกรณ์มหาวิทยาลัย

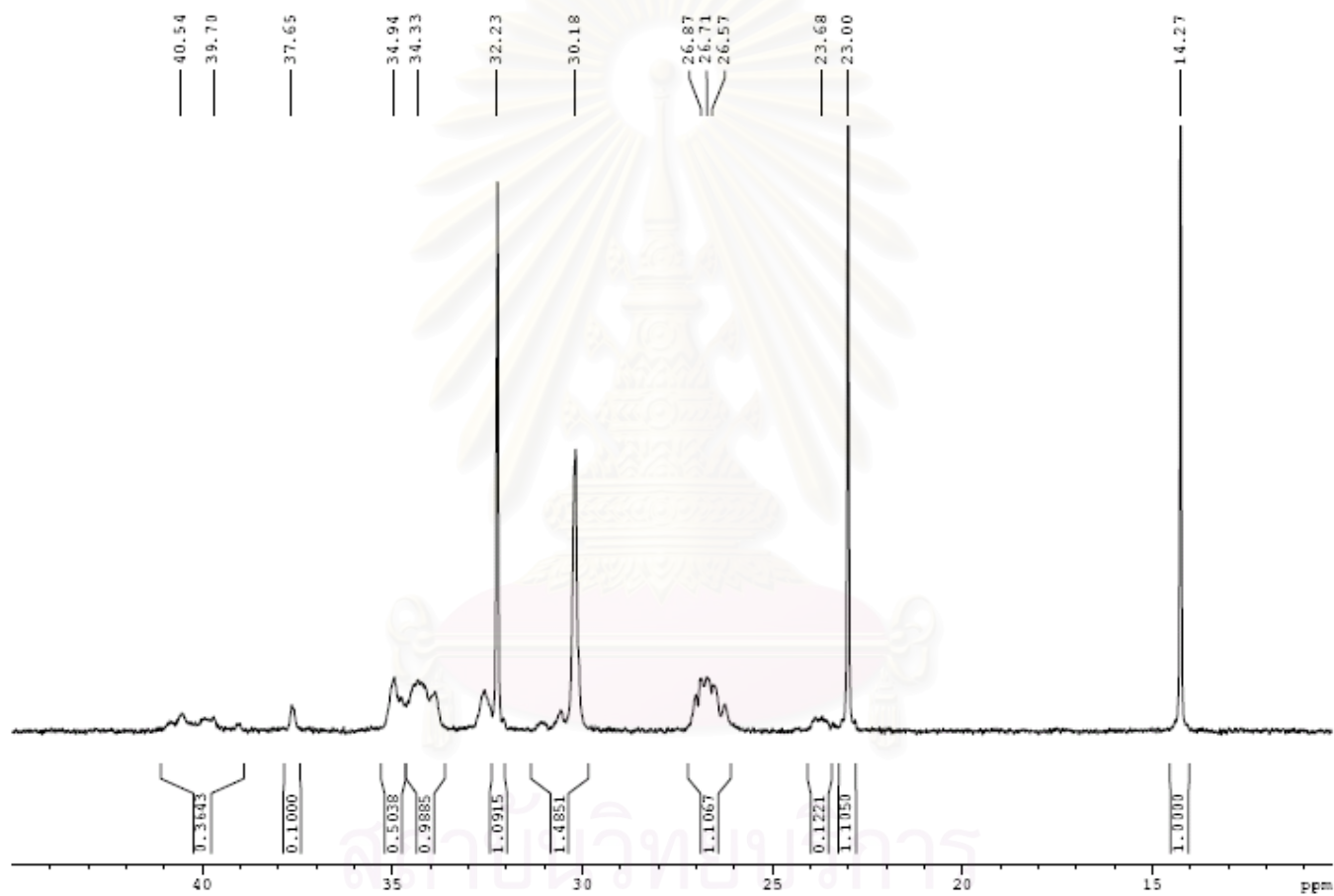


Figure B-1. ^{13}C NMR spectrum of ethylene/1-octene copolymer produced with homogeneous in toluene

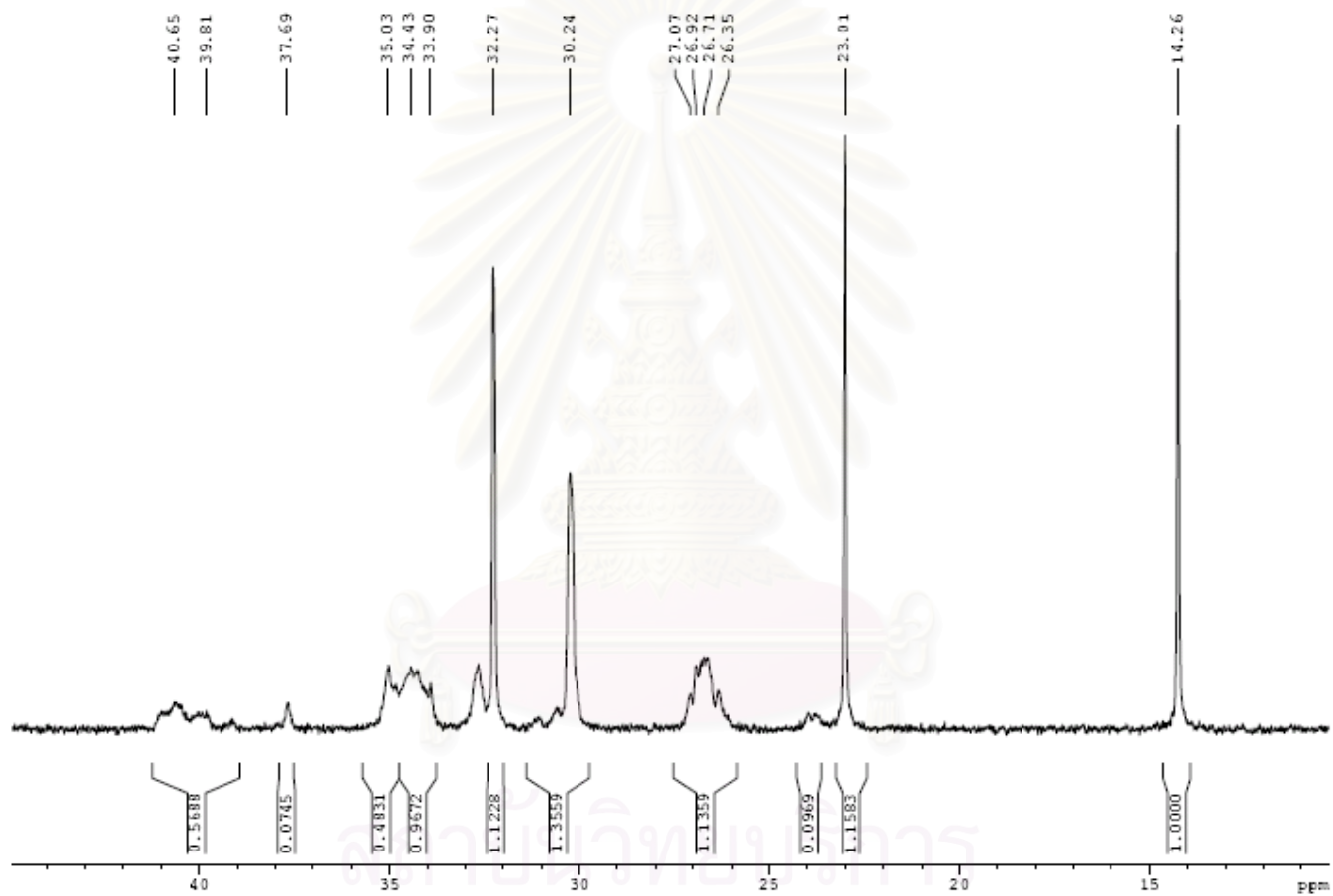


Figure B-2. ^{13}C NMR spectrum of ethylene/1-octene copolymer produces with SiO_2 support in toluene

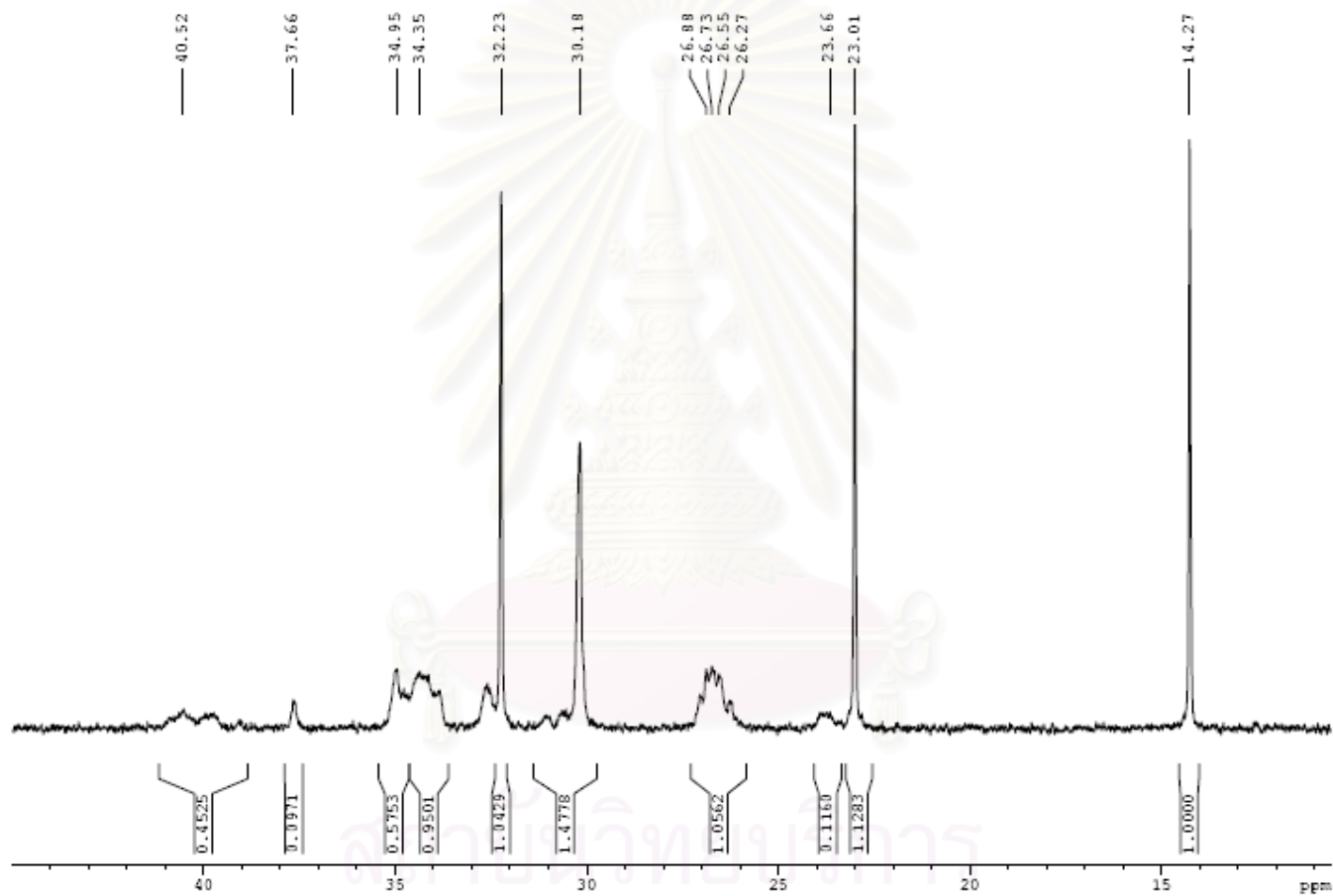


Figure B-3. ^{13}C NMR spectrum of ethylene/1-octene copolymer produces with $\text{SiO}_2\text{-TiO}_2$ support in toluene

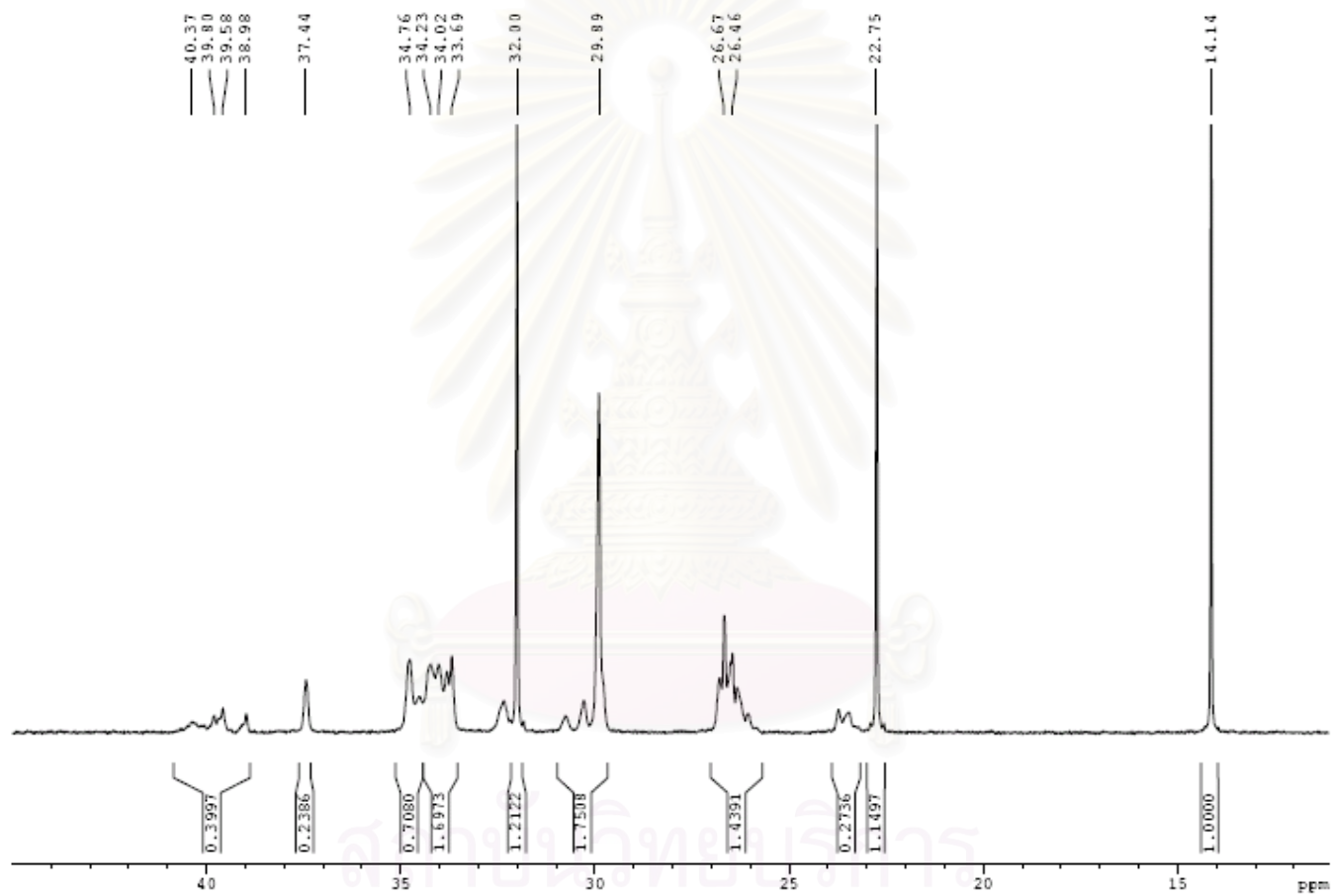


Figure B-4. ^{13}C NMR spectrum of ethylene/1-octene copolymer produced with TiO_2 support in toluene

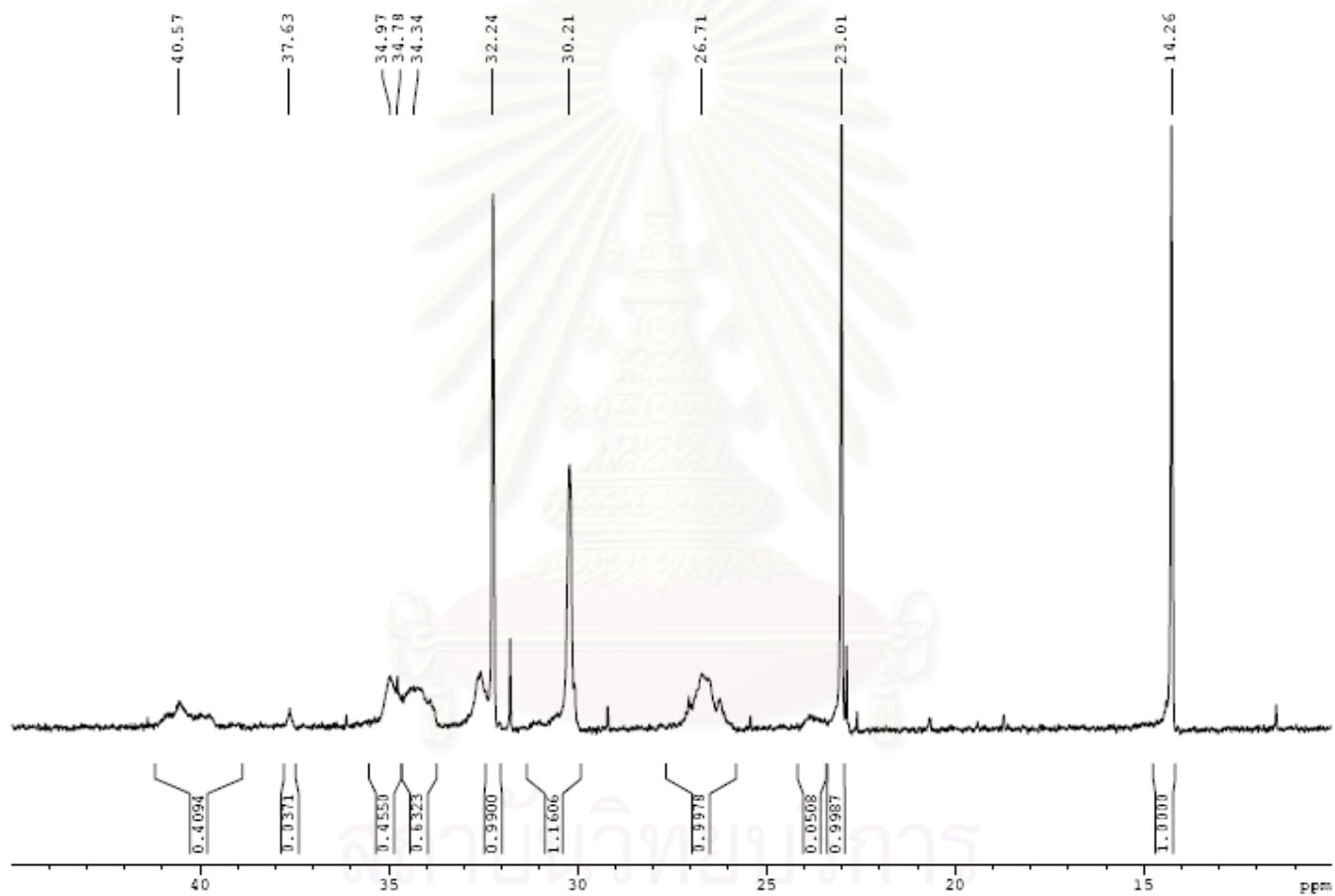


Figure B-5. ^{13}C NMR spectrum of ethylene/1-octene copolymer produced with homogeneous in chlorobenzene

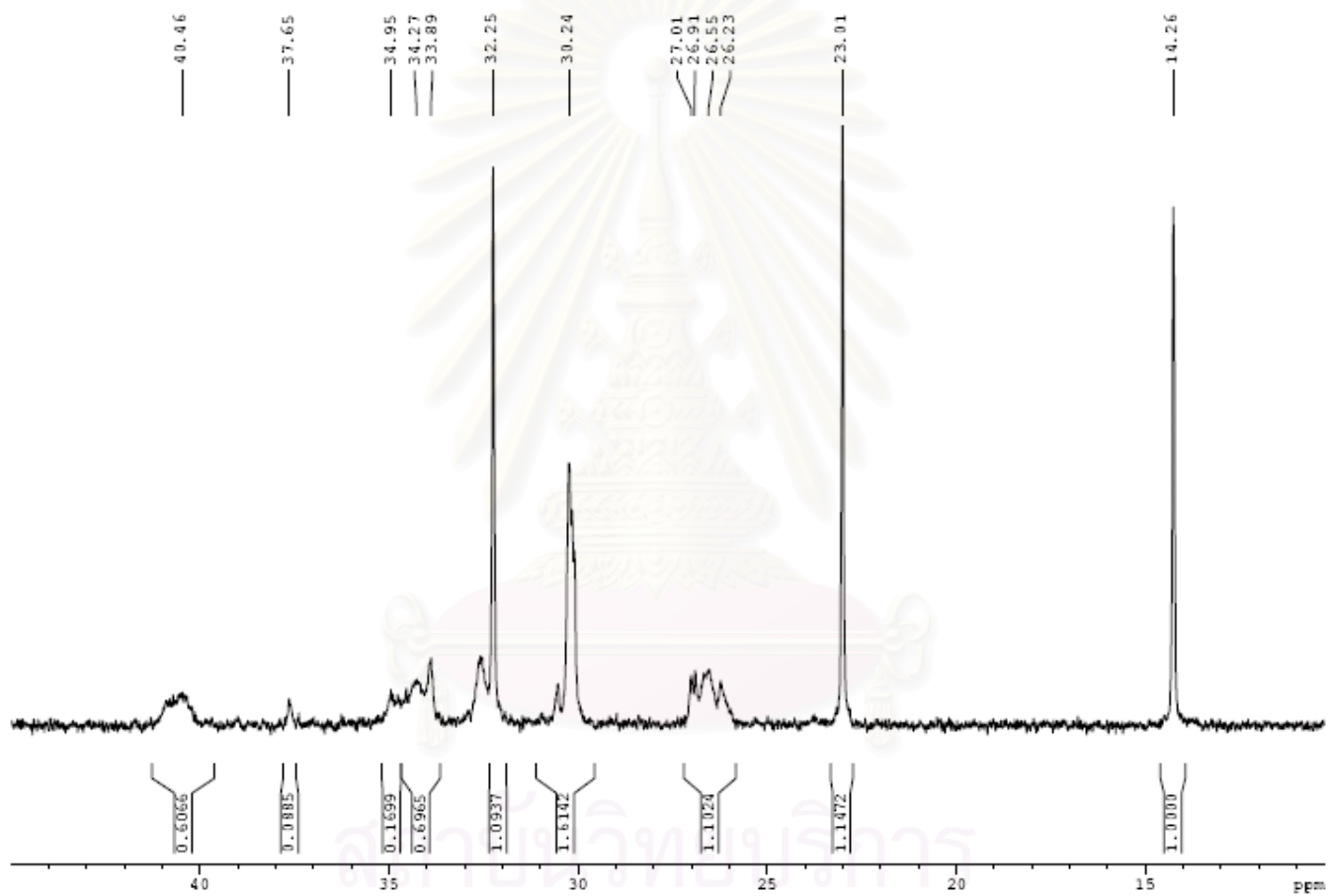


Figure B-6. ^{13}C NMR spectrum of ethylene/1-octene copolymer produced with SiO_2 support in chlorobenzene

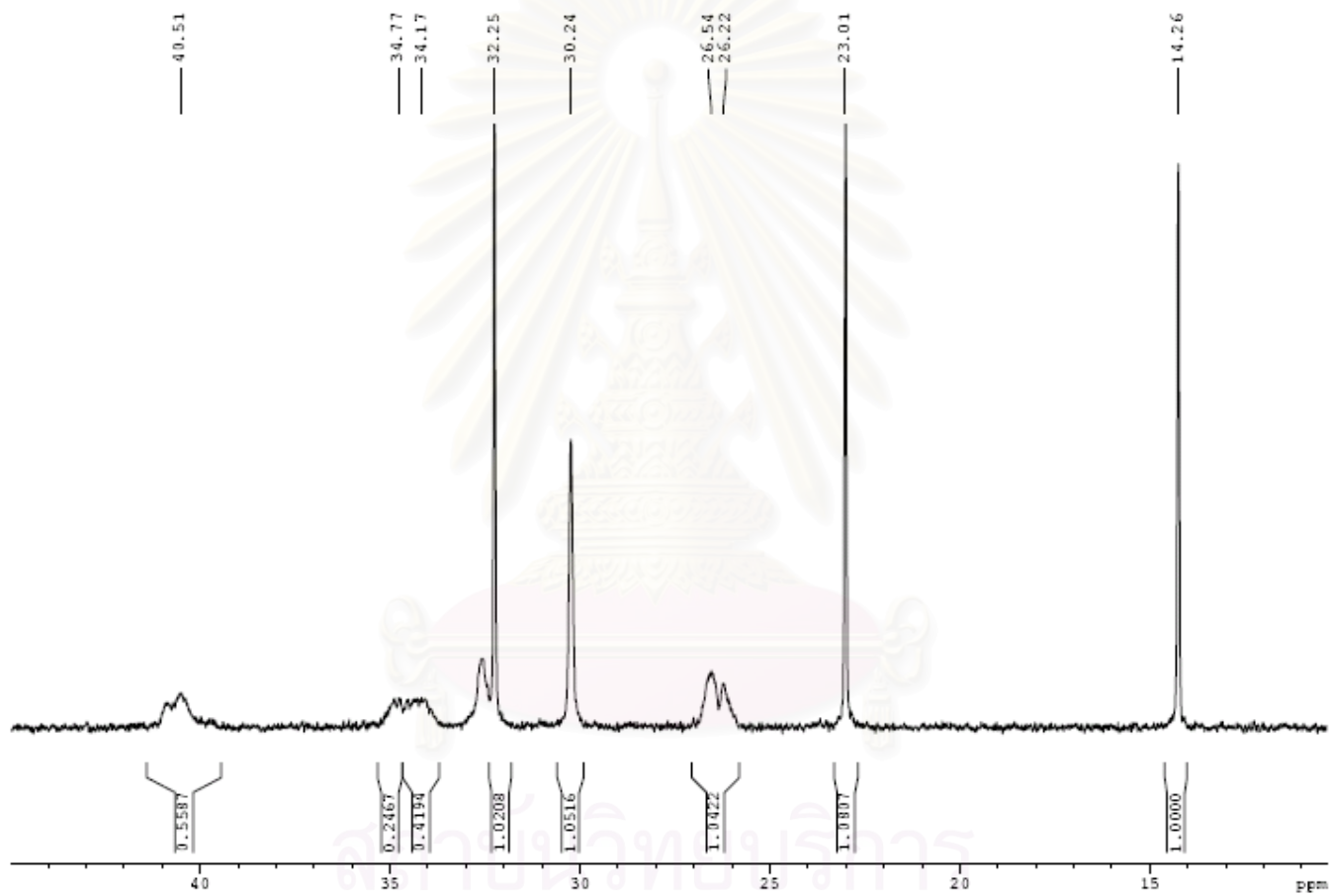


Figure B-7. ^{13}C NMR spectrum of ethylene/1-octene copolymer produced with $\text{SiO}_2\text{-TiO}_2$ support in chlorobenzene

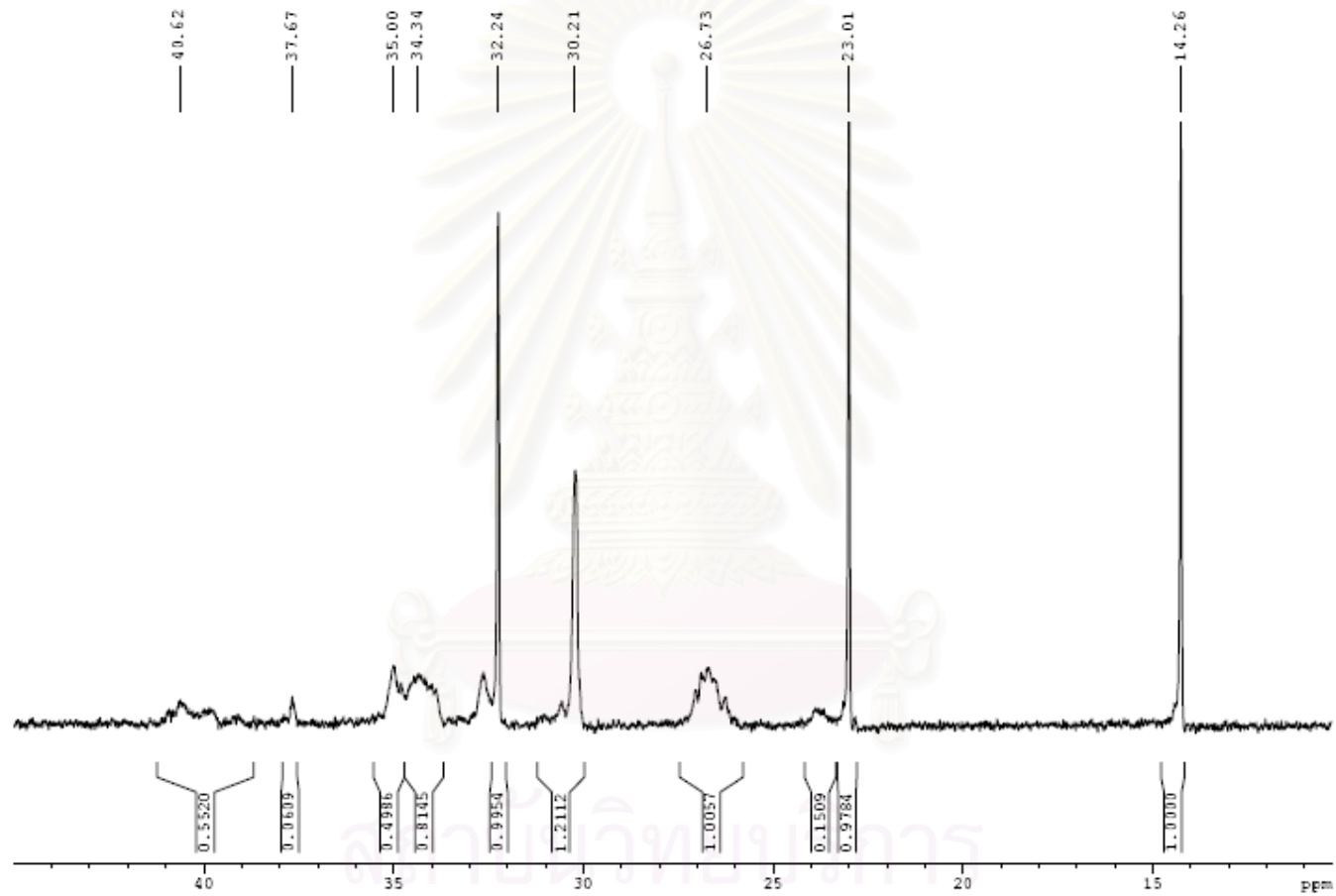


Figure B-8. ^{13}C NMR spectrum of ethylene/1-octene copolymer produced with TiO_2 support in chlorobenzene



APPENDIX C
(Differential Scanning Calorimeter)

สถาบันวิทยบริการ
จุฬาลงกรณ์มหาวิทยาลัย

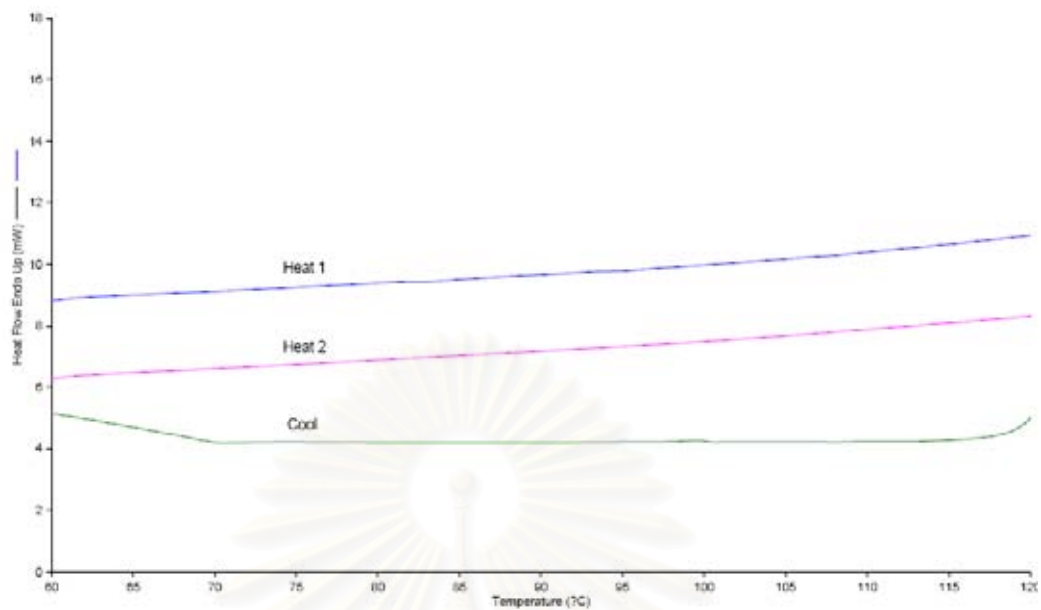


Figure C-1. DSC curve of ethylene/1-octene copolymer produce with homogeneous in toluene

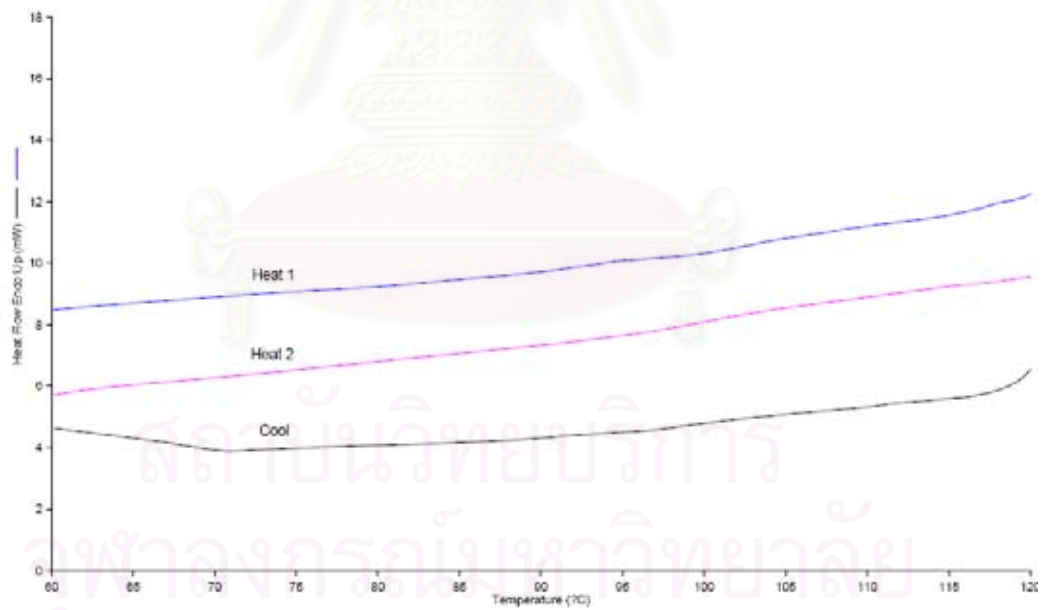


Figure C-2. DSC curve of ethylene/1-octene copolymer produce with SiO₂ support in toluene

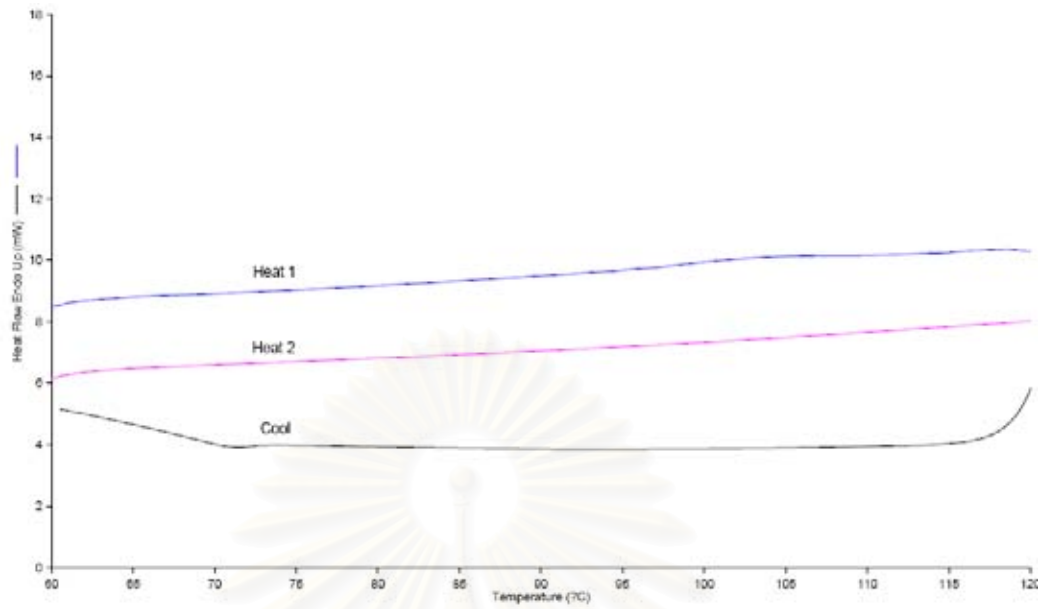


Figure C-3. DSC curve of ethylene/1-octene copolymer produce with $\text{SiO}_2\text{-TiO}_2$ support in toluene

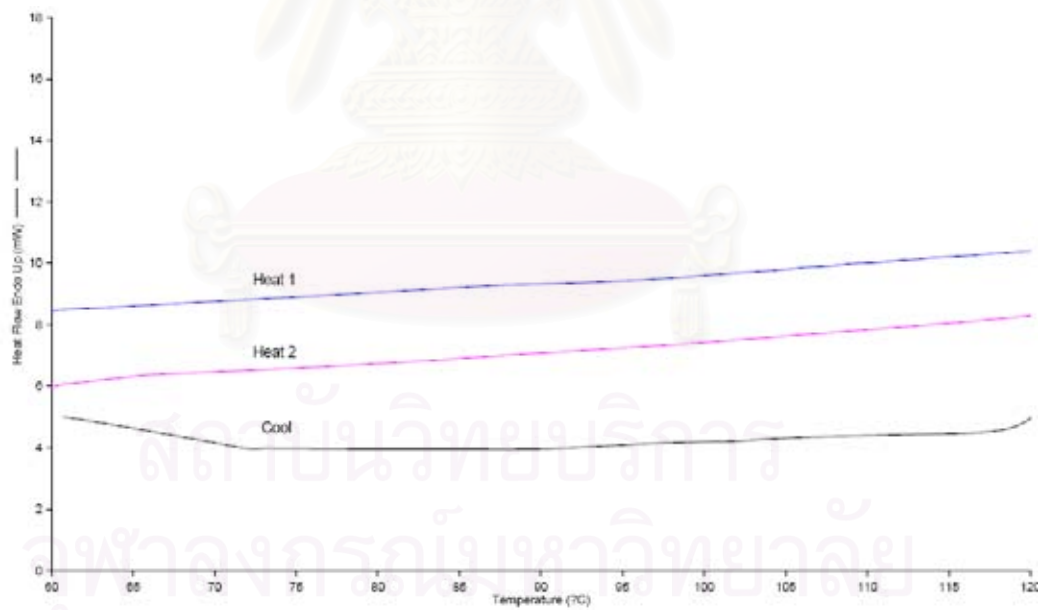


Figure C-4. DSC curve of ethylene/1-octene copolymer produce with TiO_2 support in toluene

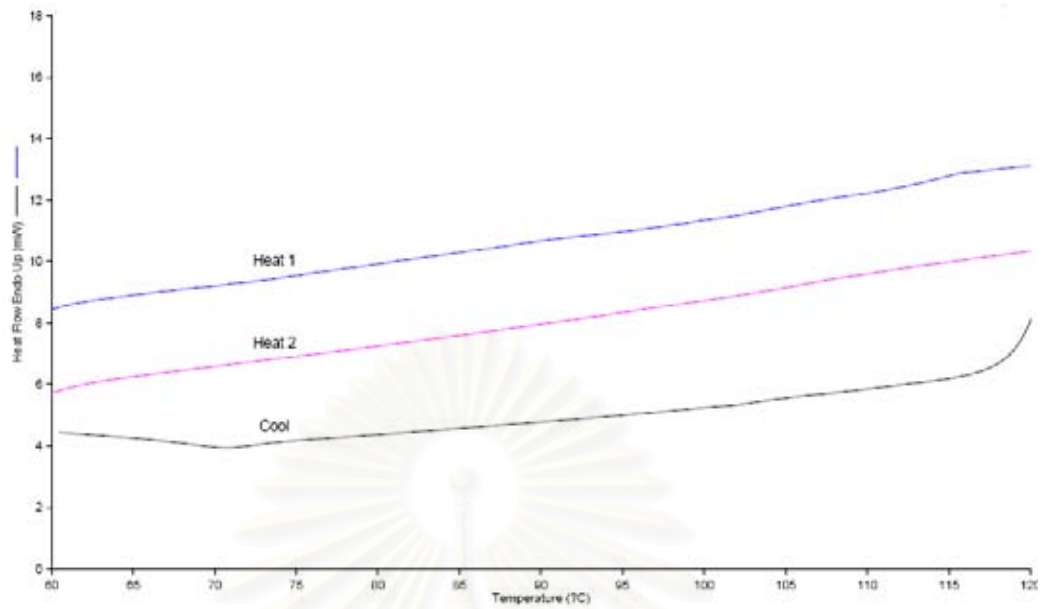


Figure C-5. DSC curve of ethylene/1-octene copolymer produce with homogeneous in chlorobenzene

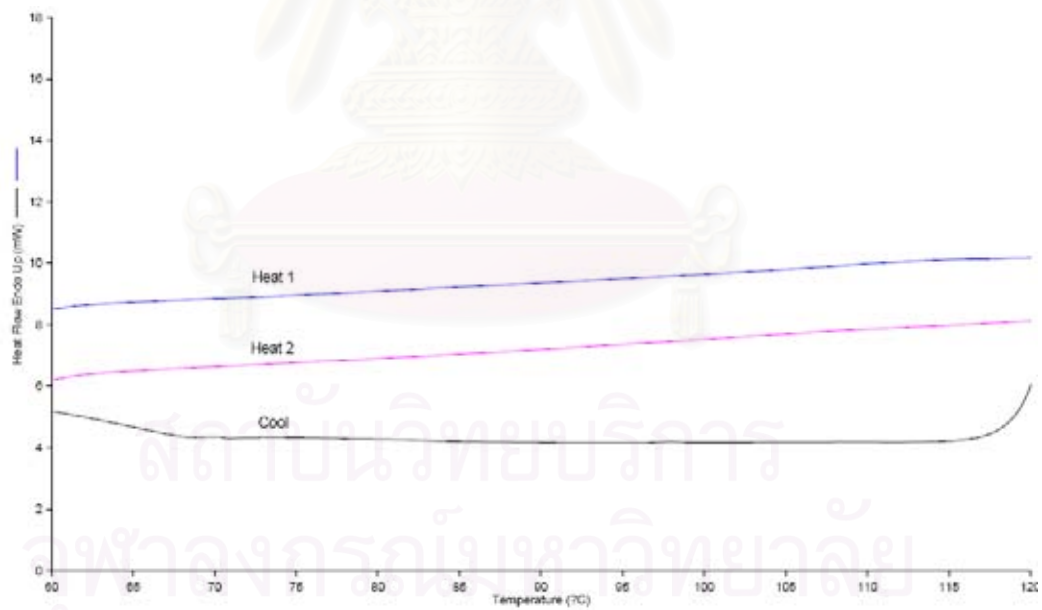


Figure C-6. DSC curve of ethylene/1-octene copolymer produce with SiO₂ support in chlorobenzene

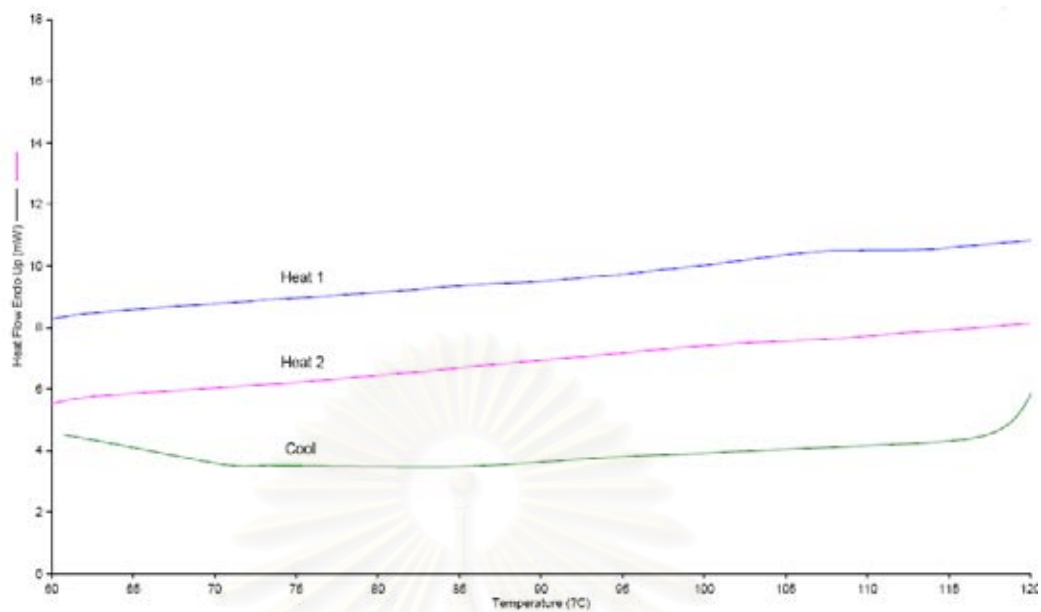


Figure C-7. DSC curve of ethylene/1-octene copolymer produce with $\text{SiO}_2\text{-TiO}_2$ support in chlorobenzene

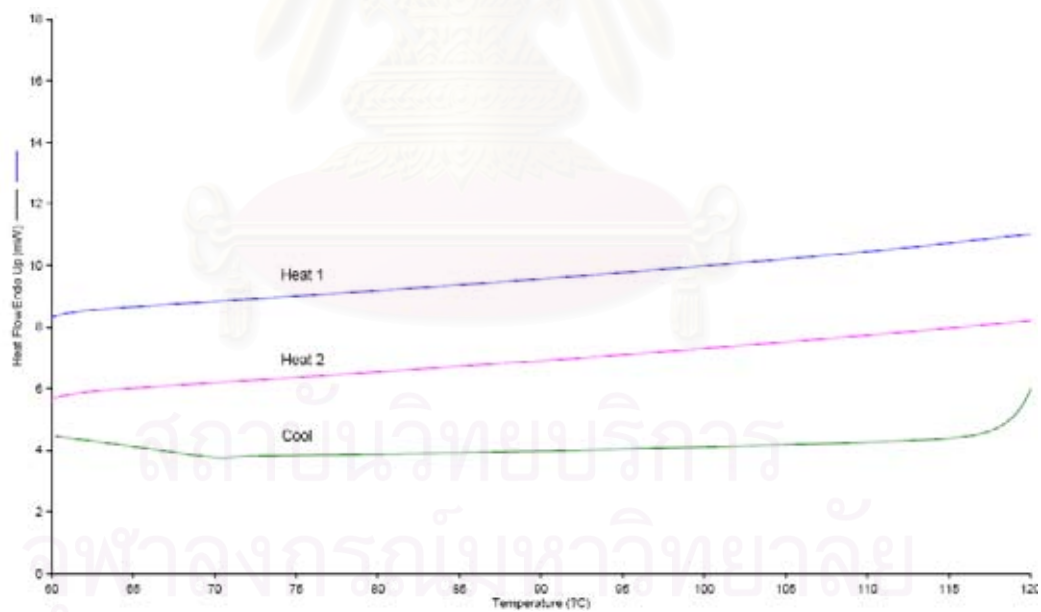


Figure C-8. DSC curve of ethylene/1-octene copolymer produce with TiO_2 support in chlorobenzene

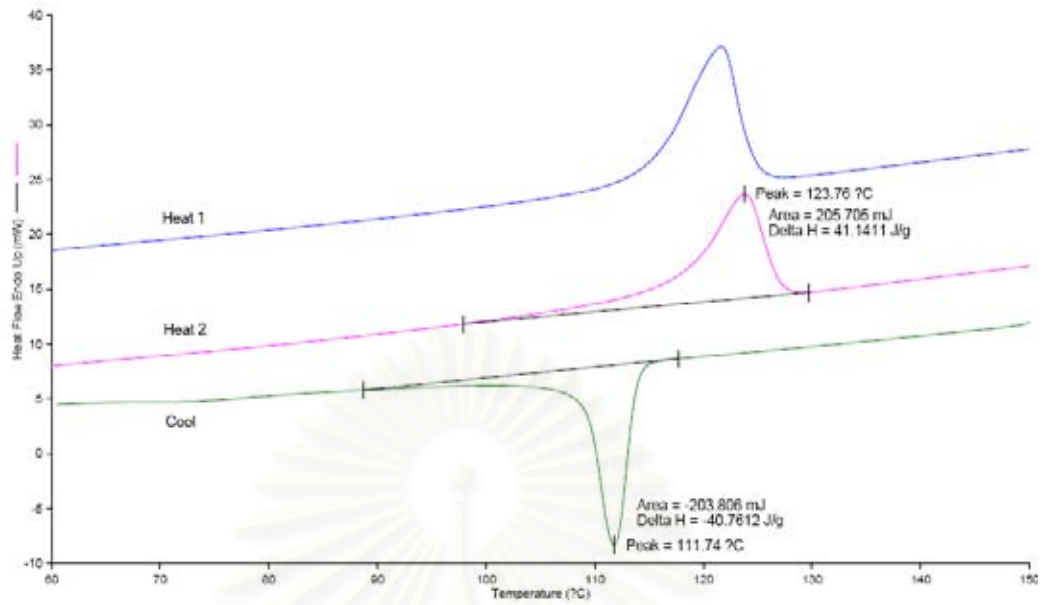


Figure C-9. DSC curve of polyethylene produce with homogeneous in toluene

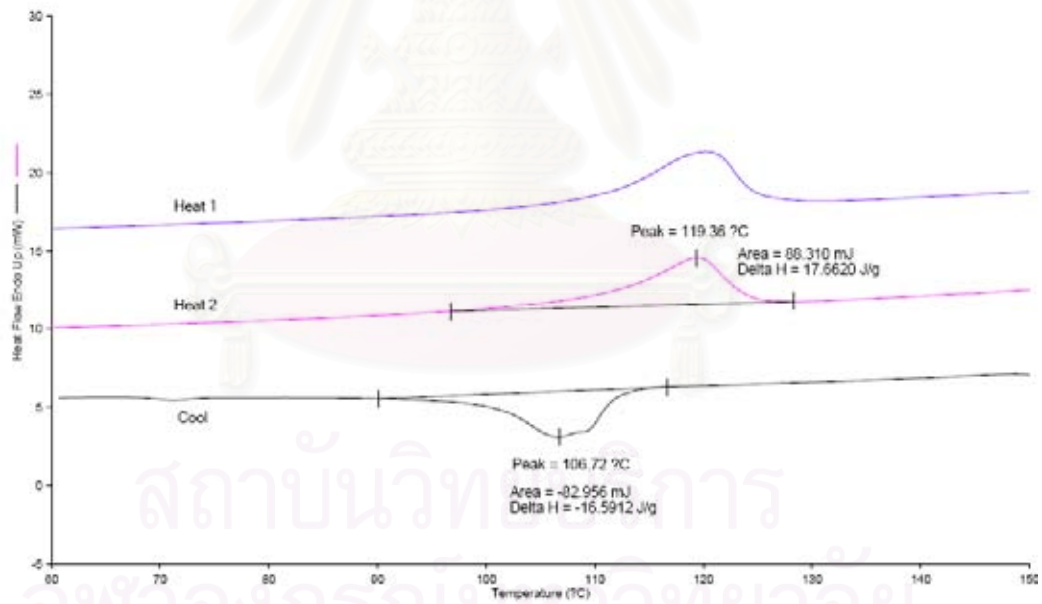


Figure C-10. DSC curve of polyethylene produce with SiO₂ support in toluene

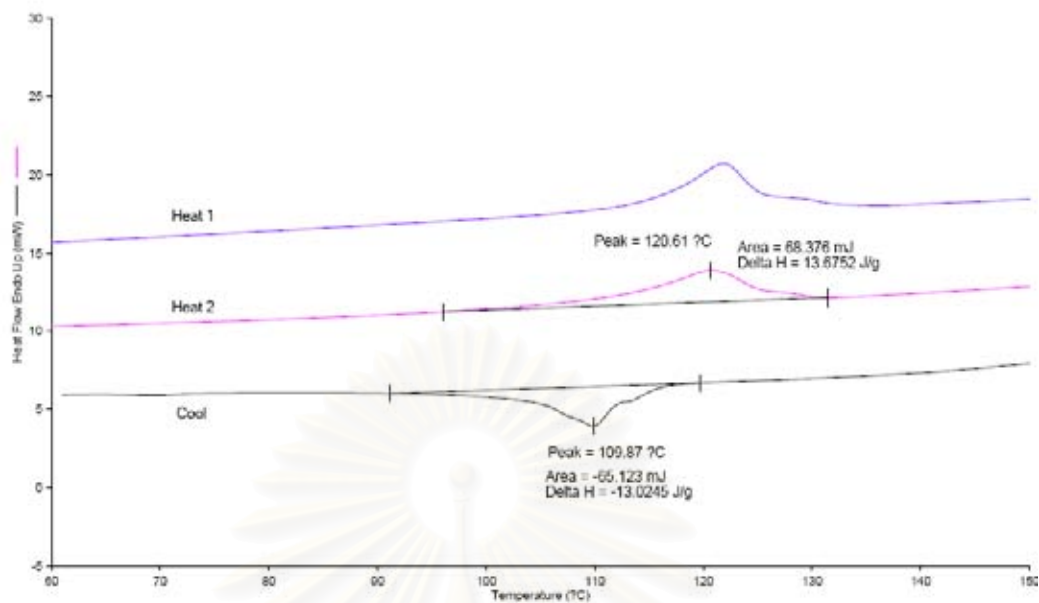


Figure C-11. DSC curve of polyethylene produce with SiO₂-TiO₂ support in toluene

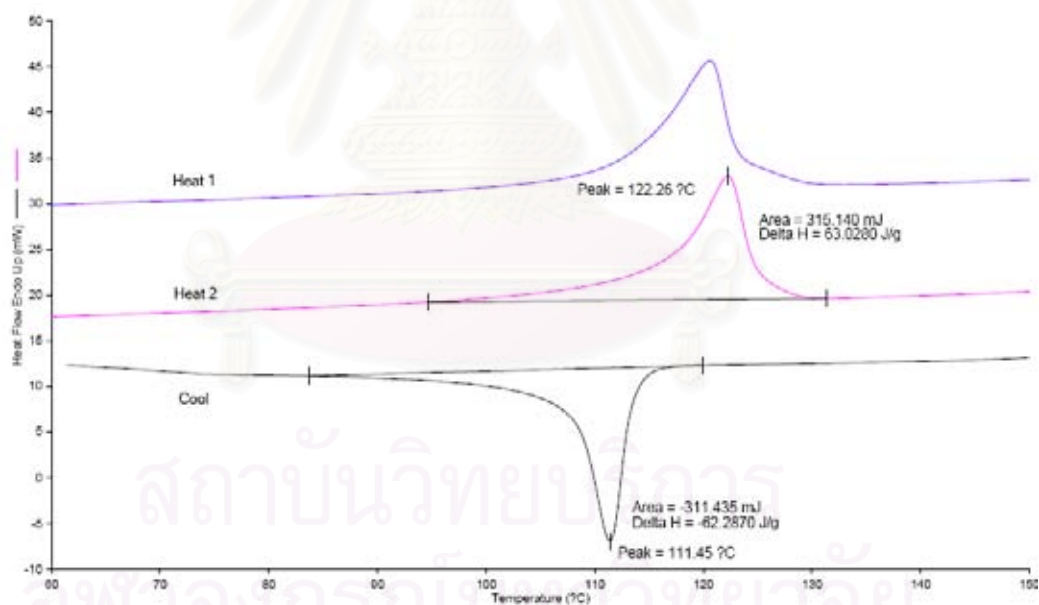


Figure C-12. DSC curve of polyethylene produce with TiO₂ support in toluene

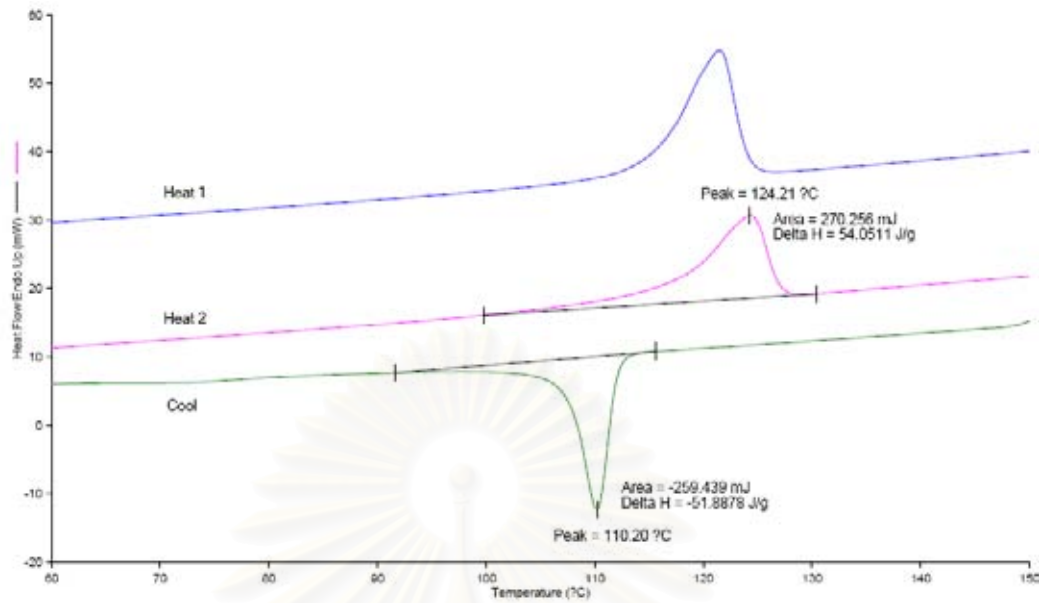


Figure C-13. DSC curve of polyethylene produce with homogeneous in chlorobenzene

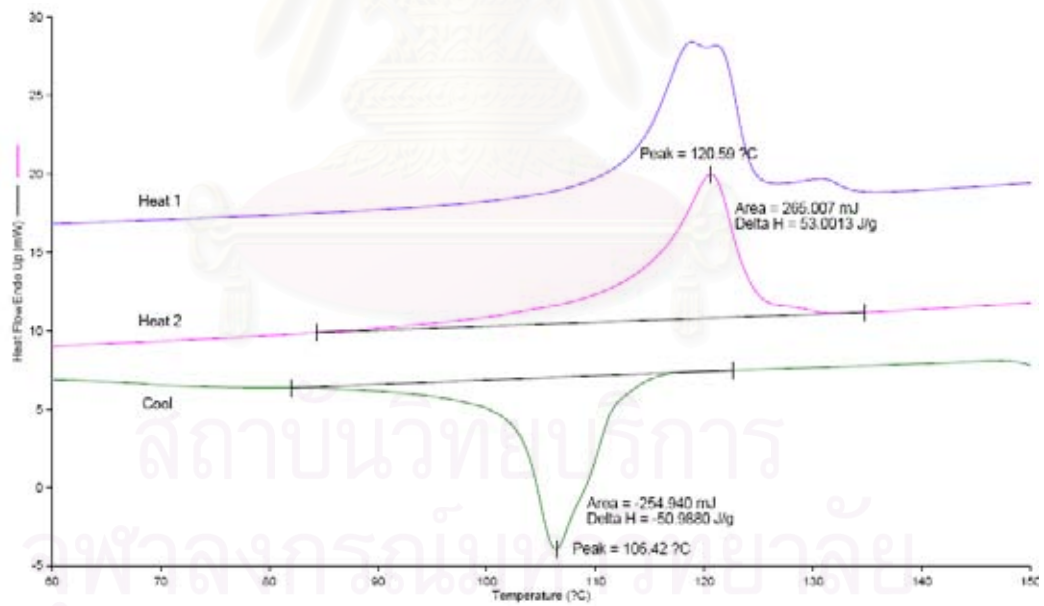


Figure C-14. DSC curve of polyethylene produce with SiO₂ support in chlorobenzene

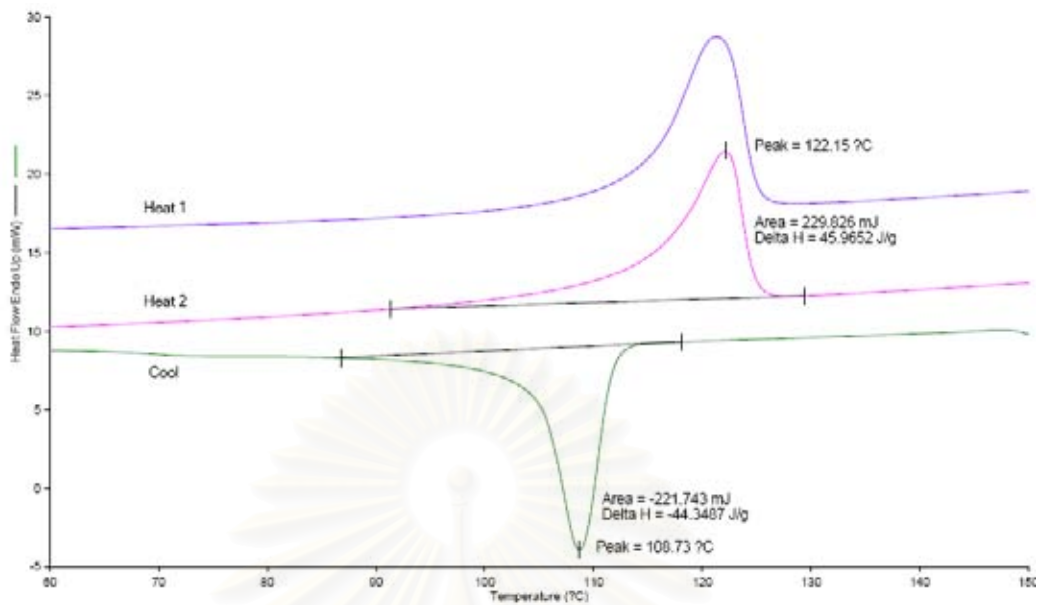


Figure C-15. DSC curve of polyethylene produce with SiO₂-TiO₂ support in chlorobenzene

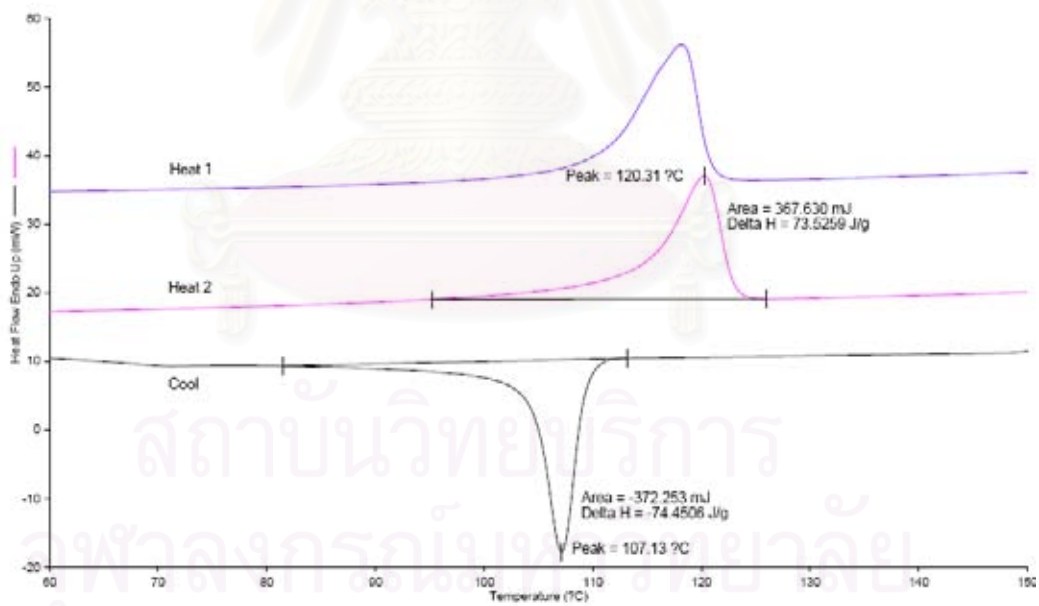


Figure C-16. DSC curve of polyethylene produce with TiO₂ support in chlorobenzene



APPENDIX D
(Calculation of Polymer Properties)

สถาบันวิทยบริการ
จุฬาลงกรณ์มหาวิทยาลัย

D.1 Calculation of crystallinity for ethylene and ethylene/ α -olefin polymer

The crystallinities of copolymers were determined by differential scanning calorimeter. %Crystallinity of copolymers is calculated from equation [95].

$$\chi(\%) = \frac{\Delta H_m}{\Delta H_m^0} \times 100$$

Where $\chi(\%)$ = %crystallinity
 ΔH_m = the heat of fusion of sample (J/g)
 ΔH_m^0 = the heat of fusion of perfectly crystalline polyethylene (286 J/g)

D.2 Calculation of polymer microstructure

Polymer microstructure and also triad distribution of monomer can be calculated according to the Prof. James C. Randall [87] in the list of reference. The detail of calculation for ethylene/1-octene copolymer was interpreted as follow.

The integral area of ^{13}C -NMR spectrum in the specify range are listed.

T_A	=	39.5 - 42	ppm
T_B	=	38.1	ppm
T_C	=	36.4	ppm
T_D	=	33 - 36	ppm
T_E	=	32.2	ppm
T_F	=	28.5 - 31	ppm
T_G	=	25.5 - 27.5	ppm
T_H	=	24 - 25	ppm
T_I	=	22 - 23	ppm
T_J	=	14 - 15	ppm

Triad distribution was calculated as the followed formula.

$k[\text{OOO}]$	=	$T_A - 0.5T_C$
$k[\text{EOO}]$	=	T_C
$k[\text{EOE}]$	=	T_B
$k[\text{EEE}]$	=	$0.5T_F - 0.25T_E - 0.25T_G$

$$\begin{aligned} k[\text{OEE}] &= T_G - T_E \\ k[\text{OEO}] &= T_H \end{aligned}$$

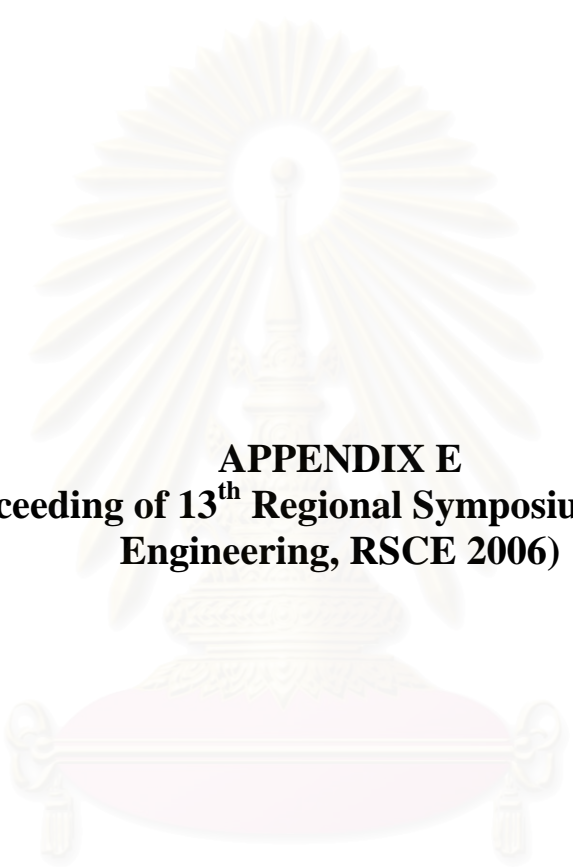
All copolymer was calculated for the relative comonomer reactivity (r_E for ethylene and r_C for the comonomer) and monomer insertion by using the general formula below.

$$r_E = 2[\text{EE}]/([\text{EC}]\text{X}) \qquad r_C = 2[\text{CC}]\text{X}/[\text{EC}]$$

where

$$\begin{aligned} r_E &= \text{ethylene reactivity ratio} \\ r_C &= \text{comonomer } (\alpha\text{-olefin}) \text{ reactivity ratio} \\ [\text{EE}] &= [\text{EEE}] + 0.5[\text{CEE}] \\ [\text{EC}] &= [\text{CEC}] + 0.5[\text{CEE}] + [\text{ECE}] + 0.5[\text{ECC}] \\ [\text{CC}] &= [\text{CCC}] + 0.5[\text{ECC}] \\ \text{X} &= [\text{E}]/[\text{C}] \text{ in the feed} = \text{concentration of ethylene (mol/L)} / \\ &\quad \text{concentration of comonomer (mol/L) in the feed.} \\ \%E &= [\text{EEE}] + [\text{EEO}] + [\text{OEO}] \\ \%O &= [\text{OOO}] + [\text{OOE}] + [\text{EOE}] \end{aligned}$$

สถาบันวิทยบริการ
จุฬาลงกรณ์มหาวิทยาลัย



APPENDIX E
**(The Proceeding of 13th Regional Symposium on Chemical
Engineering, RSCE 2006)**

สถาบันวิทยบริการ
จุฬาลงกรณ์มหาวิทยาลัย

Supporting effect of [*t*-BuNSiMe₂Flu]TiMe₂ complex during ethylene/1-octene copolymerization

Chanintorn Ketloy, Bunjerd Jongsomjit* and Piyasan Praserttham

*Center of Excellence on Catalysis and Catalytic Reaction Engineering,
Department of Chemical Engineering, Faculty of Engineering
Chulalongkorn University, Bangkok 10330 Thailand*

* Corresponding author, Phone: (662) 218-6869, Fax: (662) 218-6769

E-mail: bunjerd.j@chula.ac.th

ABSTRACT

In the present study, the supporting effects on the catalyst behaviors of [*t*-BuNSiMe₂Flu]TiMe₂ complex during ethylene/1-octene (EO) copolymerization were investigated. The various supports such as silica (SiO₂), titania (TiO₂), and mixed silica-titania (SiO₂-TiO₂) were studied. It revealed that using the mixed SiO₂-TiO₂-supported MMAO resulted in the highest catalyst activity among any other supports. It can be concluded that the presence of TiO₂ in SiO₂ can decrease the support interaction between MMAO and the support leading to increased activity during ethylene/1-octene copolymerization.

1. INTRODUCTION

Up to date, the new generation of polymerization catalysts such as metallocene and the transition metal complexes has been captivating. These catalysts have the capability to control the degree of α -olefin insertion upon the stereochemistry. They can also provide the uniform distribution of composition in the polymer chain as well. It should be noted that different distributions and compositions in the polymer backbone would result in various properties for polymer [1-5]. Therefore, by knowing the nature of catalysts, properties of polymer can be altered. It is known that supported metallocene catalysts are preferred for the gas phase and slurry phase polymerization [6]. As reported, the supports used can play important roles for polymerization behaviors. Hence, besides the nature of catalyst itself, the supporting effect is also crucial.

In this present study, the ethylene/1-octene copolymerization using three supports such as SiO₂, TiO₂ and SiO₂-TiO₂ mixed oxide supported-MMAO with titanocene catalyst was investigated and compared with the homogeneous system. The supports and catalyst precursors were prepared, characterized and investigated for the effect of supports on the catalyst activity and properties of copolymers. The role of supports and the microstructure of copolymer were further discussed.

2. EXPERIMENTAL SECTION

Ethylene/1-octene copolymerization reaction was carried out in a 100 mL semibatch stainless steel autoclave reactor equipped with a magnetic stirrer. At first, the desired amount of the supported MMAO and the toluene (to make the total volume of 30 mL) were introduced into the reactor. The titanium complex in toluene (10 μ mol/mL) was put into the reactor to make the $[Al]_{MMAO}/[Ti]_{cat} = 400$. Then, the reactor was immersed in liquid nitrogen. 1-Octene (0.018 moles) was added into the frozen reactor. The reactor was heated up to the polymerization temperature at 70 °C. By feeding ethylene into the reactor, the polymerization was started. The ethylene pressure and reactor temperature were kept constant during the polymerization. After

5 min, the reaction was terminated by adding acidic methanol and stirred for 30 min. After filtration, the copolymer obtained was washed with methanol and dried at room temperature.

3. RESULTS AND DISCUSSION

The polymerization activities via various supports are shown in Table 1. It was found that the mixed SiO₂-TiO₂ support exhibited the highest activity among other supports employed. It can be proposed that the presence of TiO₂ in SiO₂ can decrease the interaction between MMAO and the support without any changes in the amounts of MMAO at surface determined by XPS. Thus, it can be concluded that TiO₂ acted as a spacer group to reduce the support interaction resulting in increased activity during polymerization of ethylene/1-octene. The characteristics of polymer obtained will be further discussed in the near future.

Table 1 Polymerization^a activity

System	Polymerization	Time (min)	Yield (g)	Activity (kg of Polymer/mol Ti.h)
Homogeneous	EO	5	3.2475	3,897
SiO ₂ support	EO	5	2.4868	2,984
SiO ₂ -TiO ₂ support	EO	5	2.6092	3,131
TiO ₂ support	EO	5	2.3292	2,795

^a Polymerization condition: Ti = 10 μmol, Al/Ti = 400, Temp = 70 °C, Time = 5 min, 50 psi of ethylene pressure was applied.

Acknowledgements

We thank the Thailand Research Fund (TRF) and the financial support from the graduate school at Chulalongkorn University (90th Anniversary of Chulalongkorn University).

References

- [1] Mader, D., Heinemann, J., Walter, P. and Mulhaupt, R. (2000). *Influence of n-alkyl branches on glass-transition temperatures of branched polyethylenes prepared by means of metallocene- and palladium-based catalysts*. *Macromolecules* 33, 1245-1261.
- [2] Simanke, A. G., Galland, G. B., Neto, R. B., Quijada, R. and Mauler, R. S. (1999). *Influence of the type and the comonomer contents on the mechanical behavior of ethylene/α-olefin copolymers*. *J. Appl. Polym. Sci.* 74, 1194-1200.
- [3] Simanke, A. G., Galland, G. B., Freitas, L., da Jornada, J. A. H., Quijada, R. and Mauler, R. S. (1999). *Influence of the comonomer content on the thermal and dynamic mechanical properties of metallocene ethylene/1-octene copolymers*. *Polymer* 40, 5489-5495.
- [4] Xu, X. R., Xu, J. T., Feng, L. X. and Chen, W. (2000). *Effect of short chain-branching distribution on crystallinity and modulus of metallocene-based ethylene-butene copolymers*. *J. Appl. Polym. Sci.* 77, 1709-1715.
- [5] Hasan, T., Ioku, A., Nishii, K., Shiono, T. and Ikeda, T. (2001). *Syndiospecific living polymerization of propylene with [t-BuNSiMe₂Flu]TiMe₂ using MAO as cocatalyst*. *Macromolecules* 34, 3142-3145.
- [6] Hlatky, G. G. (2000). *Heterogeneous single-site catalysts for olefin polymerization*. *Chem. Rev.* 100, 1347-1376.



APPENDIX F
(The Submitted Paper to Applied Catalysis A: General)

สถาบันวิทยบริการ
จุฬาลงกรณ์มหาวิทยาลัย

**Characteristics and catalytic properties of [*t*-BuNSiMe₂Flu]TiMe₂/dMMAO
catalyst dispersed on various supports towards ethylene/1-octene
copolymerization**

Chanintorn Ketloy, Bunjerd Jongsomjit* and Piyasan Praserttham

*Center of Excellence on Catalysis and Catalytic Reaction Engineering,
Department of Chemical Engineering, Faculty of Engineering
Chulalongkorn University, Bangkok 10330 Thailand*

* Corresponding author, Phone: (662) 218-6869, Fax: (662) 218-6769

E-mail: bunjerd.j@chula.ac.th



สถาบันวิทยบริการ
จุฬาลงกรณ์มหาวิทยาลัย

Abstract

In the present study, the characteristics and catalytic properties of [*t*-BuNSiMe₂Flu]TiMe₂/dMMAO catalyst dispersed on various supports towards ethylene/1-octene copolymerization were investigated. First, the dMMAO was impregnated onto various supports such as SiO₂, SiO₂-TiO₂, and TiO₂. Then, copolymerization of ethylene/1-octene was conducted with and without the presence of supports in different solvent mediums. It revealed that the SiO₂-TiO₂ support exhibited the highest activity among the other support. The high activity observed for the SiO₂-TiO₂ support can be attributed to fewer interactions between the support and dMMAO as confirmed by XPS and TGA results. It can be proposed that the different solvents can possibly alter the nature of catalyst in two ways; (i) changing the interaction between the support and cocatalyst and/or (ii) changing the form of active species i.e., active ion-pair and solvent-separated ion-pair as seen in the homogeneous system. However, there was no effect with regards to activity of the solvent mediums employed for the homogeneous system. It is worth noting that the Ti-complex rendered pronouncedly high incorporation of 1-octene having the triblock (OOO) and diblock (EOO) copolymers. The properties of copolymer by means of GPC, DSC, and ¹³C NMR were further discussed in more details.

Keywords: metallocene catalyst; copolymerization; Ti complex; silica; titania; supports

สถาบันวิทยบริการ
จุฬาลงกรณ์มหาวิทยาลัย

1. Introduction

Linear low density polyethylene (LLDPE) is one of the most important commercial products. As far, industrial efforts have been directed towards finding novel and efficient polymerization catalysts for the synthesis of the desired copolymer. Metallocene catalysts are particularly useful for the production of LLDPE through the copolymerization of ethylene and α -olefins such as 1-butene, 1-hexene, and 1-octene [1]. The single-site characteristic of metallocene makes it possible to improve polymer properties; control the degree of α -olefin insertion upon the stereochemistry and provide higher activity, than those obtained by conventional Ziegler-Natta catalyst. They can also result in a narrow molecular weight distribution (MWD) and the uniform distribution of short-chain branches in the polymer chain as well [2]. It should be noted that different distributions and compositions in the polymer backbone would result in various properties for polymer [3-5]. Therefore, by knowing the nature of catalysts, properties of polymer can be altered.

Several studies comparing different group 4 metallocene structures in ethylene/ α -olefin copolymerization have been reported [6-9]. Nevertheless, the homogeneous catalyst systems based on metallocene require high aluminum-to-transition metal molar ratios and extensive polymer washing, so as to remove residual aluminum. In addition, they are not suitable for industrial applications such as gas-phase and slurry polymerization processes. To overcome these disadvantages, metallocene compounds have been supported mainly on inorganic carriers such as SiO_2 , Al_2O_3 , TiO_2 and zeolites [10-12]. These carriers have been extensively studied for supported cocatalyst for years. The heterogeneous metallocene system is necessary to produce polymer particle of desired morphology to avoid reactor fouling with finely dispersed swelling of polymers [5].

It is known that the catalytic behaviors depend on polymerization conditions, catalytic compositions, metal dispersion, and types of supports used. In the case of solution and slurry polymerization, the kind of solvent is also one of factors which can influence the polymerization behaviors [13]. Indeed, literature data regarding α -olefin homopolymerization reports that the polarity of solvent remarkably affects the catalytic activities [14] and, in some case, also the microstructure of polymer [15-18].

In the previous studies, a unique catalyst called “constrained geometry catalyst” (CGC) using half-sandwich titanocenes, have been found that they can afford to give highly activity and incorporate a large amount of α -olefin in to copolymer [19, 20]. It revealed that [*t*-BuNSiMe₂Flu]TiMe₂ complex was employed to polymerize propylene, norbornene and ethylene [21-25]. Several papers reported that [*t*-BuNSiMe₂Flu]TiMe₂ catalyst was suitable for the propylene polymerization in various polymerization conditions due to effect of activators and solvents used. They found that the kind of activators and the polarity of solvents played important roles on the catalytic activities and microstructure of polymer as well [17, 18, 26, 27]. A few papers, however, reported on the copolymerization of ethylene with α -olefins [28, 29] and only one that reported the supported system [30].

The present work has focused on the effect of supports in different solvent mediums in ethylene/1-octene copolymerization using three supports such as SiO₂, TiO₂ and SiO₂-TiO₂. The solvent mediums such as toluene and chlorobenzene (CB) having different dielectric constant values (ϵ) were studied. The supports and catalyst precursors were prepared, characterized and tested for the catalyst activity. The properties of copolymers obtained were further investigated by means of GPC, DSC, and ¹³C NMR analysis.

2. Experimental Section

2.1 Materials

All operations were manipulated under an argon atmosphere using glove box and/or standard Schlenk techniques. The [*t*-BuNSiMe₂Flu]TiMe₂ (Ti-complex) was synthesized according to the procedure described by Hagihara et al. [29]. Ethylene (polymerization grade) was obtained from the National Petrochemical Co., Ltd., Thailand. 1-Octene (98%, 0.715 g/mL) was purchased from Aldrich Chemical Company and further purified by distilling over CaH₂ for 6 h. Modified methyl aluminoxane, MMAO (1.86 M in toluene) was donated by Tosoh Akzo, Japan. Silica gel (Cariact P-10) from Fuji Silysia Chemical Ltd., Japan. Titanium (IV) oxide (pure anatase) was obtained from Aldrich Chemical Company. Toluene was donated from the Exxon Chemical, Thailand Co., Ltd. It was dried over dehydrated CaCl₂ and distilled over sodium/benzophenone.

2.2 Preparation of SiO₂-TiO₂ mixed oxide support

SiO₂-TiO₂ mixed oxide support [surface area of SiO₂ = 281 m²g⁻¹ and TiO₂ = 70 m²g⁻¹] was prepared according to the method described by Conway et al. [31]. In particular, 1 g of SiO₂-TiO₂ (4:1 by weight) [32] mixed oxide support was physically mixed by dispersing in toluene (ca. 20 ml). The mixture was stirred for 30 min, filtered, and then dried under vacuum.

2.3 Removal of trialkylaluminiums from MMAO

Removal of trialkylaluminiums from MMAO was carried out according to the reported procedure [33]. The toluene solution of MMAO was dried under vacuum for 6 h at room temperature to evaporate the solvent, AlMe₃, and Al(*i*Bu)₃. Then, continue to dissolve with 100 ml of heptane and the solution was evaporated under vacuum to remove the remaining AlMe₃ and Al(*i*Bu)₃. This procedure was repeated 4 times and the white powder of dried MMAO (dMMAO) was obtained.

2.4 Preparation of supported dMMAO

Silica-supported dMMAO (dMMAO/SiO₂) was prepared according to the literature [33]. SiO₂ was calcined at 573 K for 6 h. A toluene solution (100 mL) of dMMAO (15 g) was added into the SiO₂ slurry in toluene (20 g, 250 mL), and the mixture was stirred for 30 min at room temperature. After the toluene was evaporated under vacuum, then washed with hexane (150 mL × 7) and finally dried under vacuum for 5 h to give SiO₂/dMMAO. Similarly, silica-titania mixed oxide-supported dMMAO (dMMAO/SiO₂-TiO₂) and titania-supported dMMAO (dMMAO/TiO₂) were prepared according to the method as described above.

2.5 Polymerization procedure

Ethylene/1-octene copolymerization reaction was carried out in a 100 mL semibatch stainless steel autoclave reactor equipped with a magnetic stirrer. At first, the desired amount of the supported dMMAO and the toluene (CB) [to make the total volume of 30 mL] were introduced into the reactor. The titanium complex in toluene

(10 $\mu\text{mol/mL}$) was put into the reactor to make the $[\text{Al}]_{\text{dMMAO}}/[\text{Ti}]_{\text{cat}} = 400$. Then, the reactor was immersed in liquid nitrogen. 1-Octene [5 mL (0.031 mole)] was added into the frozen reactor. The reactor was heated up to the polymerization temperature at 343 K. By feeding ethylene into the reactor, the polymerization was started. The ethylene pressure and reactor temperature were kept constant during the polymerization (pressure in reactor = 50 psi). After 5 min, the reaction was terminated by adding acidic methanol and stirred for 30 min. After filtration, the copolymer obtained was washed with methanol and dried at room temperature.

2.6 Supports and supported dMMAO Characterization

Scanning electron microscopy and energy dispersive X-ray spectroscopy: SEM and EDX were used to determine the sample morphologies and elemental distribution throughout the sample granules, respectively. The SEM of JEOL mode JSM-6400 was applied. EDX was performed using Link Isis series 300 program.

X-ray diffraction: XRD was performed to determine the bulk crystalline phases of samples. It was conducted using a SIEMENS D-5000 X-ray diffractometer with $\text{CuK}\alpha$ ($\lambda = 1.54439 \text{ \AA}$). The spectra were scanned at a rate of $2.4 \text{ }^\circ/\text{min}$ in the range $2\theta = 20\text{-}80^\circ$.

Raman spectroscopy: The Raman spectra of the samples were collected by projecting a continuous wave YAG laser of neodymium (Nd) red (810 nm) through the samples at room temperature. A scanning range of $100\text{-}1000 \text{ cm}^{-1}$ with a resolution of 2 cm^{-1} was applied.

X-ray photoelectron spectroscopy: XPS was used to determine the binding energies (BE) and the amount of Al on sample surfaces. It was carried out using the Shimadzu AMICUS with VISION 2-control software. Spectra were recorded at room temperature in high-resolution mode (0.1 eV step, 23.5 eV pass energy) for Al 2p core-level region. The samples were mounted on an adhesive carbon tape as pellets. The energies reference for Ag metal (368.0 eV for $3d_{5/2}$) was used for this study.

Thermogravimetric analysis: TGA was performed using TA Instruments SDT Q 600 analyzer. The samples of 10-20 mg and a temperature ramping from 298 to 873 K at 2 K/min were used in the operation. The carrier gas was N_2 UHP.

2.7 Polymer Characterization

Gel permeation chromatography: The molecular weight and molecular weight distribution of polymer was determined using GPC (PL-GPC-220). Samples were prepared having approximately concentration of 1 to 2 mg/ml in trichlorobenzene (mobile phase) by using the sample preparation unit (PL-SP 260) with filtration system at a temperature of 423 K. The dissolved and filtered samples were transferred into the GPC instrument at 423 K. The calibration was conducted using the universal calibration curve based on narrow polystyrene standards.

Differential scanning calorimetry (DSC): Thermal analysis measurements were performed using a Perkin-Elmer DSC P7 calorimeter. The DSC measurements reported here were recorded during the second heating/cooling cycle with the rate of 20 K/min. This procedure ensured that the previous thermal history was erased and provided comparable conditions for all samples. Approximately, 10 mg of sample was used for DSC measurement at a time.

¹³C NMR spectroscopy: ¹³C NMR spectroscopy was used to determine the α -olefin incorporation and copolymer microstructure. Chemical shift were referenced internally to the CDCl₃ and calculated according to the method described by Randall [34]. Sample solution was prepared by dissolving 50 mg of copolymer in 1,2,4-trichlorobenzene and CDCl₃. ¹³C NMR spectra were taken at 333 K using BRUKER AVANCE II 400 operating at 100 MHz with an acquisition time of 1.5 s and a delay time of 4 s.

3. Results and discussion

3.1 Catalytic activities

Here, the various supports such as silica, titania, and mixed silica-titania (4:1 by weight) were used for supporting the [*t*-BuNSiMe₂Flu]TiMe₂ (the Ti-complex)/dMMAO catalyst. Prior to impregnation of the supports with dMMAO, they are characterized by means of XRD and Raman spectroscopy. XRD patterns of the supports before impregnation to dMMAO are shown in **Figure 1**. It was observed that silica exhibited a broad XRD peak as seen typically for the conventional amorphous silica. Similar to silica, the XRD patterns for titania indicated only the

characteristics peaks of anatase titania at 25° (major), 37°, 48°, 55°, 56°, 62°, 71°, and 75°. XRD patterns of the mixed silica-titania revealed the combination of silica and titania being present as mentioned above. Raman spectra of supports are shown in **Figure 2**. It was found that the titania support exhibited the Raman bands at 639, 516, and 397 cm^{-1} for titania in its anatase form as seen from our previous work [35, 36] whereas silica was the Raman insensitive upon the scanning range applied. After impregnation with dMMAO, the $[\text{Al}]_{\text{dMMAO}}$ content was measured using EDX. The typical measurement curve for the quantitative analysis using EDX is shown in **Figure 3**. The amounts of $[\text{Al}]_{\text{dMMAO}}$ in various supports are also listed. It can be seen that the amount of $[\text{Al}]_{\text{dMMAO}}$ in various supports were varied due to the adsorption ability of each support. It revealed that titania exhibited the highest amount of $[\text{Al}]_{\text{dMMAO}}$ being present among other supports probably due to its strong interaction. On the other hand, increased amount of $[\text{Al}]_{\text{dMMAO}}$ can be observed with the presence of titania as also seen in the mixed silica-titania compared with that in the sole silica. Besides the content of $[\text{Al}]_{\text{dMMAO}}$ in supports, one should consider the distribution of $[\text{Al}]_{\text{dMMAO}}$ in the supports. The elemental distribution was also performed using EDX mapping on the external surface. The $[\text{Al}]_{\text{dMMAO}}$ distribution in the various supports is shown in **Figure 4**. As seen, all samples exhibited good distribution of Al without any changes in the support morphology.

For comparative studies, the catalytic activities towards the copolymerization of ethylene/1-octene upon various supports were measured. The polymerization activities of the homogeneous system and various supports employed in toluene are shown in **Table 1**. It can be observed that the polymerization activities were in the order of homogeneous system > $\text{SiO}_2\text{-TiO}_2$ > SiO_2 > TiO_2 . As known, the supported system exhibited lower activity than the homogeneous one due to the supporting effect. Considering the supported system, the $\text{SiO}_2\text{-TiO}_2$ rendered the highest activity among the other supports. In fact, the presence of TiO_2 in SiO_2 can result in decreased interaction between the cocatalyst and SiO_2 supports. It was reported that TiO_2 may acted as a spacer group to anchor MAO to the SiO_2 support resulting in less steric hindrance and less interaction on the support surface as seen for the zirconocene/MAO system as well [32]. Hence, the similar effect was consistently observed for the titanocene/dMMAO system. It should be mentioned that the lowest polymerization activity obtained for the TiO_2 support was due to the strong support

interaction [37]. In order to give a better understanding on species present on supports, the XPS study of the dMMAO on various supports was conducted. In fact, the binding energy (BE) of Al 2p core-level of $[Al]_{dMMAO}$ was measured. The typical XPS profile of Al 2p on various supports is shown in **Figure 5** indicating the BE of 74.6-74.8 eV. These values were also in accordance with the MMAO present on the silica support as reported by Hagimoto et al. [33]. This was suggested that no significant change in the oxidation state of $[Al]_{dMMAO}$ upon the various support employed. As a matter of fact, the differences in polymerization activities observed on various supports were not caused by any changes of the surface species. The surface concentrations of Al 2p measured by XPS were also shown in **Table 2**. On the other hand, changes in activity upon various supports were mainly attributed to both the amounts of $[Al]_{dMMAO}$ present and its interaction with the support. Considering the various supports employed, the surface concentrations of Al 2p were in the order of $TiO_2 > SiO_2-TiO_2 > SiO_2$ as seen from the bulk using EDX. It was obvious that the TiO_2 support contained the highest amount of surface Al 2p due to strong interaction resulting in less leaching of dMMAO during the preparation. The presence of TiO_2 in the mixed SiO_2-TiO_2 also enhanced the interaction of dMMAO due to the synergistic effect arising from TiO_2 . Based on, the surface concentrations of Al 2p, one might argue that with TiO_2 support, the polymerization activity should be the highest since it apparently had the highest concentration of Al 2p. However, based on our results, the polymerization activity using the TiO_2 was the lowest. This indicated that besides the surface concentration of $[Al]_{dMMAO}$, the interaction between the $[Al]_{dMMAO}$ and support was substantially important. In fact, the strong interaction of species with TiO_2 or other supports employed in this study was referred to the interaction between the support and the cocatalyst (dMMAO). Based on this study, dMMAO was dispersed by impregnation onto the support prior to polymerization. The degree of interaction between the support and dMMAO can be determined by the TGA measurement. In order to give a better understanding, the interaction of support and dMMAO can be proposed based on the review paper by Severn et al. [38]. They mentioned that the connection of the support and cocatalyst occurred via the $O_{support} \sim Al_{cocatalyst}$ linkage. In particular, the TGA can only provide useful information on the degree of interaction for the dMMAO bound to the support in terms of weight loss and removal temperature. The stronger interaction can result in being more difficult for the dMMAO bound to the support to react with the Ti-complex during

activation process leading to lower catalytic activity for polymerization. As mentioned, the TiO_2 support is known to have a strong interaction with species being present on it. In order to proof the interaction between the $[\text{Al}]_{\text{dMMAO}}$ and various supports, the TGA measurement was performed. The TGA profiles of $[\text{Al}]_{\text{dMMAO}}$ on various supports are shown in **Figure 6** indicating the similar profiles for various supports. It was observed that the weight loss of $[\text{Al}]_{\text{dMMAO}}$ present on various supports were in the order of SiO_2 (22%) > $\text{SiO}_2\text{-TiO}_2$ (21%) > TiO_2 (19%). The species having strong interaction with the support was removed at ca. 538, 542 and 588 K for SiO_2 , $\text{SiO}_2\text{-TiO}_2$ and TiO_2 , respectively. This indicated that $[\text{Al}]_{\text{dMMAO}}$ present on TiO_2 had the strongest interaction, thus, lowest polymerization activity observed. However, in the case of $\text{SiO}_2\text{-TiO}_2$ support, although it had stronger interaction than that of SiO_2 , it exhibited higher polymerization interaction due to higher concentration of $[\text{Al}]_{\text{dMMAO}}$ at surface as mentioned above. Besides, the presence of TiO_2 in SiO_2 as a spacer group was also counted for higher activity.

In order to investigate the solvent effect on this polymerization system. The solvent having different dielectric constant values (ϵ) such as chlorobenzene (CB) was employed for the corresponding polymerization system. The dielectric constant (ϵ) is in the order of CB (5.68) > toluene (2.38) [39]. The polymerization activity results in CB are also shown in **Table 1**. It can be observed that there was no significant change regarding to activity for the homogeneous system when changing the solvent medium. However, the dramatic increases in activity was apparently found in the supported system especially with SiO_2 and $\text{SiO}_2\text{-TiO}_2$ supports when CB was employed as the solvent medium. It indicated that the polymerization activities substantially increased with SiO_2 and $\text{SiO}_2\text{-TiO}_2$ supports in CB almost 4 times higher compared with those in toluene. The activity for TiO_2 support in CB only slightly increased compared to that in toluene. It can be proposed that the different solvents can possibly alter the nature of catalyst in two ways; (i) changing the interaction between the support and cocatalyst and/or (ii) changing the form of active species i.e., active ion-pair and solvent-separated ion-pair as seen in the homogeneous system as reported by Nishii et al. [17] and Intaragamjon et al. [28]. It is worth noting that the dramatic increases in polymerization activities in CB compared to those in toluene can be perhaps attributed to increased propagation rate presuming that the $[\text{Al}]_{\text{dMMAO}}$ species present on SiO_2 and $\text{SiO}_2\text{-TiO}_2$ supports were similar by means of the XPS measurement. Nishii et al.

[17] investigated the propylene polymerization using the Ti complex in various solvents having different dielectric constants value in homogeneous system. They reported that the high polarity of solvent resulted in increased activity due to the increased propagation rate. It revealed that the enhancement of the separation of the active metal cation and the MMAO-derived anion in the polar solvent occurred. It should be also noted that there was no solvent effect observed with the support having the strong interaction such as TiO₂ as seen in **Table 1**.

3.2 Characteristics of polymer

The various copolymers obtained were further characterized by means of GPC, DSC and ¹³C NMR. The GPC was performed in order to determine the M_w, M_n and MWD of polymers. The GPC results are shown in **Table 3**. The GPC curves for EO copolymers using various supports in toluene and CB are shown in **Figures 7 and 8**, respectively. It indicated that all copolymers obtained exhibited only the unimodal molecular weight distribution. Considering polymerization in toluene, the supported system (except for TiO₂ support) gave the higher M_w than that of the homogeneous system, however, without any significant changes in MWD. It was suggested that using TiO₂ apparently promoted the chain transfer reaction consequently resulting in lower M_w. The effect of TiO₂ support on the zirconocene/MAO system was also reported in our previous work [32]. However, it was obvious that the titanocene/dMMAO system gives much higher M_w. It can be observed that polymerization in CB exhibited higher M_w than those in toluene without a significant change in MWD. The increased M_w in CB can be attributed to the solvent-separated ion-pair active species occurred which allowed inserting more monomers into the growing chain. Thus, the solvent-separated ion-pair can provide the high activity while also enhancing the insertion of monomer to the growing chain. The DSC was performed to measure the thermal properties of polymers. It revealed that no melting temperature (T_m) was found indicating non-crystalline polymer produced in this specified polymerization system. The non-crystalline polymers were attributed to the high degree of 1-octene insertion, which can be confirmed by ¹³C NMR.

The quantitative analysis of triad distribution for all copolymers was conducted on the basic assignment of the ¹³C NMR spectra of ethylene/1-octene (EO) copolymer [34]. The ¹³C NMR spectra for EO copolymers using various supports in

toluene and CB are shown in **Figures 9 and 10**, respectively indicating the characteristic peaks of the typical EO copolymer. The triad distribution of all polymers is shown in **Table 4**. It can be observed that the incorporation of 1-octene increased with the CB system for the homogeneous system, the SiO₂-TiO₂, and TiO₂-supported systems. This indicated that the solvent-separated ion-pair obtained from CB exhibited less steric hindrance, then enhancing the insertion of 1-octene in the growing polymer. However, for the SiO₂-supported system, a slight decrease in 1-octene incorporation was found when CB was employed. This was probably due to the inhibition arising from more steric hindrance in SiO₂-supported system. Nishii et al. [17] also investigated the effect of Ti-complex on the syndiospecificity of polypropylene in the homogeneous system. They reported that the presence of the solvent-separated ion-pair allowed the growing chain to migrate between the two enantiomeric ligand sites on the Ti cation without monomer insertion. However, with the contact ion-pair obtained from the non-polar solvent, the migration of the growing chain was not allowed. Based on their work, it can be concluded that migration of the growing chain in different solvent mediums was the main factor for controlling the stereospecificity of polymer. However, in the present work, the copolymerization of ethylene/1-octene was conducted on both homogeneous and supported catalytic systems. Based on the ¹³C NMR results, it can be observed that the microstructure of polymer was similar in regardless of solvents employed. Therefore, the migration of the growing chain did not occurred when compared to the corresponding propylene polymerization system. Considering the triad distribution, it revealed that the polymers obtained from both solvent mediums were block polymer ($r_E \cdot r_O > 1$) indicating the large amounts of triblock (OOO) for the CB system and diblock (EEO) for the toluene system as seen in **Table 4**.

4. Conclusions

In summary, the SiO₂-TiO₂-supported dMMAO with Ti-complex exhibited the highest activity towards ethylene/1-octene copolymerization in different solvent mediums due to decreased support interaction and steric hindrance. In particular, the dramatic increase in catalytic activity can be achieved using the high dielectric constant solvent medium such as chlorobenzene (CB). It can be proposed that the different solvents can possibly alter the nature of catalyst in two ways; (i) changing

the interaction between the support and cocatalyst and/or (ii) changing the form of active species i.e, active ion-pair and solvent-separated ion-pair as seen in the homogeneous system. However, there was no significant change in the observed activity upon the different solvent mediums in the homogeneous system. The presence of CB also resulted in high M_w of polymer. In all cases, the block copolymer was obtained along with high insertion of 1-octene.

Acknowledgement

We thank the Thailand Research Fund (TRF) and the graduate school of CU for the financial support of this project. The guidance of the Ti-complex preparation by Professor Takeshi Shiono from Hiroshima University is greatly appreciated.

References

- [1] P. Tait and I. Berry, *Comp. Polm. Sci.* 4 (1989) 575.
- [2] H.-H. Brintzinger, D. Fischer, R. Mulhaupt, B. Rieger and R.M. Waymouth, *Angew. Chem. Int. Ed. Engl.* 34 (1995) 1143.
- [3] A.G. Simanke, G.B. Galland, L. Freitas, J.A.H. da Jornada, R. Quijada and R.S. Mauler, *Polymer* 40 (1999) 5489.
- [4] X.R. Xu, J.T. Xu, L.X. Feng and W. Chen, *J. Appl. Polym. Sci.* 77 (2000) 1709.
- [5] G.G. Hlatky, *Chem. Rev.* 100 (2000) 1347.
- [6] M. Dankova, R.M. Waymouth, *Macromolecules* 36 (2003) 3815.
- [7] M. Galimberti, F. Piemontesi, N. Mascellani, I. Camurati, O. Fusco and M. Destro, *Macromolecules* 32 (1999) 7968.
- [8] M.J. Schneider, J. Suhm, R. Mulhaupt, M.-H. Prosenc and H.-H. Brintzinger, *Macromolecules* 30 (1997) 3164.
- [9] A. Yano, S. Hasegawa, T. Kaneko, M. Sone, M. Sato and A. Akimoto, *Macromol. Chem. Phys.* 200 (1999) 1542.
- [10] M. Marques, A. Conte, F.C. De Resende and E.G. Chaves, *J. Appl. Polym. Sci.* 82 (2001) 724.
- [11] G. Jacobs, T.K. Das, Y. Zhang, J. Li, G. Racoillet and B.H. Davis, *Appl. Catal. A: Gen.* 233 (2002) 263.

- [12] R. Quijada, J. Retuert, J.L. Gurvara, R. Rojas, M. Valle, P. Saavedra, H. Palza and G.B. Galland, *Macromol. Symp.* 189 (2002) 111.
- [13] C.V. JAMES, C. W. C. JAMES, N. B. CADDAM and A. N. RICHARD, J. *Appl. Polym. Sci. Part A: Polym. Chem.* 32 (1994) 2049.
- [14] D. Coevoet, H. Cramail and A. Deffieux, *Macromol. Chem. Phys.* 197 (1996) 885.
- [15] S.H. Yang, J. Huh and W.H. Jo, *Macromolecules* 38 (2005) 1402.
- [16] F. Forlini, E. Princi, I. Tritto, M.C. Sacchi and F. Piemontesi, *Macromol. Chem. Phys.* 203 (2002) 645.
- [17] K. Nishii, T. Matsumae, E.O. Dare, T. Shiono and T. Ikeda, *Macromol. Chem. Phys.* 205 (2004) 363.
- [18] K. Nishii, T. Shiono and T. Ikeda, *Macromol. Rapid Commun.* 25 (2004) 1029.
- [19] W. Kaminsky and A. Laban, *Appl. Catal. A: Gen.* 222 (2001) 47.
- [20] K. Soga, T. Uozumi, S. Nakamura, T. Toneri, T. Teranishi, T. Sano, T. Arai and T. Shiono, *Macromol. Chem. Phys.* 197 (1996) 4237.
- [21] T. Hasan, K. Nishii, T. Shiono and T. Ikeda, *Macromolecules* 35 (2002) 8933.
- [22] K. Nishii, H. Hagihara, T. Ikeda, M. Akita and T. Shiono, *J. Organometallic Chem.* 691 (2006) 193.
- [23] K. Nishii, T. Ikeda, M. Akita and T. Shiono, *J. Mol. Catal. A: Chem.* 231 (2005) 241.
- [24] T. Hasan, T. Ikeda and T. Shiono, *Macromolecules* 38 (2005) 1071.
- [25] T. Hasan, T. Ikeda and T. Shiono, *Macromolecules* 37 (2004) 8503.
- [26] A. Ioku, T. Hasan, T. Shiono and T. Ikeda, *Macromol. Chem. Phys.* 202 (2002) 748.
- [27] T. Shiono, S. Yoshida, H. Hagihara and T. Ikeda, *Appl. Catal. A: Gen.* 200 (2000) 145.
- [28] N. Intaragamjon, T. Shiono, B. Jongsomjit and P. Praserttham, *Catal. Commun.* 7 (2006) 721.
- [29] H. Hagihara, T. Shiono and T. Ikeda, *Macromolecules* 31 (1998) 3184.
- [30] A. Ioku, T. Shiono and T. Ikeda, *Appl. Catal. A: Gen.* 226 (2002) 15.
- [31] S.J. Conway, J.W. Falconer and C.H. Rochester, *J. Chem. Soc. Faraday Trans.* 185 (1989) 71.
- [32] B. Jongsomjit, S. Ngamposri, and P. Praserttham, *Catal. Lett.* 100 (2005) 139.

- [33] H. Hagimoto, T. Shiono and T. Ikeda, *Macromol. Chem. Phys.* 205 (2004) 19.
- [34] J.C. Randall, *J. Macromol. Sci., Rev. Macromol. Chem. Phys.* C29 (1989) 201.
- [35] B. Jongsomjit, C. Sakdamnusun, J.G. Goodwin, Jr., and P. Praserthdam, *Catal. Lett.* 94 (2004) 209.
- [36] B. Jongsomjit, T. Wongsalee, and P. Praserthdam, *Mater. Chem. Phys.* 97 (2006) 343.
- [37] R. Riva, H. Miessner, R. Vitali, and G.D. Piero, *Appl. Catal. A:Gen.* 196 (2000) 111.
- [38] J.R. Severn, J.C. Chadwick, R. Duchateau, and N. Friederichs, *Chem. Rev.* 105 (2005) 4073.
- [39] R. Klienschmidt, Y. Griebenow, G. Fink, *J. Mol. Catal. A: Chem.* 201 (2000) 401.



สถาบันวิทยบริการ
จุฬาลงกรณ์มหาวิทยาลัย

Table 1 Polymerization^a activity

System	Solvent	Yield (g)	Activity (kg of Polymer/mol Ti.h)
Homogeneous	Toluene	3.25	3897
SiO ₂ support		2.49	2984
SiO ₂ -TiO ₂ support		2.61	3131
TiO ₂ support		2.33	2795
Homogeneous	CB	3.23	3871
SiO ₂ support		1.68 ^b	10095
SiO ₂ -TiO ₂ support		2.69 ^c	12127
TiO ₂ support		2.53	3032

^a Polymerization condition: Ti = 10 μ mol, Al/Ti = 400, Temp = 343 K, Time = 5 min, 50 psi of ethylene pressure was applied.

^b Polymerization time = 1 min

^c Polymerization time = 1.5 min

สถาบันวิทยบริการ
จุฬาลงกรณ์มหาวิทยาลัย

Table 2 XPS data of Al 2p core-level of cocatalysts

Cocatalyst	BE (eV) for Al ³⁺	Amount of Al ³⁺ at surface (% mass)
dMMAO	74.7	28.5
dMMAO/SiO ₂	74.6	25.0
dMMAO/SiO ₂ -TiO ₂	74.8	25.6
dMMAO/TiO ₂	74.7	27.1



สถาบันวิทยบริการ
จุฬาลงกรณ์มหาวิทยาลัย

Table 3 Polymer characterization

System	Solvent	GPC Analysis (g/mol)			T _m ^a
		M _w (10 ⁴)	M _n (10 ⁴)	MWD	
Homogeneous	Toluene	13.43	4.95	2.7	- ^b
SiO ₂		36.37	13.80	2.6	-
SiO ₂ -TiO ₂		36.60	16.02	2.3	-
TiO ₂		6.91	4.25	1.6	-
Homogeneous	CB	27.24	8.11	3.4	-
SiO ₂		50.98	26.52	1.9	-
SiO ₂ -TiO ₂		37.86	9.64	4.0	-
TiO ₂		18.16	6.50	2.8	-

^a Melting temperature was measured by DSC analysis

^b Value not be detected from the measurement

สถาบันวิทยบริการ
จุฬาลงกรณ์มหาวิทยาลัย

Table 4 Triad distribution of copolymer obtained from ^{13}C NMR

System	Solvent	OOO	EOO	EOE	EEE	OEE	OEO	%Octene incorporation
Homogeneous	Toluene	0.107	0.481	0.096	0.184	0.015	0.117	68
	SiO_2	0.295	0.436	0.067	0.102	0.012	0.087	80
	$\text{SiO}_2\text{-TiO}_2$	0.140	0.487	0.082	0.181	0.011	0.098	71
	TiO_2	0.027	0.415	0.140	0.125	0.133	0.160	58
Homogeneous	CB	0.223	0.558	0.045	0.102	0.010	0.062	83
	SiO_2	0.498	0.162	0.085	0.247	0.008	0.000	75
	$\text{SiO}_2\text{-TiO}_2$	0.610	0.346	0.000	0.014	0.030	0.000	96
	TiO_2	0.268	0.442	0.054	0.093	0.009	0.134	76

สถาบันวิทยบริการ
จุฬาลงกรณ์มหาวิทยาลัย

List of Figures

- Figure 1** XRD patterns of various supports prior to impregnation with dMMAO
- Figure 2** Raman spectra of various supports prior to impregnation with dMMAO
- Figure 3** A typical spectrum of the supported dMMAO from EDX analysis used to measure the average [Al]dMMAO concentration on various supports
- Figure 4** SEM/EDX mapping for Al distributions on (a) SiO₂, (b) SiO₂-TiO₂, and (c) TiO₂ supports
- Figure 5** A typical XPS spectrum of Al 2p core-level of dMMAO and dMMAO on various supports
- Figure 6** TGA profiles of supported dMMAO on various supports
- Figure 7** Molecular weight distribution measured by GPC of EO copolymers obtained from various supports in toluene
- Figure 8** Molecular weight distribution measured by GPC of EO copolymers obtained from various supports in CB
- Figure 9** ¹³C NMR spectra of EO copolymers obtained from various supports in toluene
- Figure 10** ¹³C NMR spectra of EO copolymers obtained from various supports in CB

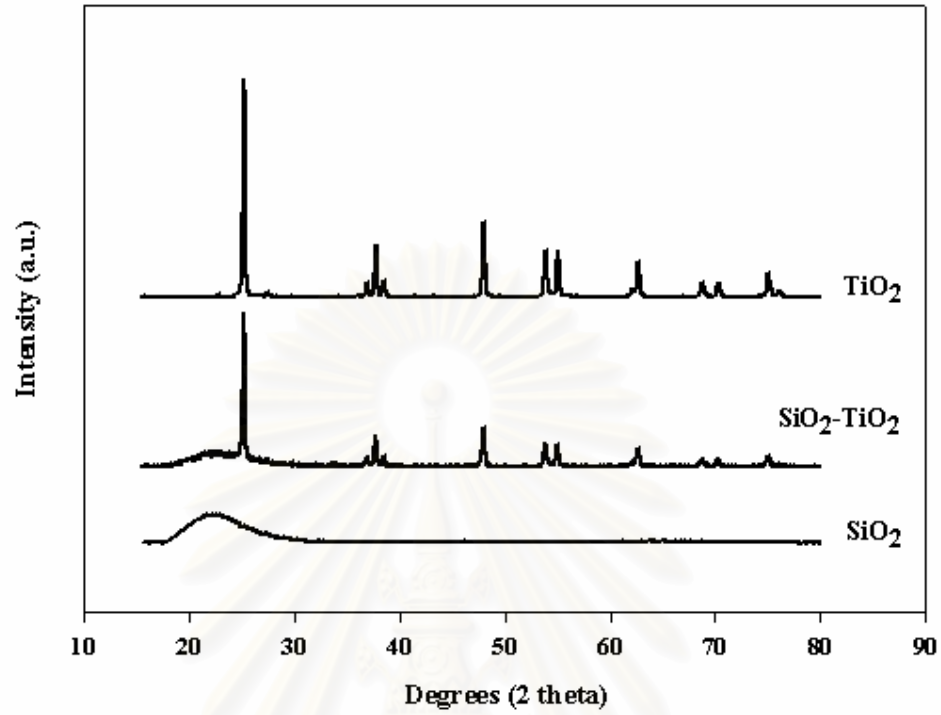


Figure 1

สถาบันวิทยบริการ
จุฬาลงกรณ์มหาวิทยาลัย

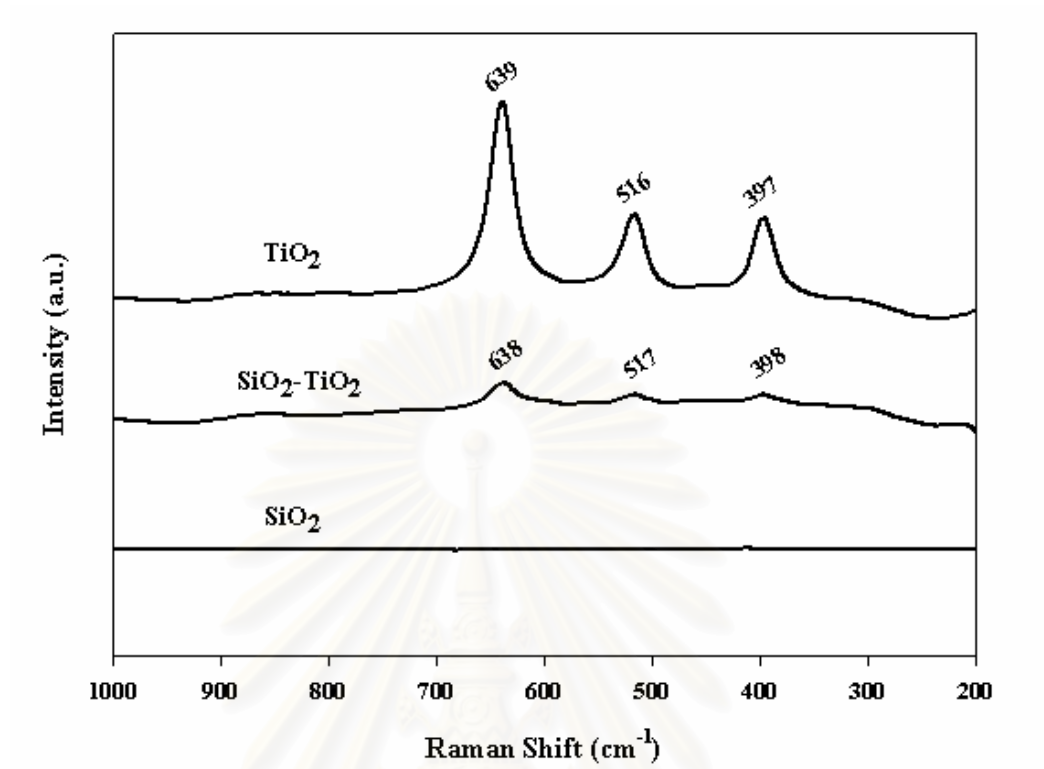
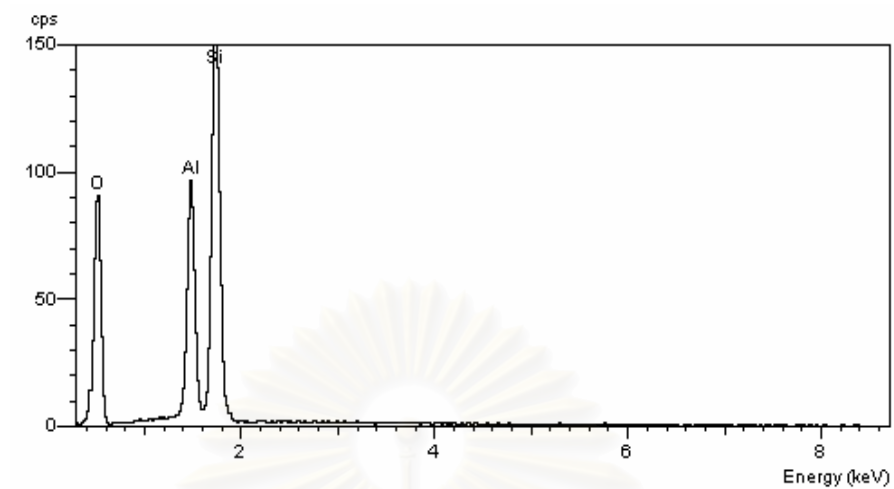


Figure 2

สถาบันวิทยบริการ
จุฬาลงกรณ์มหาวิทยาลัย



Cocatalyst	[Al] _{dMMAO} (% mass)
dMMAO/SiO ₂	12.56
dMMAO/SiO ₂ -TiO ₂	14.69
dMMAO/TiO ₂	18.56

Figure 3

สถาบันวิทยบริการ
จุฬาลงกรณ์มหาวิทยาลัย

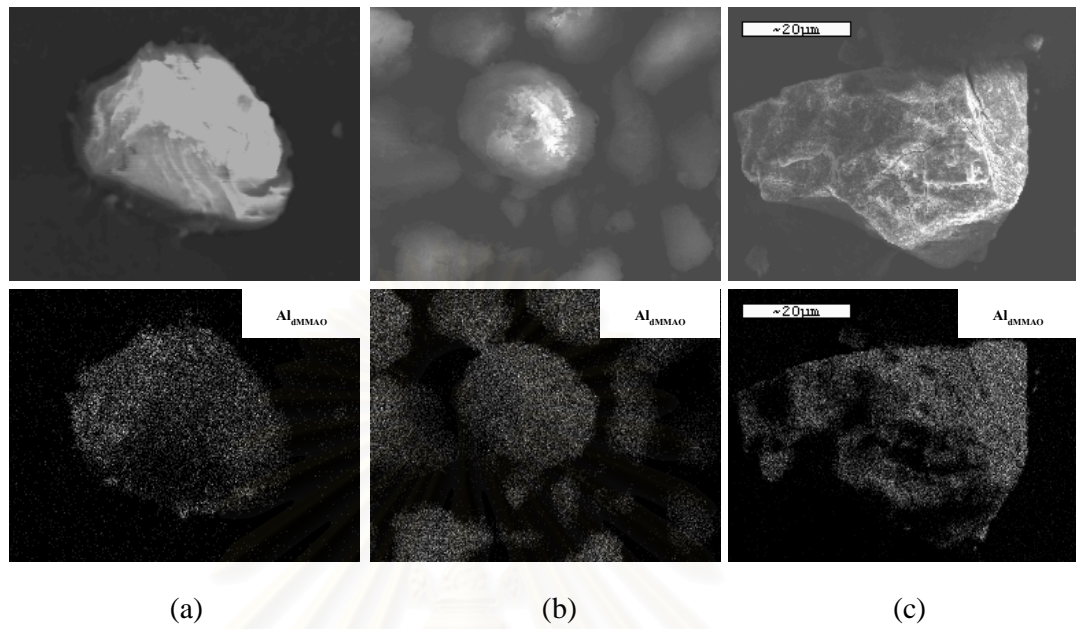


Figure 4

สถาบันวิทยบริการ
จุฬาลงกรณ์มหาวิทยาลัย

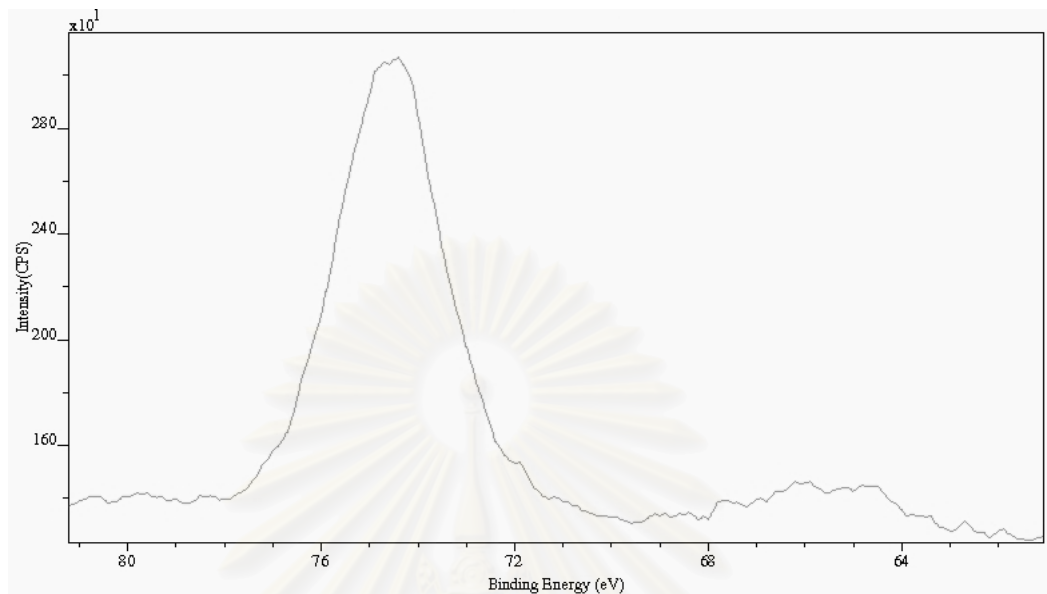


Figure 5

สถาบันวิทยบริการ
จุฬาลงกรณ์มหาวิทยาลัย

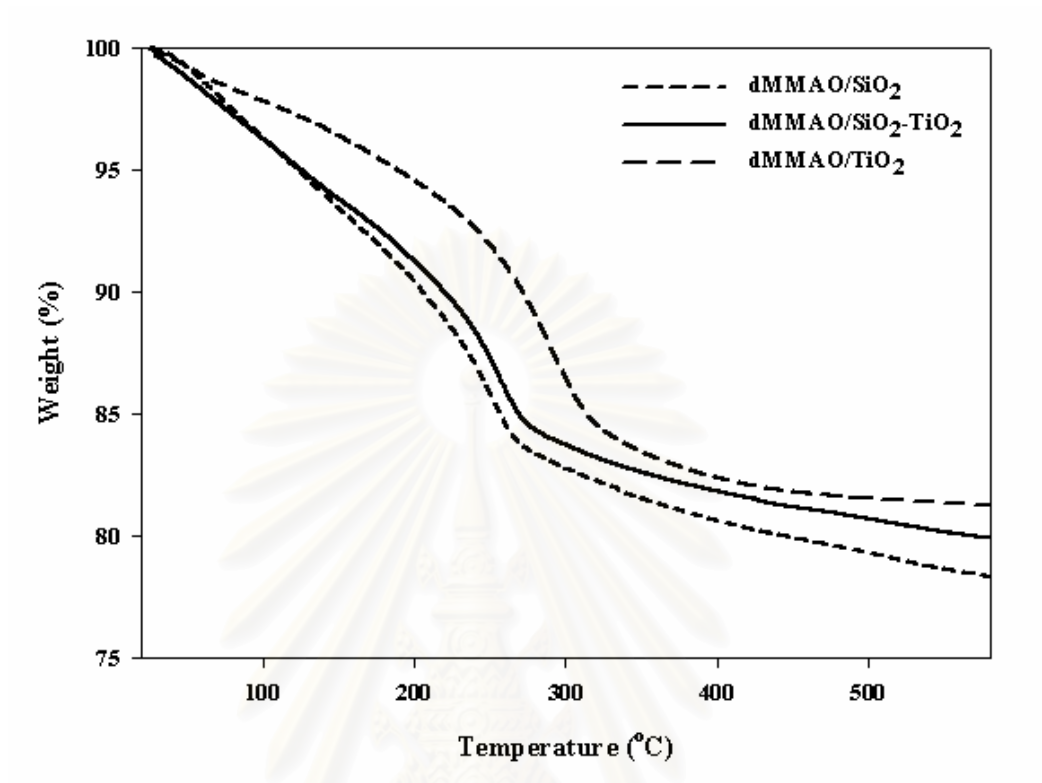


Figure 6

สถาบันวิทยบริการ
จุฬาลงกรณ์มหาวิทยาลัย

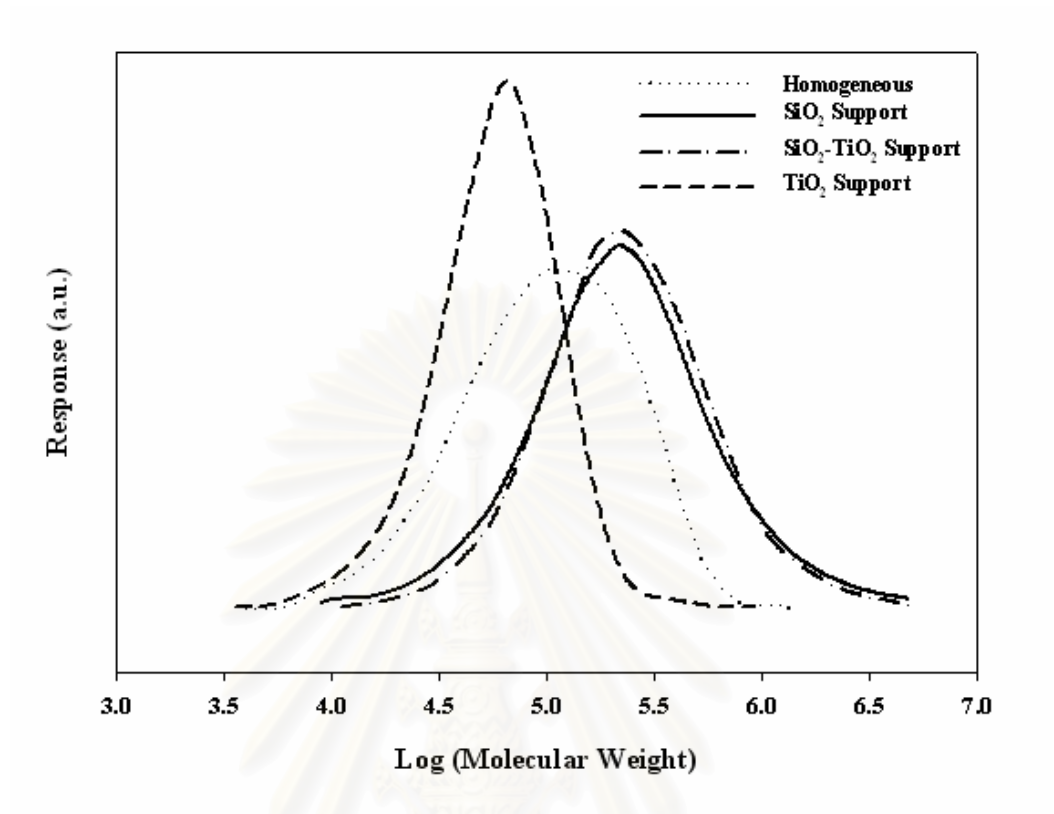


Figure 7

สถาบันวิทยบริการ
จุฬาลงกรณ์มหาวิทยาลัย

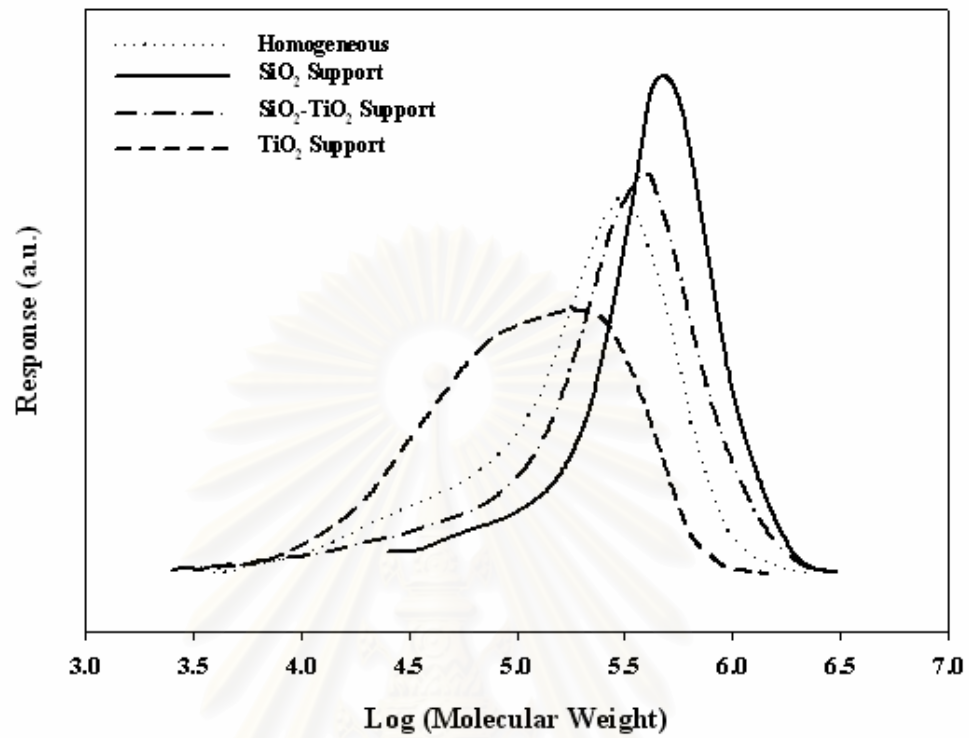


Figure 8

สถาบันวิทยบริการ
จุฬาลงกรณ์มหาวิทยาลัย

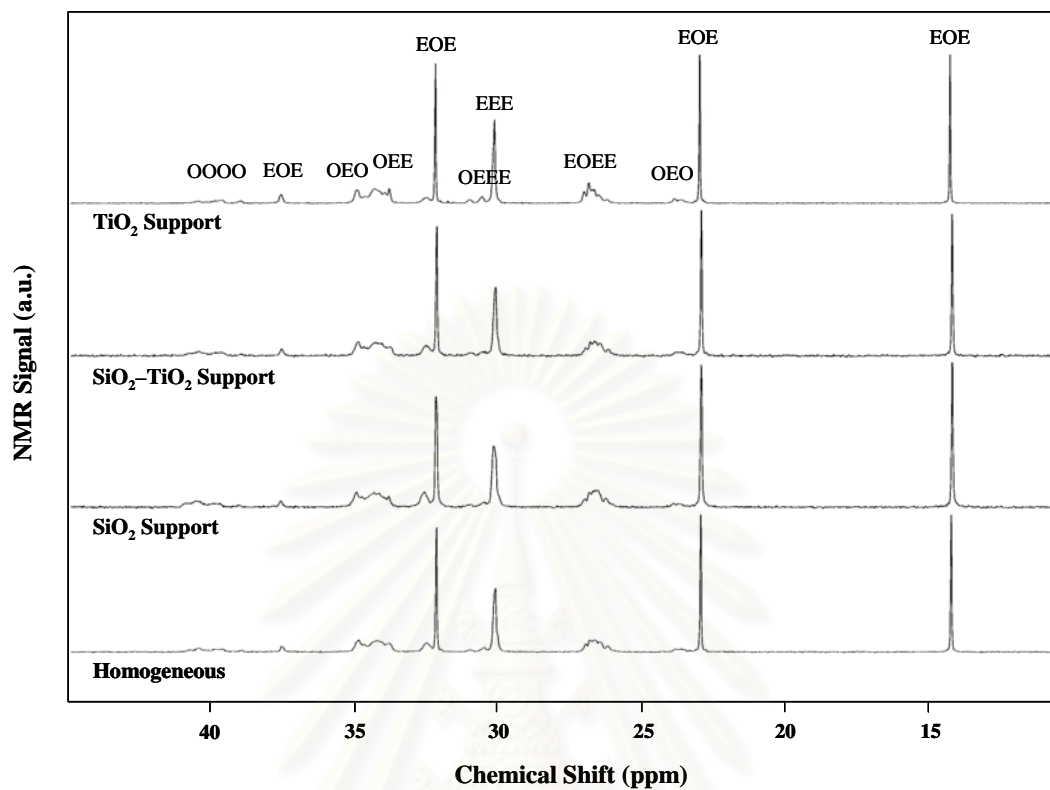


Figure 9

สถาบันวิทยบริการ
จุฬาลงกรณ์มหาวิทยาลัย

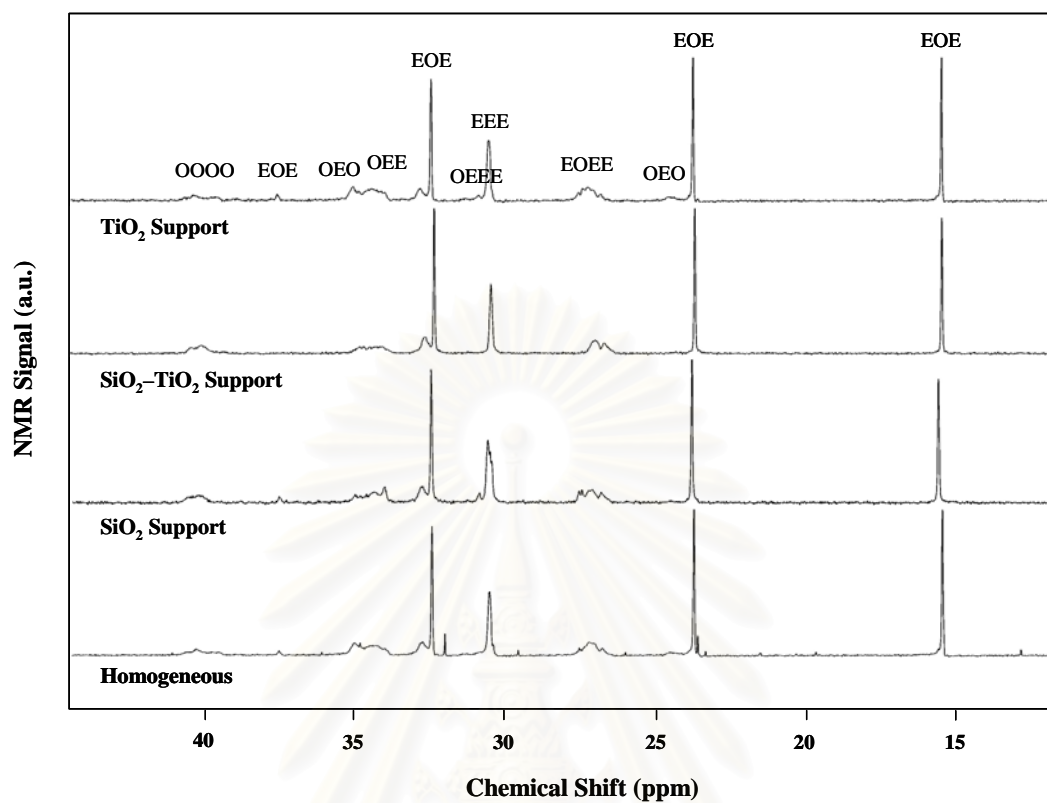


Figure 10

สถาบันวิทยบริการ
จุฬาลงกรณ์มหาวิทยาลัย

VITA

Miss Chanintorn Ketloy was born on July 23, 1982 in Bangkok, Thailand. She received the Bachelor's Degree of Science from the Department of Chemical Technology, Faculty of Science, Chulalongkorn University in May, 2005. She continued her Master's Degree study at Chulalongkorn University in June, 2005.



สถาบันวิทยบริการ
จุฬาลงกรณ์มหาวิทยาลัย